WCAP-10081-A
Addendum 1

ADDENDUM TO THE WESTINGHOUSE SMALL BREAK ECCS EVALUATION MODEL USING THE NOTRUMP CODE FOR THE COMBUSTION ENGINEERING NSSS

S. M. Bajorek

M. R. Wengerd

March 1987

WESTINGHOUSE ELECTRIC CORPORATION
Energy Systems
P. O. Box 355
Pittsburgh, Pennsylvania 15230

8706220214 870604
PDR TOPRP EMVWEST
B PDR



UNITED STATES
NUCLEAR REGULATORY COMMISSION
WASHINGTON, D. C. 20555
November 28, 1986

Mr. E. P. Rahe, Jr, Manager
Nuclear Safety Department
Westinghouse Electric Corporation
Nuclear Technology Division
P. O. Box 355
Pittsburgh, PA 15230-0355

Dear Mr. Rahe:

SUBJECT: ACCEPTANCE FOR REFERENCING OF LICENSING TOPICAL REPORT WCAP-10054, ADDENDUM 1, "ADDENDUM TO THE WESTINGHOUSE SMALL BREAK ECCS EVALUATION MODEL (WCAP-10054) USING THE NOTRUMP CODE FOR THE COMBUSTION ENGINEERING NSSS."

The Nuclear Regulatory Commission (NRC) staff has completed its review of the Topical Report WCAP-10054, Addendum 1.

We find the report to be acceptable for referencing in license applications to the extent specified and under the limitations delineated in the report and the associated NRC evaluation, which is enclosed. The evaluation defines the basis for acceptance of the report.

We do not intend to repeat our review of the matters described in the report and found acceptable when the report appears as a reference in license applications, except to assure that the material presented is applicable to the specific plant involved. Our acceptance applies only to the matters described in the report.

In accordance with procedures established in NUREG-0390, it is requested that Westinghouse publish an accepted version of this report within three months of receipt of this letter. The accepted version shall incorporate this letter and the enclosed evaluation after the title page. The accepted version shall include an -A (designating accepted) following the report identification symbol.

Should our criteria or regulations change such that our conclusions as to the acceptability of the report are invalidated, Westinghouse and/or the applicants referencing the topical report will be expected to revise and resubmit their respective documentation, or submit justification for the continued effective applicability of the topical report without revision of their respective documentation.

Sincerely,

Dennis M. Crutchfield

Dennis M. Crutchfield, Assistant Director
Division of PWR Licensing-B
Office of Nuclear Reactor Regulation

Enclosure:
Safety Evaluation

SAFETY EVALUATION REPORT
OF
WESTINGHOUSE TOPICAL REPORT
WCAP-10054, ADDENDUM 1

1.0 INTRODUCTION

NUREG-0737 Item II.K.3.30 required industry to demonstrate its small break loss of coolant accident (SBLOCA) methods continue to comply with the requirements of Appendix K to 10 CFR 50. In response to this requirement, Westinghouse submitted a description of its NOTRUMP code (Reference 1) and its SBLOCA evaluation model (Reference 2) as applied to a Westinghouse nuclear steam supply system (NSSS). These topical reports were reviewed by the staff and found acceptable as documented in Reference 3.

Westinghouse submitted WCAP-10054, Addendum 1 (Reference 4) which describes the application of the Westinghouse SBLOCA evaluation model to the Combustion Engineering (CE) NSSS and is intended to satisfy NUREG-0737 Item II.K.3.30 for these plants. Supplemental information supporting the topical report was provided in Reference 5.

This report evaluates WCAP-10054, Addendum 1. It specifically addresses compliance of the Westinghouse SBLOCA evaluation model for the CE NSSS to the requirements of Appendix K to 10 CFR 50 and compliance with the requirements of NUREG-0737 Item II.K.3.30.

2.0 EVALUATION OF COMPLIANCE TO APPENDIX K TO 10 CRF 50

WCAP-10054, Addendum 1 describes the methodology used to apply the Westinghouse NOTRUMP code to the CE NSSS. The report specifically

discusses the differences in the CE NSSS, as compared to the Westinghouse NSSS, and examines the application of the Westinghouse SBLOCA evaluation model to the CE NSSS. This evaluation included an examination of the specific modeling features (i.e., equations and assumptions) utilized in the NOTRUMP code, and their applicability to the CE NSSS. Other modeling features of the NOTRUMP code such as the solution techniques and general code formulations, which were not impacted by the NSSS design differences were not modified. The staff has concluded that this approach is acceptable and limited its review of the previously approved SBLOCA evaluation model using the NOTRUMP code to assuring that the impact of the NSSS design differences were properly accomodated. Detailed discussions of this assessment is provided in this section.

In addition to examining the impact of design differences, a sample small break LOCA spectrum was provided in WCAP-10054, Addendum 1. This analysis was reviewed by the staff and the results are reported in Section 2.8.

2.1 Loop Layout

The CE NSSS has a two hot leg, four cold leg layout which is different from the Westinghouse "n" hot leg, "n" cold leg design. To simulate this design difference, the noding utilized for the NOTRUMP code has been modified from that described in Reference 2. The staff has reviewed the differences in the noding utilized for representing the CE NSSS as compared to that approved for the Westinghouse NSSS. The staff has concluded that the noding utilized appropriately reflects the loop layout and is, therefore, acceptable.

The CE design specifies a 42" I.D. hot leg in comparison to the Westinghouse design which has a hot leg of 29.5" I.D. The differences in the hot leg diameter are accounted for by the input data used for the NOTRUMP code. Additionally, it was noted that the transition boundary in horizontal two-phase flow is only weakly dependent on pipe diameter for large diameter pipes. The staff reviewed the models utilized in the NOTRUMP code and has concluded that the effect of the larger diameter pipes is appropriately considered in the equations utilized. Thus, accounting for the effects of the larger hot leg pipe diameter via the code input is acceptable.

The primary flow from the hot leg enters the steam generator through an inclined steam generator inlet nozzle. The inclination of this nozzle is different for the two NSSS designs. Westinghouse examined the effect of the nozzle inclination on the flooding correlation utilized in the NOTRUMP code to represent this portion of the NSSS. It was shown, via a sensitivity study, that the difference in the flooding correlations for the two NSSS designs result in essentially the same total mass behavior during the SBLOCA. Thus, the staff finds that the flooding correlation proposed in WCAP-10054, Addendum 1 for the CE NSSS is acceptable.

The loop seal venting behavior plays an important role for small cold leg LOCAs in which the break size is large enough to deplete

the system mass inventory so that the break becomes uncovered yielding predominantly steam break flow. There are significant geometric differences in the loop seals between the two NSSS designs. For the CE NSSS, the horizontal section of the loop seal is at approximately the same elevation as the top of the core, whereas in the Westinghouse NSSS design, the horizontal loop seal pipe elevation lies at nearly the mid-core elevation. As a result, there is much less of an inner vessel, (i.e., upper plenum, core and lower plenum) level depression required to initiate loop seal venting in the CE NSSS design.

Geometric differences in the loop seals are explicitly treated in the NOTRUMP input. Modifications to the loop seal noding were made for the application of NOTRUMP to the CE NSSS design due to loop layout differences. The staff has reviewed these noding differences and, based upon the break spectrum analyses presented in Section 4 of WCAP-10054, Addendum 1, noted that the noding utilized for the CE NSSS design produces consistent behavior in the loop seal venting behavior. Thus, the staff finds the loop seal noding acceptable.

WCAP-10054, Addendum 1 did not address differences in the steam generator design and their impact on the SBLOCA evaluation model. Westinghouse provided supplemental information, in response to a staff request, in Reference 5 to address this impact. The staff noted that the NOTRUMP code description includes mechanical separator

models and questioned their applicability to the CE NSSS. Westinghouse stated that these models are not used in the SBLOCA evaluation model. Thus, the staff finds that differences in the separator design does not affect the evaluation model.

With respect to the steam generator heat transfer models, Westinghouse noted that the heat transfer coefficients in the NOTRUMP code are regime dependent and that the correlations used consider the effects of geometry differences via the code input. Based upon staff review of the NOTRUMP heat transfer models, as given in Reference 3, and the fact that the models appropriately account for the effect of geometriv differences, the staff finds that no modifications to the NOTRUMP code are needed to simulate the CE plant steam generators.

2.2 Control Element Assembly (CEA) design

The CE upper internals design provides for several flowpaths for communication between the upper plenum and the upper head. The CEAs can include a shroud through which flow from the upper head can reach the upper plenum in addition through flow through the CEAs themselves. Westinghouse performed sensitivity studies to investigate the modeling of the flow between the upper head and upper plenum.

The results showed that the noding scheme proposed in WCAP-10054, Addendum 1 provided nearly identical inner vessel mixture levels in comparison to detailed representation of the various flow paths available. Based upon these sensitivity studies, the staff concludes that the modeling utilized to represent the CE upper intervals design is acceptable.

2.3 Upper Head Bypass Flow

The CE upper head design provides for negligible bypass flow from the top of the downcomer through the upper head in comparison to that available for a Westinghouse plant with a cold upper head. To reflect this difference, the SBLOCA evaluation model was modified and included a revised assumption for the initial upper head fluid temperature. The staff has examined the approach proposed in WCAP-10054, Addendum 1 and concluded it will result in a conservative prediction of SBLOCA behavior. Thus, the staff finds the treatment of upper head bypass flow for the CE NSSS acceptable.

2.4 Fuel Assembly Design

Both the NOTRUMP and LOCTA-IV (Reference 6) codes calculate the core heat transfer during periods of steam cooling based upon the correlations developed in Reference 7. Westinghouse verified that these steam cooling relations are equally applicable to the range of hydraulic

diameters typical of Westinghouse designed assemblies being reloaded into CE plants. Since the steam cooling correlations explicitly include the hydraulic diameter effect and the hydraulic diameters for the Westinghouse-designed assemblies being reloaded into CE plants are comparable to the range of hydraulic diameters for Westinghouse fuel in Westinghouse plants, the staff concludes that the steam cooling relations in References 1 and 6 are applicable for the CE NSSS.

2.5 Fuel Rod Design

The fuel clad swelling and rupture model in LOCTA-IV is described in Reference 6. Modifications to the LOCTA-IV code to represent the rod burst behavior for the fuel loaded into the CE NSSS is described in Reference 8 and is applied in an identical manner in the SBLOCA evaluation model for the CE NSSS. Since this model has previously been approved by the staff, the staff finds this approach acceptable.

2.6 Pumped Safety and Accumulator Injection

The angle between the cold leg and safety injection line of the CE NSSS is different than that of the Westinghouse NSSS. In WCAP-10054, Addendum 1, the impact of this design difference was evaluated. It was determined that the behavior of the safety injection fluid entering the NSSS would be similar for both designs. In addition, the approach utilized in the NOTRUMP code to represent the non-equilibrium behavior

of the injected fluid is based upon conservative input assumptions. The staff has examined the information provided and has concluded that the evaluation model will conservatively model the non-equilibrium behavior of the injected fluid and is, therefore, acceptable.

The accumulator polytropic expansion coefficient utilized in NOTRUMP is based upon the accumulator blowdown test performed at the Callaway site in 1982. For CE plants with 600 psig accumulators, the coefficient which was derived from this test is directly applicable. For those CE plants with 200 psig accumulators, Westinghouse reexamined these tests using the final portion, wherein the pressure varied from 223.6 to 194.0 psig, to determine the polytropic expansion coefficient. The staff has reviewed the results of these tests and has confirmed that the coefficients specified in WCAP-10054, Addendum 1 an acceptable.

2.7 Reactor Coolant Pumps

The reactor coolant pumps are modelled using the equivalent density model described in Reference 1. CE pump specific parameters and homologous curves are to be used as input to the NOTRUMP code when applied to the CE NSSS. Based upon a review of the discussion presented in Section 3.7 of WCAP-10054, Addendum 1, the staff finds the proposed model acceptable.

2.8 Break Spectrum Analyses

Within Sections 4 and 5 of WCAP-10054, Addendum 1, a sample break spectrum analysis was performed. This break spectrum was performed for the Millstone 2 plant. Analyses were performed for 3-, 4-, and 6-inch cold leg pump discharge breaks. These cases resulted in peak cladding temperatures of 1301°F, 1975°F and 1165°F, respectively. In addition, 4-inch line breaks were also analyzed in the pump suction and hot leg piping resulting in peak cladding temperatures of 1412°F and 1673°F, respectively. Thus, based upon these analyses, it was concluded that a 4-inch line break in the cold leg pump discharge piping was the worst case break.

The staff reviewed these calculations for conformance with Section C.1 of Appendix K. With respect to the specific plant analyzed (Millstone 2), the staff was concerned that a break size which did not rely upon the accumulator injection to recover the core inventory could result in a higher peak cladding temperature. In Reference 5, Westinghouse submitted additional information which demonstrated that a break of approximately a 3.5 inch line would not result in accumulator injection. Westinghouse conservatively estimated the peak cladding temperature for this break and demonstrated that it was bounded by the 4-inch line break. Based upon these results, the staff concludes that the spectrum analyses performed for Millstone 2 satisfies the requirements of Section C.1 of Appendix K.

The staff also expressed concern that this break spectrum analysis may not be applicable for all CE plants. In Reference 5, Westinghouse stated that any future analyses for a CE plant will include analysis of a representative spectrum of small breaks to identify the limiting break. The staff finds this commitment acceptable.

2.9 Summary of Compliance with Appendix K to 10 CFR 50

Within Reference 3, the staff concluded that the NOTRUMP code and its application to the Westinghouse NSSS fully complied with the requirements of Appendix K to 10 CFR 50. Within WCAP-10054, Addendum 1, Westinghouse described the modifications to the NOTRUMP code and its application for the CE NSSS. As discussed in detail above, the staff finds all the proposed modifications acceptable. Thus, the staff finds that the application of the NOTRUMP code to the CE NSSS, as described in WCAP-10054, Addendum 1, complies with the requirements of Appendix K to 10 CFR 50, with the exception of the break spectrum requirements of Section C.1 of Appendix K. The staff has concluded that the analyses is WCAP-10054, Addendum 1 demonstrates compliance to this section for the Millstone 2 plant, however, the results may not be generically applicable for all CE plants. The staff finds the Westinghouse commitment to perform representative break spectrum analyses for future calculations for other CE NSSS designs acceptable for demonstrating compliance with this section.

3.0 EVALUATION OF COMPLIANCE TO NUREG-0737 ITEM II.K.3.30

NUREG-0737, Item II.K.3.30 required industry to demonstrate its SBLOCA methods continued to comply with the requirements of Appendix K to 10 CFR 50. As stated in II.K.3.30, specific staff concerns regarding small-break LOCA models were provided in the analysis sections of the Bulletin and Orders Task Force reports for each LWR vendor. NUREG-0611 and NUREG-0635 addressed the staff concerns regarding the Westinghouse and CE NSSS methods, respectively.

Within Reference 3, the staff evaluated the conformance of References 1 and 2 to the concerns documented in NUREG-0611. The staff reviewed NUREG-0635 and determined that it contained many of the concerns expresssd in NUREG-0611. Thus, many of the previous staff evaluations in Reference 3 are equally applicable to application of the NOTRUMP code to the CE NSSS.

Three concerns were identified from NUREG-0635 which needed to be examined specifically for the CE NSSS design or were not identified in NUREG-0611. Westinghouse addressed these concerns in Reference 5. These concerns are evaluated below.

3.1 Noncondensible Affects on Condensation Heat Transfer

NUREG-0635 requested an assessment of the effects of noncondensible gases on condensation heat transfer in the CE plants.

Within Reference 2, Westinghouse demonstrated that the effect of noncondensible gases on the small-break LOCA transient for a Westinghouse NSSS would be minimal. Westinghouse stated, in Reference 5, that the effects of noncondensible gases for a CE plant would be the same. The staff concluded in Reference 3, that due to the limited amount of noncondensible gases available during a design bases SBLOCA event, minimal impact is expected. This was also confirmed by test results obtained from Semiscale experiments. Based upon the foregoing, the staff agrees that noncondensible gases is also expected to have a minimal impact on the CE NSSS. Thus, this concern is resolved.

3.2 Primary Metal Heat

NUREG-0635 requested confirmation that adequate accounting of stored energy (heat) within the primary system metal structures are included in the CE plant model. Westinghouse described, in Reference 5, the components in the plant for which metal heat is modeled. Verification of the primary metal heat modeling was provided by the LOFT and SEMISCALE simulations documented in Reference 2. Based upon the verification results, the staff concludes that adequate accounting of stored metal heat is included in the NOTRUMP model for the CE NSSS and this item is resolved.

3.3 Modeling of Break Flow

NUREG-0635 requested validation of applying a 1.0 discharge coefficient on both the subcooled and saturated break flow models. Westinghouse concluded that its subcooled break flow model slightly overpredicts subcooled break flow, while the Moody break flow model provides an accurate calculation of the break flow for steam discharge. Two-phase discharge through the break is expected to occur over a short time period.

The staff reviewed the break flow results presented in Section 4 of WCAP-10054, Addendum 1 and agrees that the two-phase break flow occurs over a small time period. Additionally, the staff believes that the Westinghouse subcooled break flow model will produce reasonable, but somewhat conservative, break flow rates; the Moody break flow model is also reasonable for steam discharges. Thus, the staff has concluded that the use of a 1.0 discharge coefficient for both the subcooled and saturated break flow models is acceptable.

3.4 Summary of Compliance to NUREG-0737 Item II.K.3.30

Based upon the foregoing, the staff has concluded that WCAP-10054, Addendum 1 addresses the concerns of NUREG-0635 and NUREG-0611.

As noted in Section 2.9, the staff also finds that the Westinghouse SBLOCA evaluation model satisfies the requirements of Appendix K to 10 CFR 50. Therefore, the staff finds that WCAP-10054, Addendum 1 satisfies NUREG-0737, Item II.K.3.30.

4.0 REFERENCES

1. Meyer, P. E. and Kornfilt, J., "NOTRUMP-A Nodal Transient Small Break and General Network Code," WCAP-10079, November 1982.

2. Lee, N., Tauche, W. D. and Schwarz, W. R., "Westinghouse Small Break ECCS Evaluation Model Using the NOTRUMP Code," WCAP-10054, December 1982.

3. Letter, C. O. Thomas (NRC) to E. P. Rahe (Westinghouse), Subject: Acceptance for Referencing of Licensing Topical Report WCAP-10054 (Westinghouse Small Break ECCS Evaluation Model Using the NOTRUMP Code), May 21, 1985.

4. Bajorek, S. M., "Addendum To The Westinghouse Small Break ECCS Evaluation Model (WCAP-10054) Using the NOTRUMP Code for the Combustion Engineering NSSS," WCAP-10054, Addendum 1, July 1984.

5. Letter, Rahe, E. P., Jr. (Westinghouse) to Lyons, J. (NRC), "Response to the NRC Request for Additional Information on Topical Report WCAP-10054, Addendum 1," October 23, 1976.

6. Bordelon, F. M. et al., "LOCTA-IV Program: Loss of Coolant Transient Analysis," WCAP-8305, June 1974.

7. Yeh, H. C. et al., "Heat Transfer Above the Two-Phase Mixture Level Under Core Uncovery Conditions in a 336-Rod Bundle," EPRI-NP-2161, December 1981.

8. Ferguson, K. L. and Kemper, R. M., "ECCS Evaluation Model for Westinghouse Fuel Reloads of Combustion Engineering NSSS," WCAP-9528, June 1979.

ACKNOWLEDGMENTS

The work of the following contributors is acknowledged:

P. E. Meyer

R. J. Skwarek

M. J. Parvin

W. D. Tauche

W. R. Schwarz

N. Lee

B. A. McIntyre

D. W. Sklarsky

TABLE OF CONTENTS

Section	Title	Page
1	INTRODUCTION	1-1
2	SYSTEM DESCRIPTION	2-1
3	SYSTEM EVALUATION	3-1
	3.1 Loop Layout	3-1
	3.1.a Loop Representation	3-1
	3.1.b Large Diameter Hot Leg	3-2
	3.1.c Hot Leg - SG Inlet Plenum Flooding	3-2
	3.1.d Loop Seal Behavior	3-5
	3.2 Control Element Assembly Design	3-8
	3.3 Upper Head Bypass Flow	3-11
	3.3.a Representation	3-11
	3.3.b Upper Head Temperature	3-12
	3.4 Fuel Assembly Design	3-13
	3.5 Fuel Rod Design	3-16
	3.5.a Rod Burst Calculation	3-16
	3.5.b Fuel Crack and Dish Volumes	3-16

Section	Title	Page
	5.3 4-Inch Pump Suction Leg Break	5-2
	5.4 Conclusion	5-3
	5.5 Additional Sensitivity Studies	5-3
6	CONCLUSIONS	6-1
7	REFERENCES	7-1
APPENDIX A	Response to NRC Questions	A-1

LIST OF ILLUSTRATIONS

Figure	Title	Page
3-1	CE-NOTRUMP Small Break Evaluation Model Noding Diagram	3-21
3-2	Flooding Correlation Sensitivity Study Inner Vessel Mixture Level Comparison	3-22
3-3	Flooding Correlation Sensitivity Study SG Tube Mixture Level Comparison	3-22
3-4	Flooding Correlation Sensitivity Study Total System Mass Comparison	3-23
3-5	Upper Head Flow Path Sensitivity Study [ ]^{a,c} Path Model	3-24
3-6	Upper Head Flow Path Sensitivity Study [ ]^{a,c} Path Model	3-24
3-7	Upper Head Flow Path Sensitivity Study Upper Head Mixture Level Comparison	3-25
3-8	Upper Head Flow Path Sensitivity Study Inner Vessel Mixture Level Comparison	3-25
3-9	Comparison of F_{froth} Correlation with Data and Maximum CE Rod Size Deviation	3-26
4-1	Core Pressure for Sample 3-Inch Cold Leg Break	4-9

TABLE OF CONTENTS

Section	Title	Page
1	INTRODUCTION	1-1
2	SYSTEM DESCRIPTION	2-1
3	SYSTEM EVALUATION	3-1
	3.1 Loop Layout	3-1
	3.1.a Loop Representation	3-1
	3.1.b Large Diameter Hot Leg	3-2
	3.1.c Hot Leg - SG Inlet Plenum Flooding	3-2
	3.1.d Loop Seal Behavior	3-5
	3.2 Control Element Assembly Design	3-8
	3.3 Upper Head Bypass Flow	3-11
	3.3.a Representation	3-11
	3.3.b Upper Head Temperature	3-12
	3.4 Fuel Assembly Design	3-13
	3.5 Fuel Rod Design	3-16
	3.5.a Rod Burst Calculation	3-16
	3.5.b Fuel Crack and Dish Volumes	3-16

Section	Title	Page
	3.6 Pumped Safety and Accumulator Injection	3-17
	3.6.a Injection Angle	3-17
	3.6.b Safety Injection Flow Geometry	3-17
	3.6.c Polytropic Expansion Coefficient	3-18
	3.7 Reactor Coolant Pumps	3-20
4	SAMPLE BREAK SPECTRUM	4-1
	4.1 Steady State Conditions	4-1
	4.2 Transient Analysis	4-3
	4.3 Small Break Spectrum Results	4-3
	4.3.a Three Inch Cold Leg Break	4-4
	4.3.b Four Inch Cold Leg Break	4-5
	4.3.c Six Inch Cold Leg Break	4-5
	4.3.d Summary of Loop Seal Behavior	4-6
	4.3.e Summary of Cold Leg Break Results	4-6
5	SENSITIVITY STUDIES	5-1
	5.1 Introduction	5-1
	5.2 4-Inch Hot Leg Break	5-1

Section	Title	Page
	5.3 4-Inch Pump Suction Leg Break	5-2
	5.4 Conclusion	5-3
	5.5 Additional Sensitivity Studies	5-3
6	CONCLUSIONS	6-1
7	REFERENCES	7-1
APPENDIX A	Response to NRC Questions	A-1

LIST OF ILLUSTRATIONS

Figure	Title	Page
3-1	CE-NOTRUMP Small Break Evaluation Model Noding Diagram	3-21
3-2	Flooding Correlation Sensitivity Study Inner Vessel Mixture Level Comparison	3-22
3-3	Flooding Correlation Sensitivity Study SG Tube Mixture Level Comparison	3-22
3-4	Flooding Correlation Sensitivity Study Total System Mass Comparison	3-23
3-5	Upper Head Flow Path Sensitivity Study [ ]^{a,c} Path Model	3-24
3-6	Upper Head Flow Path Sensitivity Study [ ]^{a,c} Path Model	3-24
3-7	Upper Head Flow Path Sensitivity Study Upper Head Mixture Level Comparison	3-25
3-8	Upper Head Flow Path Sensitivity Study Inner Vessel Mixture Level Comparison	3-25
3-9	Comparison of F_{froth} Correlation with Data and Maximum CE Rod Size Deviation	3-26
4-1	Core Pressure for Sample 3-Inch Cold Leg Break	4-9

Figure	Title	Page
4-2	Inner Vessel Mixture Level for Sample 3-Inch Cold Leg Break	4-9
4-3	Break Liquid Flow for Sample 3-Inch Cold Leg Break	4-10
4-4	Break Steam Flow for Sample 3-Inch Cold Leg Break	4-10
4-5	Total System Inventory for Sample 3-Inch Cold Leg Break	4-11
4-6	Broken Loop Seal Steam Flow for Sample 3-Inch Cold Leg Break	4-11
4-7	Intact Loop Seal Adjacent to Broken Leg Steam Flow for Sample 3-Inch Cold Leg Break	4-12
4-8	Lumped Intact Loop Seal Steam Flow for Sample 3-Inch Cold Leg Break	4-12
4-9	Vessel Mixture Mass for Sample 3-Inch Cold Leg Break	4-13
4-10	Hot Rod Clad Temperature for Sample 3-Inch Cold Leg Break	4-13
4-11	Core Pressure for Sample 4-Inch Cold Leg Break	4-14
4-12	Inner Vessel Mixture Level for Sample 4-Inch Cold Leg Break	4-14
4-13	Break Liquid Flow for Sample 4-Inch Cold Leg Break	4-15
4-14	Break Steam Flow for Sample 4-Inch Cold Leg Break	4-15

Figure	Title	Page
4-15	Total System Inventory for Sample 4-Inch Cold Leg Break	4-16
4-16	Broken Loop Seal Steam Flow for Sample 4-Inch Cold Leg Break	4-16
4-17	Intact Loop Seal Adjacent to Broken Leg Steam Flow for Sample 4-Inch Cold Leg Break	4-17
4-18	Lumped Intact Loop Seal Steam Flow for Sample 4-Inch Cold Leg Break	4-17
4-19	Vessel Mixture Mass for Sample 4-Inch Cold Leg Break	4-18
4-20	Accumulator Pressure for Sample 4-Inch Cold Leg Break	4-18
4-21	Hot Rod Clad Temperature for Sample 4-Inch Cold Leg Break	4-19
4-22	Core Pressure for Sample 6-Inch Cold Leg Break	4-20
4-23	Inner Vessel Mixture Level for Sample 6-Inch Cold Leg Break	4-20
4-24	Break Liquid Flow for Sample 6-Inch Cold Leg Break	4-21
4-25	Break Steam Flow for Sample 6-Inch Cold Leg Break	4-21
4-26	Total System Inventory for Sample 6-Inch Cold Leg Break	4-22

Figure	Title	Page
4-27	Broken Loop Seal Steam Flow for Sample 6-Inch Cold Leg Break	4-22
4-28	Intact Loop Seal Adjacent to Broken Leg Steam Flow for Sample 6-Inch Cold Leg Break	4-23
4-29	Lumped Intact Loop Seal Steam Flow for Sample 6-Inch Cold Leg Break	4-23
4-30	Vessel Mixture Mass for Sample 6-Inch Cold Leg Break	4-24
4-31	Accumulator Pressure for Sample 6-Inch Cold Leg Break	4-24
4-32	Hot Rod Clad Temperature for Sample 6-Inch Cold Leg Break	4-25
5-1	Core Pressure for 3-Inch Hot Leg Break	5-4
5-2	Inner Vessel Mixture Level for 4-Inch Hot Leg Break	5-4
5-3	Break Liquid Flow for 4-Inch Hot Leg Break	5-5
5-4	Break Steam Flow for 4-Inch Hot Leg Break	5-5
5-5	Total System Inventory for 4-Inch Hot Leg Break	5-6
5-6	Single Intact Loop Seal Steam Flow for 4-Inch Hot Leg Break	5-6

Figure	Title	Page
5-7	Single Intact Loop Seal Steam Flow for 4-Inch Hot Leg Break	5-7
5-8	Lumped Intact Loop Seal Steam Flow for 4-Inch Hot Leg Break	5-7
5-9	Vessel Mixture Mass for 4-Inch Hot Leg Break	5-8
5-10	Hot Rod Clad Temperature for 4-Inch Hot Leg Break	5-8
5-11	Core Pressure for 4-Inch Pump Suction Leg Break	5-9
5-12	Inner Vessel Mixture Level for 4-Inch Pump Suction Leg Break	5-9
5-13	Break Liquid Flow for 4-Inch Pump Suction Leg Break	5-10
5-14	Break Steam Flow for 4-Inch Pump Suction Leg Break	5-10
5-15	Total System Inventory for 4-Inch Pump Suction Leg Break	5-11
5-16	Broken Loop Seal Steam Flow for 4-Inch Pump Suction Leg Break	5-11
5-17	Intact Loop Seal Adjacent to Broken Leg Steam Flow for 4-Inch Pump Suction Leg Break	5-12
5-18	Lumped Intact Loop Seal Steam Flow for 4-Inch Pump Suction Leg Break	5-12

Figure	Title	Page
5-19	Vessel Mixture Mass for 4-Inch Pump Suction Leg Break	5-13
5-20	Hot Rod Clad Temperature for 4-Inch Pump Suction Leg Break	5-13
A-1	Pressure Comparison	A-13
A-2	Mixture Level Comparison	A-14
A-3	Core Steam Flow Comparison	A-15
A-4	Break Steam Flow Comparison	A-16
A-5	Break Liquid Flow Comparison	A-17
A-6	Vessel Liquid Mass Comparison	A-18
A-7	Total System Mass Comparison	A-19
A-8	Clad Average Temperature	A-20

LIST OF TABLES

Table	Title	Page
3-1	Maximum Steam Cooling Deviation	3-15
4-1	Steady State Operating Conditions	4-2
4-2	Comparison of Event Sequence	4-7
4-3	Fuel Cladding Data Comparison	4-8
5-1	Break Location Comparison	5-3
A-1	All Steam Break Flow Comparisons	A-10
A-2	Fraction of Core Power	A-12

NOMENCLATURE

Symbol	Meaning	Units
C_d	Drag coefficient	
d	Diameter	ft
D_e	Hydraulic diameter	ft
g	Gravitational acceleration	ft/sec^2
g_c	32.174	$lbm-ft/lbf-sec^2$
G	Mass flux	lbm/ft^2-sec
h	Heat transfer coefficent	Btu/ft^2-sec-^oF
j	Superficial velocity	$ft^3/sec-ft^2$
k	Thermal conductivity	$Btu/ft-sec-^oF$
K	Kutateladze number	
m	Constant	
n	Constant	
Nu	Nusselt number	
P	Pressure	psia
Pr	Prandtl number	
Re	Reynolds number	
u	Velocity	ft/sec
[ ] a,c		
Z	Elevation	ft

Greek Symbols	Meaning	Units
α	Void fraction	
ρ	Density	lbm/ft^3
σ	Surface tension	lbf/ft
μ	Viscocity	lbm/ft/sec

Subscripts	Meaning
g	Vapor phase
f	Liquid phase
scon	Steam cooling

SECTION 1

INTRODUCTION

This report presents a description of the application of the Westinghouse (W) Small Break Evaluation Model using NOTRUMP[1,2] and LOCTA-IV[3] for the Combustion Engineering (CE) nuclear steam supply systems (NSSS). The intended application of the model described in this report is for use in demonstrating compliance with II.K.3.30 of NUREG-0737 and Appendix K of 10CFR50 for the analysis of the Combustion Engineering nuclear steam supply system. The Evaluation Model discussed in this report is intended to be a generic small break Evaluation Model for the CE NSSS design. This report is therefore an addendum to Reference 1 providing supplementary information and plant sensitivity studies to demonstrate the applicability of the NOTRUMP code to CE plants. A detailed code description of NOTRUMP is provided in Reference 2.

The Westinghouse small break Loss Of Coolant Accident (LOCA) Evaluation Model using NOTRUMP and LOCTA-IV is conservative and in conformance with the previously mentioned regulations. This report addresses the design differences between the CE and Westinghouse steam supply systems and evaluates the effects of those differences on a small break LOCA.

[ ]^{a,c} Modification of the application of the model is done to preserve accuracy in the analysis while preserving a sufficient margin of conservativism in the analysis of a CE NSSS. The unaltered details and aspects of the model are discussed in the References 1-3 and are not specifically repeated here.

This topical report also provides results of generic small break sensitivity studies for a CE plant which have been performed utilizing Appendix K assumptions. These studies identify the limiting break and plant conditions with respect to the emergency core cooling system (ECCS) performance on small break LOCA peak clad temperature (PCT) for CE NSSSs. Since model sensitivity studies performed and documented in Reference 1

for W NSSS designs remain generally applicable to CE NSSS designs, the sensitivity studies examined in this report are limited to those which are particular to the CE NSSS design.

The sections that follow provide the supporting documentation that justifies the application of the Westinghouse small break Evaluation Model for CE plants. Section 2 identifies those design aspects of the CE NSSS that are important departures from the Westinghouse design. Section 3 evaluates those design differences and demonstrates the appropriateness of the application of the small break Evaluation Model for the CE design. Section 4 provides a sample cold leg small break spectrum and demonstrates conformance of the Evaluation Model for CE plants. In Section 5, a sensitivity study to break location is presented in order to demonstrate the ability of the Evaluation Model to analyze other types of small break LOCAs in a CE NSSS and to verify the cold leg as the limiting break location.

SECTION 2

SYSTEM DESCRIPTION

The CE NSSS design has been evaluated in order to confirm the applicability of the Westinghouse Small Break Evaluation Model using NOTRUMP and LOCTA-IV for analysis of the CE NSSS. The assessment has confirmed the application of the Westinghouse (W) plant Small Break Evaluation Model [1-3] generically for CE plant designs. Certain design aspects of the CE NSSS have led to either modification of the application of the Westinghouse Small Break Evaluation Model, or to the performance of sensitivity studies to address the impact of differences between the Westinghouse and CE NSSS with regards to small break ECCS analysis. This chapter discusses those design aspects of the CE NSSS which are addressed in the modification of the Westinghouse Small Break Evaluation Model. Section 3 evaluates these design differences and justifies the methodology used in the application of NOTRUMP for the CE NSSS.

Loop Layout: The CE design incorporates a system of two hot legs feeding two steam generators which in turn feed into four cold legs by way of four crossover legs and four pumps. This feature has been accounted for by modification of the Westinghouse control volume noding scheme and through verification of the flow models which may depend on geometry. The CE design also has loop seals which are relatively high with respect to the top of the core in contrast with the W design. This feature has been been taken into account through geometric input and a noding scheme which provides a more fully explicit representation of a CE NSSS.

Control Assembly Design: The CE upper internals design includes a shroud for the control element assemblies (CEA). Within a given plant, there may be more than one type of shroud design. This design feature is accounted for in the NOTRUMP input description of the CE plant.

Upper Head Bypass Flow: The CE upper head design provides only a small flowpath between the downcomer and the upper head region. This flow is limited due to small flow area with high resistance. Verification for

[ ]^{a,c} is provided. Because of this [

]^{a,c}

Fuel Assembly Design: The steam cooling correlation used in both NOTRUMP and LOCTA-IV is examined and justified for use in the analysis of fuel assemblies with dimensions typical of the CE fuel assembly design. The CE fuel assembly design utilizes guide tubes with diameters that are several times larger than those of neighboring fuel rods. The effect of this is that [

]^{a,c} as is the case of a Westinghouse fuel assembly. However, this beneficial aspect has [

]^{a,c}

Fuel Rod Design: Fuel compatibility considerations result in designs of fuel to be reloaded into CE plants to be similar in all aspects to those of the original CE fuel. However, in some cases, the dimensions of reload fuel rods for CE plants differs somewhat from typical Westinghouse fuel. These differences have been considered in the input description for the fuel residing in the CE core. These differences have been incorporated into all fuel rod models, such as the rod burst calculation in LOCTA-IV.

Safety Injection Flowrate/Injection Angle: The CE pumped safety injection (SI) flowrate under minimum SI assumptions may be lower than that of a typical Westinghouse plant at pressures in the range of 1200 to 600 psia. As in a large number of Westinghouse plants, the safety injection line is connected at an angle to the cold leg pipe. The modelling of the interaction of injected ECCS water and steam generated during the LOCA as done by the Westinghouse Evaluation Model was reviewed and verified as being appropriate for use in the small break transient of a CE NSSS.

Accumulator Injection: The accumulators in a CE plant can have an initial operating nitrogen backpressure as low as 200 psig and as high as 600 psig. The Westinghouse accumulator model is verified in this report as being

appropriate for modelling accumulator injection in a CE NSSS for initial pressures as low as 200 psig, until the pressure at which the accumulator is empty.

Pump Model and Assumptions: The CE NSSS reactor coolant pumps are of a similar design to those of a Westinghouse NSSS. This report verifies the NOTRUMP pump model to be capable of predicting the response of a CE pump during a small break LOCA. Homologous pump curves and other RCP parameters, typical of a CE designed pump are represented by the NOTRUMP RCP model inputs.

SECTION 3

SYSTEM EVALUATION

This chapter describes in detail the verification and when necessary, the modification of the Westinghouse Small Break Evaluation Model to properly represent the CE NSSS. Each design difference of the CE NSSS is evaluated with respect to the specific models and correlations used within NOTRUMP and LOCTA-IV affected by that design difference. Where the CE design requires a change to the model application or input methodology, the modifications are discussed.

3.1 Loop Layout

3.1.a Loop Representation:

The CE NSSS has a two hot leg, four cold leg layout which is different from the Westinghouse "n" hot leg, "n" cold leg design. This difference is accounted for in the W Small Break Evaluation Model for CE NSSSs (CE-NOTRUMP) [

]^{a,c} The noding diagram for the CE NSSS is presented in Figure 1. [

]^{a,c}

[

]a,c

Geometric inputs (volumes, areas, elevations) representative of the CE NSSS are used appropriately. The NOTRUMP code uses a generalized input description and thus code modification is not required to enable systems other than the W NSSS geometry to be modelled.

3.1.b Large Diameter Hot Leg:

The CE design specifies a 42" I.D. hot leg in comparison to the Westinghouse design with a hot leg of 29.5" I.D. The hot leg diameter is an input parameter and has been accounted for in the input data of the CE NSSS model in this report. [

]a,c In addition, the position of transition boundaries in horizontal two-phase flow is only weakly dependent on pipe diameter for large diameter pipes. Therefore, the NOTRUMP code sufficiently accounts for the larger diameter hot leg typical of a CE NSSS.

3.1.c Hot Leg - SG Inlet Plenum Flooding:

The primary flow from the hot leg enters the steam generator inlet plenum through an inclined steam generator inlet nozzle. The inclination of this nozzle is approximately 40° from vertical in a W NSSS while the nozzle is inclined at approximately a 50° angle in a typical CE NSSS. The flooding correlations in NOTRUMP used to represent flooding from the steam generator inlet plenum to the hot leg and is of the form:

[ ]a,c (3-1)

where:

The Kutateladze numbers are defined as:

$$K_g = \left[\frac{\rho_g j_g^2}{[\sigma g g_c \cdot (\rho_f - \rho_g)]^{1/2}} \right]^{1/2} \qquad (3\text{-}2)$$

$$K_f = \left[\frac{\rho_f j_f^2}{[\sigma g g_c \cdot (\rho_f - \rho_g)]^{1/2}} \right]^{1/2} \qquad (3\text{-}3)$$

This flooding correlation was developed from experimental data from a W run test in a one-third scale model facility with PWR geometry for the hot leg and steam generator inlet plenum. The angle of the SG inlet nozzle used in the tests was 40° from vertical. The effect of inclination on the correlation can be estimated by considering a force balance on a droplet in the inlet nozzle at flooding. The minimum vapor velocity that can suspend a droplet in an inclined tube is that velocity which will balance the gravitational and drag forces acting on the droplet:

$$\frac{1}{2} C_d \left(\frac{\pi d^2}{4}\right) \rho_g u_g^2 = \left(\frac{\pi d^3}{6}\right) (\rho_f - \rho_g) g \cos\theta \qquad (3\text{-}4)$$

The maximum stable drop size can be estimated by:

$$d = \frac{We\ \sigma}{\rho_g u_g^2} \qquad (3\text{-}5)$$

The droplet size is determined by the balance of forces that try to shatter the drop as opposed to those that try to hold the drop together. This can also apply to droplets that are torn from a slow moving liquid surface.

Solving for the minimum vapor velocity to suspend the maximum stable droplet, the superficial vapor velocity becomes:

$$j_g = \alpha \left(\frac{4\ We}{3\ C_d}\right)^{1/4} (\cos\theta)^{1/4} \frac{[\sigma g (\rho_f - \rho_g)]^{1/4}}{\rho_g^{1/4}} \qquad (3\text{-}6)$$

Using the expression for j_g, and assuming that the void fraction is high when flooding occurs, the value of K_g at flooding can be estimated from:

$$K_g = \left(\frac{4\ We}{3\ C_d}\right)^{1/4} \cos^{1/4}\theta = C^n \qquad (3\text{-}7)$$

or,

$$K_g = (\text{constant}) * \cos^{1/4}\theta \qquad (3\text{-}8)$$

This expression provides an estimate of the effect of inclination on the flooding in an inclined tube. Note that We_{crit}, C_d and cos appear to the power of 0.25. Thus, the value of C is insensitive to their exact values over small ranges. The theoretical variation of C near 50° can estimated by recalculating C and taking the inclination into account. The correlation with the angular dependence could be written as:

[ ]^{a,c} (3-9)

Note that for θ=40° this expression reverts back to the original correlation. For θ=50° the expression becomes:

[ ]^{a,c} (3-10)

The flooding constants in this and in the original equation differ by [ ]^{a,c} Thus, the flooding correlation [

]^{a,c}

In order to [

]^{a,c} a sensitivity study was conducted to examine the effect of changing the flooding constant. This was accomplished analyzing and comparing two four inch cold leg breaks. The base case used Eq. 3-1 to model the flooding in the SG inlet nozzle and additional case used Eq. 3-10 as the flooding correlation for this region.

The results of this sensitivity are presented in Figures 3-2, 3-3, and 3-4. Figure 3-2 shows a comparison of the inner vessel mixture levels. The behaviors are identical until the loop seals begin to vent and there is sufficient steam flow through the SG inlet nozzle to cause flooding. The mixture levels then diverge for approximately the next 300 seconds until

they reconverge at the 600 second mark and remain identical thereafter. The cause of the divergence in the mixture levels during the 300-600 second time period is due to increased liquid holdup in the SG tubes by the case which used Eq. 3-10 as the flooding correlation. This is shown in Figure 3-3 which compares the mixture levels in the uphill side of the broken loop steam generators. The additional heldup liquid of the second case requires a longer period of time to drain back towards the vessel. The more limiting flooding correlation of the second case does not increase liquid carry over through the steam generator resulting in higher liquid breakflow. This is clearly shown by Figure 3-4, which compares the total system mass inventory between the two cases. The total system mass behaves the same for both cases.

[

]a,c

3.1.d Loop Seal Behavior

The loop seal model used in the CE small break Evaluation Model using NOTRUMP as verified in Reference 1. This same loop seal noding is used in the W small break Evaluation Model.

The loop seal venting behavior plays an important role for small cold leg LOCAs in which the break size is large enough to deplete the system mass inventory so that the break becomes uncovered yielding predominantly steam break flow. For a CE plant, this includes small breaks approximately one to two inches in diameter and greater.

As system inventory is depleted via the break, the RCS begins a relatively slow top down drainage. Mixture levels in the pressurizer, upper head, inner vessel, and downhill sides of the steam generator tubes begin to decrease. The upper head and pressurizer completely drain, and the inner vessel mixture level decreases to the point where the hydrostatic head

developed between the downcomer and the inner vessel equals the hydrostatic head developed by the mixture levels between the uphill and downhill sections of the pump suction legs. When this occurs, the loop seals can begin to vent steam.

The geometry of the loop seal region has an effect on the hydrostatic head across the loop seal just prior to steam venting. The CE and W piping design of this region differ with regards to the relative heights between the top of the core and the elevation at which steam can slip through the loop seal. This difference is accounted for through the geometric input of the plant being simulated. In a CE plant, the horizontal section of the loop seal is at the approximate elevation as the top of the core. In a W plant however, the horizontal loop seal pipe section lies at nearly the mid-core elevation. The major reason for this is due to the lengths of the uphill and downhill sections of pipe in the loop seal. For a CE plant, these lengths are relatively short compared to those of a W plant. Therefore, the CE loop seal will have a much smaller hydrostatic pressure difference between uphill and downhill mixture levels that the same hydrostatic pressure difference in a W loop seal. Thus, it requires less of an inner vessel mixture level depression to initiate venting in a CE loop seal than in a W loop seal. Since the loop seal elevation in a CE plant is relatively high with respect to the top of the core, the loop seals can begin to vent steam before the inner vessel mixture level depresses into the core. Therefore, loop seal venting in a CE plant is a less complicated, more predictable process than in a W plant.

The noding scheme presented in Figure 1, [

] a,c

[

]a,c

Therefore, the loop seals of a CE plant can be adequetly represented using the noding scheme presented in Figure 1 and geometric input representative of the CE loop seal design. The Evaluation Model using NOTRUMP for a CE plant is [

]a,c

3.2 Control Element Assembly (CEA) Design

The CE upper internals design provides for several flowpaths for communication between the upper plenum and the upper head. The control element assemblies can include a shroud through which flow from the upper head can reach the upper plenum in addition to flow through the CEAs themselves. Within a given plant, there may be more than one type of shroud design. There are also flow areas through holes in the upper support plate and through clearances about the shrouds and CEAs. These flowpaths are [

]^{a,c} to represent flow between the upper head and upper plenum.

The effects of [ ]^{a,c} was investigated through a sensitivity study. The upper internals models for the sensitivity study are shown in Figures 3-5 and 3-6. The base case used the upper internals configuration presented in Figure 3-5 and used [

]^{a,c} The more detailed case shown in Figure 3-6 [

]^{a,c}

Results of the two cases were compared indicating a faster drain time of the upper head for the case modelling [

]^{a,c} The reason for the faster drain with [ ]^{a,c} can be explained as follows:

During the first 30 seconds of the transient, system pressure drops quickly and the flow out of the upper head is a cocurrent flow of liquid flashing to vapor. After about 30 seconds, the mixture levels in both the upper head and the upper plenum have dropped below [ ]^{a,c} Because the system pressure is not dropping as quickly as in the first 30 seconds, flashing in the upper head is less important. Thus, for liquid to be replaced by vapor in the upper head, vapor must flow from the upper plenum into the upper head. In the base case, vapor can only reach the upper head through [

]^{a,c} In the more detailed model, the bottom elevation of the [

]^{a,c} When the mixture level in the upper head drops such that the static head of liquid can no longer drive liquid out against the vapor at higher pressure in the upper plenum, vapor begins to flow into the upper head [ ]^{a,c} This provides a relatively high rate of volumetric flow into the upper head which permits [

]^{a,c}

The overall effects of the [

]^{a,c} After 100 seconds, the upper head becomes voided of liquid, [ ]^{a,c} The inner vessel mixture levels, shown in Figure 3-8, are nearly identical. The upper head is no longer an active participant in the transient behavior

after 100 seconds and is unimportant long before core uncovery or the peak clad temperature occurs. The modelling methodology also has no effect on RCS mass inventory or distribution after the initial upper head drain time. Therefore, it is acceptable to model the CE [

]^{a,c} for small break LOCA Appendix K calculations.

3.3 Upper Head Bypass Flow

3.3.a Representation

The CE upper head design provides for negligible bypass flow from the top of the downcomer through the upper head. The flow is restricted from reaching the upper head due to a small flow area with a high hydraulic resistance. For a typical CE plant, the value of [ ]^{b,g} In comparison, a Westinghouse plant with a T_{cold} upper head generally has [ ]^{a,b} It is clear from this comparison that the hydraulic resistance of the CE bypass flowpath is [ ]^{b,c} that of a W T_{cold} plant.

The flow area through the guide tubes and shrouds of a CE plant is [ ]^{b,g} Since gravity is the primary driving force for system region levels in a small break LOCA, the upper head will drain at a rate influenced by the head of the height of liquid remaining in the upper head and the break flow. Only an insignificant amount of liquid drains from the upper head back into the downcomer. Assuming it takes 100 seconds for the upper head to empty, then under the available gravity head, approximately only [

]^{b,c} On this basis, it was decided [

]^{a,c}

3.3.b Upper Head Temperature:

Due to the small upper head cooling flow, the initial upper head fluid temperature is assumed to be at [ ]^{a,c}

3.4 Fuel Assembly Design

Both the NOTRUMP and LOCTA-IV codes calculate the heat transfer during periods of steam cooling based on correlations developed in Reference 4. The tests on which these relations are based were performed on a 336 rod bundle with rods having a .374 inch O.D. The hydraulic diameter of the rods in those tests was .464 inch (.03867 ft.). The purpose of this section is to verify that the steam cooling relations derived from these tests are equally applicable to the range of hydraulic diameters typical of Westinghouse designed assemblies being reloaded into CE plants, as well as existing CE fuel. In CE plants, the fuel assembly hydraulic diameters D_e, may range between [ ]^{a,c} This range of hydraulic diameters is comparable to the range of hydraulic diameters of W fuel assemblies in W plants.

The steam cooling heat transfer relations used in NOTRUMP are:

$$Nu_{scon} = 13.7F_{froth}F_{grid}Pr^{1/3} \qquad Re<2000 \qquad (3\text{-}11)$$

$$= 0.0797F_{froth}F_{grid}Re^{0.677}Pr^{1/3} \qquad 2000<Re<25200 \qquad (3\text{-}12)$$

$$= 0.023F_{froth}F_{grid}Re^{0.8}Pr^{1/3} \qquad Re>25200 \qquad (3\text{-}13)$$

where,

$$Nu_{scon} = h_{scon}D_e/k \qquad (3\text{-}15)$$

$$F_{froth} = 1 + 5\ \exp\{-0.5(Z-Z_{froth})/D_e\} \qquad (3\text{-}16)$$

Z = elevation of point being considered

Z_{froth} = froth height

F_{grid} = [ ]^{a,c}

The hydraulic diameter D_e is explicitly included in the experimental correlation through the Nusselt number Nu_{scon} and the froth factor F_{froth}. D_e is an input parameter in the CE models for both NOTRUMP and LOCTA-IV.

Westinghouse believes that the range of D_e for Westinghouse fuel designs for CE plants are well within the range of applicability of the tests. Never-the-less, a comparison of the impact of the largest D_e for Westinghouse fuel for a CE plant was performed soley for the purpose to justify the applicability of the experiment over the range of hydraulic diameters possible. This comparison, described in the next paragraphs, indicated that the expected overall small impact of hydraulic diameter on the heat transfer coefficient is negligible, and well within the scatter of the experimental data.

It was shown earlier that the hydraulic diameter can have an effect through its dependence in the Nusselt number, the Reynolds number and in F_{froth}. The term F_{grid} [

]^{a,c} In order to more clearly see that overall effect of D_e, the above correlations can be expressed in terms of the heat transfer coefficient as the following:

$$h_{scon} = 13.7kPr^{1/3}F_{froth}/D_e \qquad Re < 2000 \qquad (3\text{-}17)$$

$$= 0.0797kPr^{1/3}\{G/\mu\}^{0.677}F_{froth}D_e^{-0.323} \qquad 2000<Re<25200 \qquad (3\text{-}18)$$

$$= 0.023kPr^{1/3}\{G/\mu\}^{0.8}F_{froth}D_e^{-0.2} \qquad Re > 25200 \qquad (3\text{-}19)$$

Note that in the expressions for h_{scon}, the hydraulic diameter is represented explicitly.

The effect of hydraulic diameter on the heat transfer coefficient can be seen by comparison of $F_{froth}D_e^m$ at two different hydraulic diameters for a range of $(Z-Z_{froth})$. The variation of $F_{froth}D_e^m$ with respect to hydraulic diameter is small in all the ranges of Re. Table 3-1 presents the

comparison of two hydraulic diameters of the test, and the largest deviation expected for fuel in CE plants for $Z-Z_{froth}$ = [ ]^{a,b}

TABLE 3-1

MAXMIMUM STEAM COOLING DEVIATION

Re	[$F_{froth}D_e^m$	$F_{froth}D_e^m$]^{b,c}	% Difference
			]^{b,c}
Re< 2000	[		]
2000<Re<25200			
Re>25200			

Figure 3-9 presents the variation of F_{froth} with $(Z-Z_{froth})$ as predicted by the correlation for F_{froth} and for the results of several of the tests. The points plotted on the figure show the predicted values of F_{froth} for [ ]^{a,c} The figure clearly shows that the diameter effect on F_{froth} is small, and within the scatter of the test data.

In conclusion, the steam cooling correlations are applicable to existing CE-designed assemblies as well as Westinghouse designed reload assemblies. The steam cooling correlation includes a hydraulic diameter effect. Furthermore, the variation of h_{scon} with D_e for the range of D_e typical of CE NSSS and Westinghouse assemblies is small, and well within the scatter of the test data. [

]^{a,c}

3.5 Fuel Rod Design

3.5.a Rod Burst Calculation:

The fuel clad swelling and rupture model in LOCTA-IV has been described in detail in Reference 3. Based on the rod burst test data, it has been determined that clad rupture is directly related to clad stress and therefore to the thickness to diameter ratio of the clad design. In determining burst temperature as a function of pressure for fuel being loaded into a CE NSSS, the pressure differential required for burst at a given temperature is [

]^{b,c} This modification to the LOCTA-IV code is presently approved for use as part of the CE large break Evaluation Model [5] and is applied to the LOCTA-IV code in an identical manner for the small break Evaluation Model presented by this report.

3.5.b Fuel Crack and Dish Volumes:

Fuel crack and dish volumes are computed internally in LOCTA-IV rather than being input. Parameters appropriate to fuel prepared for reloads into a CE NSSS have been entered in to the code, replacing the standard W values.

3.6 Pumped Safety and Accumulator Injection

3.6.a Injection Angle:

The angle between the cold leg and the safety injection line of the CE NSSS is different than that of a Westinghouse system. The injection angle in Westinghouse plants is either [ ]^{a,c} In a CE plant, the injection angle is either [ ]^{a,c} The value of the injection angle is important in calculating [

]^{a,c}

3.6.b Safety Injection Flow Geometry:

Subcooled water injected [

]^{a,c}

where $\left[\quad \right]^{a,c}$ (3-20)

To determine the safety injection flow geometry for a CE NSSS the following values were used:

Safety Injection	Accumulator and SI Injection
P = 1000 psia	P = 200 psia
ρ = 2.242 lbm/ft^3	ρ = 0.4372 lbm/ft^3
[	]^{b,c}
[	]^{b,c}

$$\sigma = 4.855 \times 10^{-3} \text{ lbf/ft} \quad @ \quad 90^{o}F$$

Substitution of these values into [

]^{b,c}

Thus, the [ ]^{a,c} for both of these safety injection flows shows that they are in the range of [ ]^{a,c} which is the same range as was determined for the Westinghouse safety injection flows. Therefore, it can be expected that the [ ]^{a,c} in a CE NSSS will behave similarily to the [ ]^{a,c} in a Westinghouse NSSS and that no modification to NOTRUMP are needed to model this aspect.

3.6.c Polytropic Expansion Coefficient:

The accumulator polytropic expansion coefficient used in small break LOCA analysis with NOTRUMP is based on the accumulator blowdown test performed at the Callaway site in December 1982. The accumulator pressure of the test ranged from an initial 598.0 psig to 194.0 psig. Test results indicated that the average value of the polytropic expansion coefficient [ ]^{b,c} during the initial portion of blowdown to an average value [ ]^{b,c} of the blowdown. These results confirmed the value of approximately 1.0 for the polytropic expansion coefficient that was indicated in LOFT L3-1. Based on these results, an accumulator polytropic expansion coefficient [ ]^{a,c} was determined to be the most

appropriate value to be used in small break analysis for 600 psig initial backfill accumulators.

The appropriate value for the accumulator polytropic expansion coefficient of a 200 psig initial backfill accumulator can be determined from the final portion of the Callaway test results. During the last quarter of the test, the pressure varied from 223.6 to 194.0 psig. The polytropic expansion coefficient calculated for this period [ ]^{a,c} Thus, based on the results at these pressures, a value [ ]^{a,c} appears to be the most appropriate value to be used for the accumulator polytropic expansion coefficient of a 200 psig initial backfill accumulator.

Therefore, a polytropic expansion coefficient [ ]^{a,c} can be used for the accumulators in the small break LOCA analysis of a CE NSSS with either 600 or 200 psig initial backfill.

3.7 Reactor Coolant Pumps

The reactor coolant pumps are modelled using the equivalent density model that is described in Reference 2. The pump model of the W small break Evaluation Model has been verified through comparison to the LOFT experiments. CE pump specific parameters and homologous curves were used in the input to NOTRUMP for the analyses reported in this document.

As presented in Reference 2, predicted RCP two phase head and torque performance is a function of Thoma's cavitation constant in the NOTRUMP RCP model. The Thoma constant is also a function of the pump specific speed, and a value of [ ]^{a,c} for the Thoma constant is appropriate for a W RCP. Because of [

]^{a,c} This is further demonstrated through verification to the LOFT L3-6 experiment. As mentioned above the pump model of the W small break Evaluation Model has been verified through comparison to the LOFT experiments. The LOFT L3-6 experiment is equally applicable for verification of either pump design, due to similarity in specific speeds.

In conclusion, [

]^{a,c}

a,c



Figure 3-1. CE-NOTRUMP Small Break Evaluation Model Noding Diagram

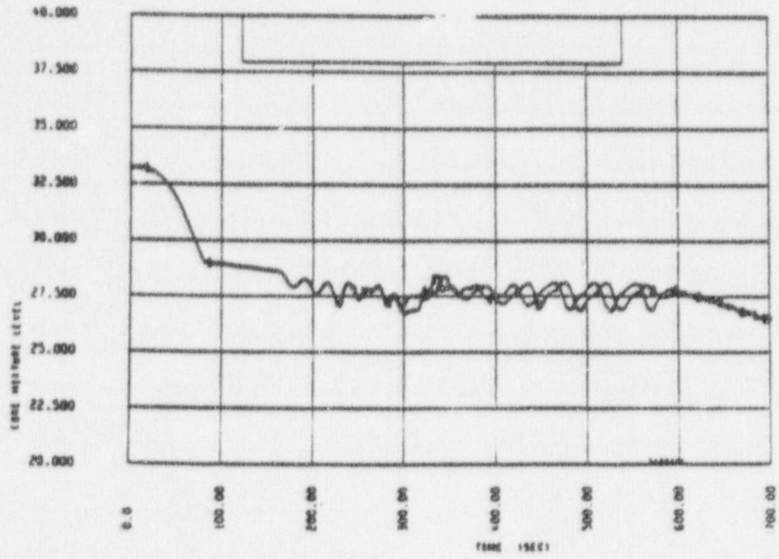


Figure 3-2. Flooding Correlation Sensitivity Study - Inner Vessel Mixture Level Comparison

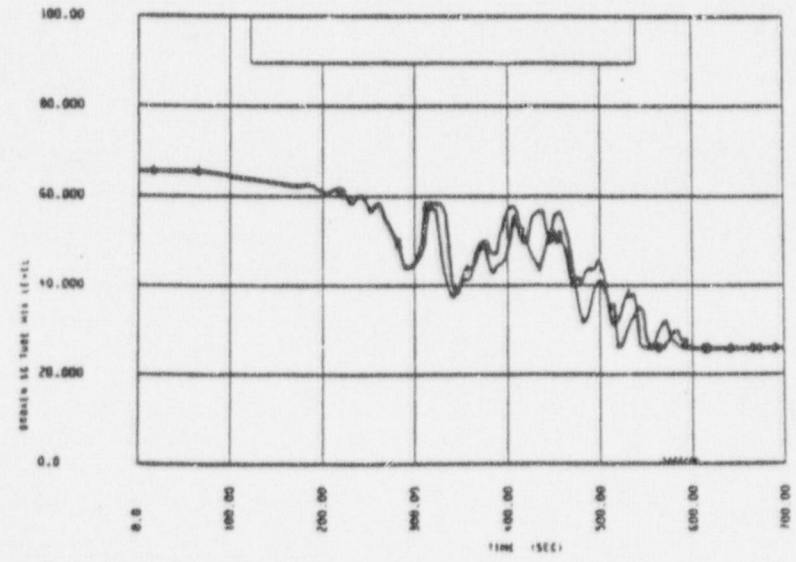


Figure 3-3. Flooding Correlation Sensitivity Study - Steam Generator Tube Mixture Level Comparison

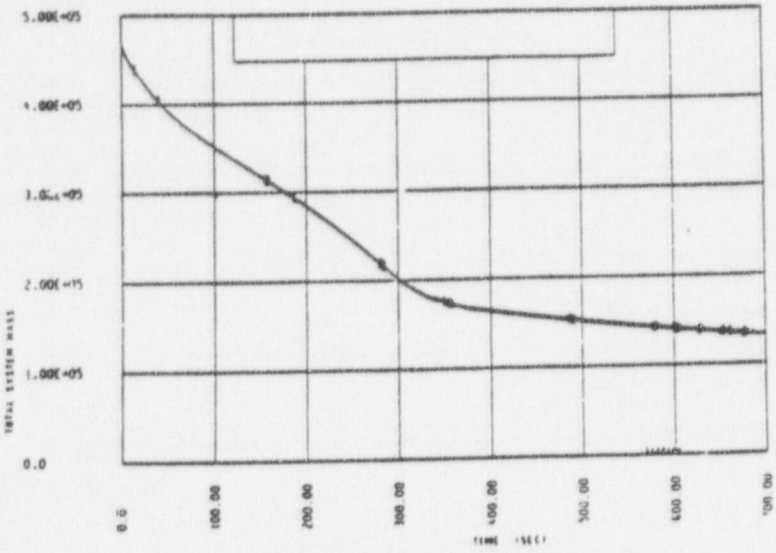


Figure 3-4. Flooding Correlation Sensitivity Study - Total System Mass Comparison

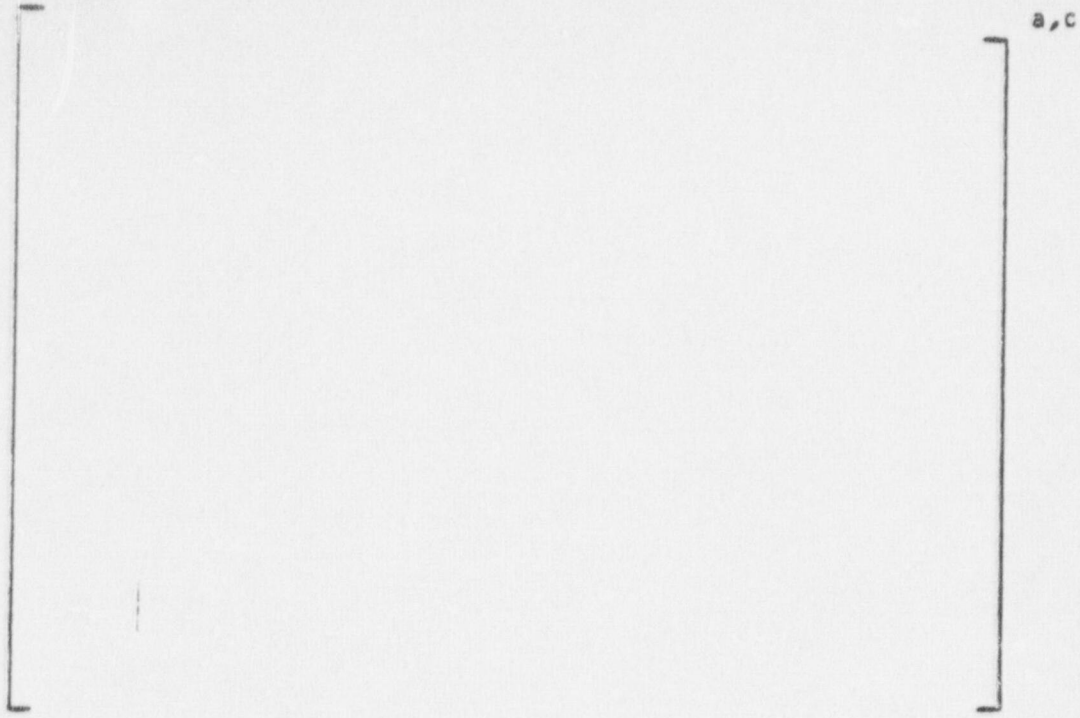


Figure 3-5. Upper Head Flow Path Study -[ ]a,c

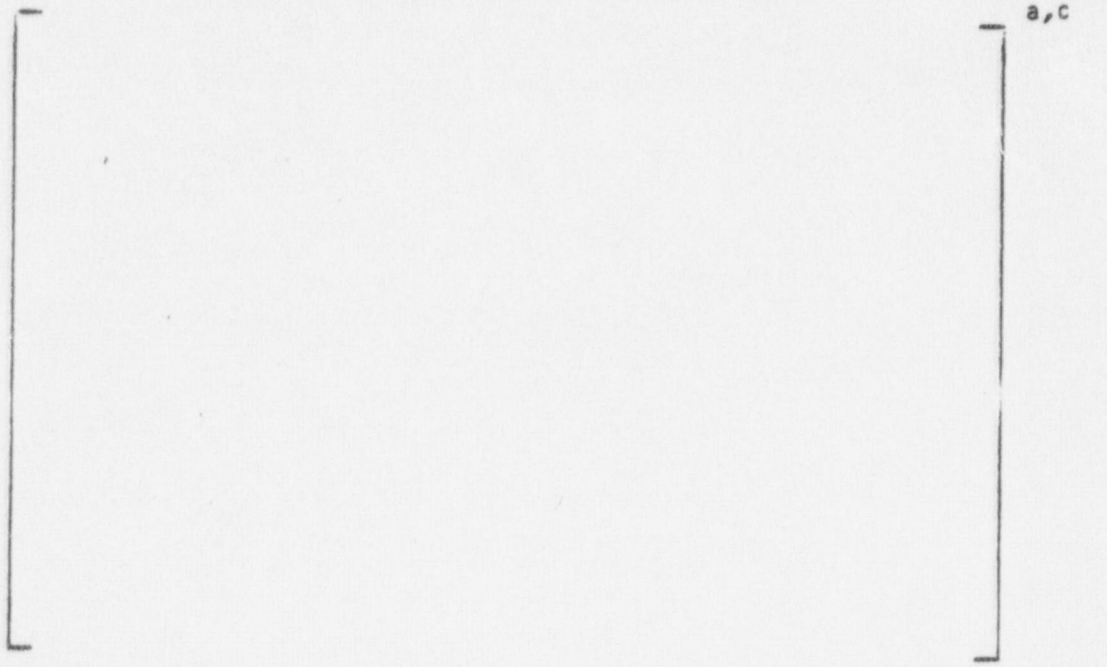


Figure 3-6. Upper Head Flow Path Study -[ ]a,c

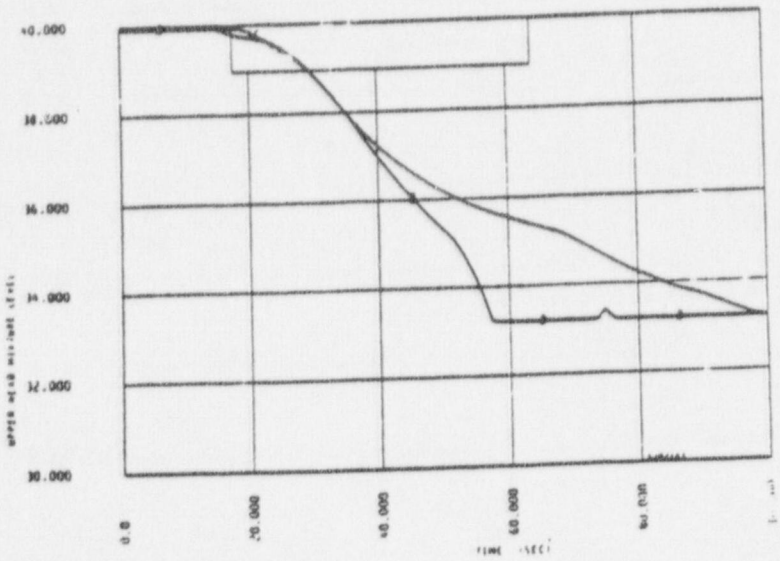


Figure 3-7. Upper Head Flow Path Study - Upper Head Mixture Level Comparison

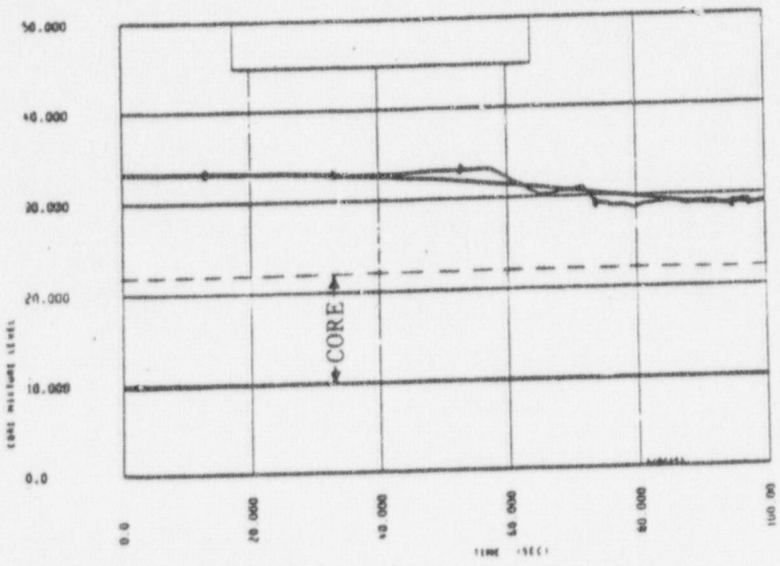


Figure 3-8. Upper Head Flow Path Study - Inner Vessel Mixture Level Comparison

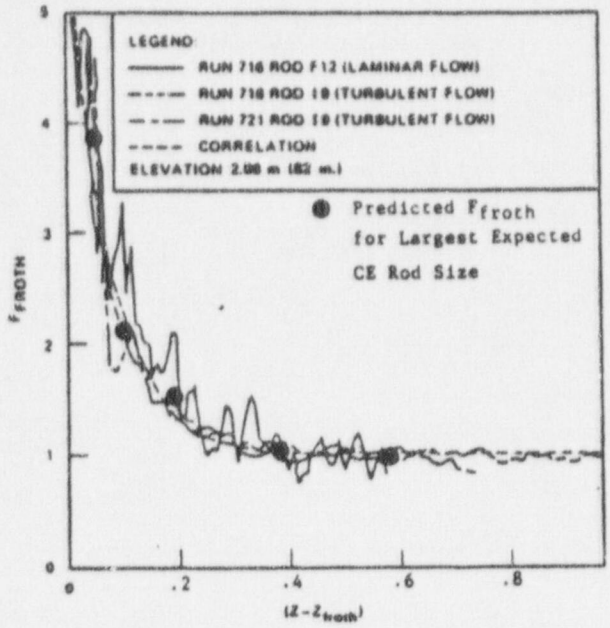


Figure 3-9. Comparison of F_{froth} Correlation with Data and Maximum CE Rod Size Deviation

SECTION 4

SAMPLE BREAK SPECTRUM

This section describes the methodology and presents the results of a range of small break size sample calculations for a CE plant using the NOTRUMP computer code. All LOCA transients are conservatively assumed to start from a 102% power steady state condition and utilize Appendix K assumptions.

4.1 Steady State Conditions

The procedure to establish the steady state set of initial conditions for a CE plant is identical to that used to establish the steady state for a W plant. This procedure is described in detail in Reference 1. For the sample break spectrum presented in this section, a CE plant with 14x14 fuel assemblies and 200 psig accumulator backfill pressure was chosen. This plant was chosen for the sample evaluation, because it is believed to have the most severe small break core uncovery among the various versions of the CE design. The power shape is a [ ]^{a,c} and represents the limiting axial power shape for small break LOCA transients. The steady state operating conditions are presented in Table 4-1.

TABLE 4-1

STEADY STATE OPERATING CONDITIONS

Licensed core power[(a)] (MWt)	2756
Rod peak linear power[(a)] (kw/ft)	15.21
Peak linear heat generation rate (kw/ft)	15.60
Total peaking factor, F_Q	2.54
Accumulator water volume (ft^3 per accumulator)	1080
Accumulator tank volume (ft^3 per accumulator)	2019
Accumulator nitrogen pressure (psia)	215.0
Initial cold leg flow (lbm/sec)	9679
Initial pressurizer pressure (psia)	2280.0
Initial SG steam pressure (psia)	890.0

(a) 2 percent is added to this power to account for calorimetric error, as required by Appendix K of 10CFR50.

4.2 Transient Analysis

A break spectrum calculation for a typical CE plant was performed for a number of break sizes in order to demonstrate the performance of the small break Evaluation Model for CE plants using the NOTRUMP and LOCTA-IV codes. The analyses are presented for a range of break sizes which produced core uncovery and the limiting small break peak clad temperature. The number of break sizes considered was sufficient to conclusively determine the worst break size in terms of peak clad temperature for the CE plant analyzed. The breaks were postulated to occur on the cold leg since this location has been demonstrated to produce the most severe core uncovery for W plants. The break location sensitivity study reported in Section 5 verifies this assumption for CE plants.

For Appendix K small break analyses, the worst single failure assumption is that one electrical train is lost when offsite power is lost at the time of reactor trip. The breaks presented here are consistent with the worst single failure assumption requirements. For small break LOCAs in the cold leg, this assumption results in a significant delay in the safety injection flow delivery. In addition, broken loop safety injection flow and broken loop accumulator flow is assumed to spill to containment. This conservative assumption results in minimum safety injection flow to the RCS.

4.3 Small Break Spectrum Results

The degree and duration of core uncovery which occurs during a small break LOCA is a good indication of the severity of the peak cladding temperature. Using the Evaluation Model, the 3-, 4-, and 6-inch cold leg small break LOCA transients were analysed. The inner vessel mixture levels, pressures, break flows, loop seal steam flows, total system masses, accumulator responses, and hot rod clad tmeperatures for these breaks are presented in Figures 4-1 through 4-32. The following paragraphs discuss each break separately and highlight important aspects of the behavior. In general, each break rapidly depressurizes to the cold leg saturation pressure while the system drains until the inner vessel mixture level is at approximately the hot leg

centerline elevation. The pressure remains fairly constant for a short period, until the loops seals begin to vent steam, and then the system continues to depressurize. Since the loop seal elevation is relatively high in a CE plant, none of the cold leg breaks exhibit a significant mixture level depression prior to loop seal venting. After the loop seal venting occurs, the inner vessel mixture level continues to decrease due to system mass inventory depletion. The mixture level eventually decreases producing core uncovery and later recovers due to safety injection and/or accumulator injection. The transient is completed when the safety injection flow exceeds the break flow and the core recovery is complete.

4.3.a Three Inch Cold Leg Break

The important parameters for the three inch break are presented in Figures 4-1 through 4-10. The three inch break rapidly depressurizes to approximately cold leg saturation pressure, as shown in Figure 4-1, and remains fairly constant until the loop seals begin to vent steam. The inner vessel mixture level transient is shown in Figure 4-2. Since the break flow, shown in Figures 4-3 and 4-4, exceeds the safety injection flow, system inventory continues to decrease and the core begins to uncover at approximately 1600 seconds. The total system inventory depletion is shown in Figure 4-5. Figures 4-6 through 4-8 present the loop seal steams flow for the three inch break. The broken loop loop seal clears and vents steam for the remainder of the transient. The intact loop seal adjacent to the broken loop vents only for a few seconds and then replugs. The lumped intact loop seal vents for a brief period, but it also replugs. Thus, by the time core uncovery begins, only the broken loop seal continues to vent steam to the break. At approximately 1900 seconds, the pumped safety injection flow reaching the downcomer exceeds the steam production in the core, and the vessel mixture mass begins to increase. The vessel mixture mass is shown in Figure 4-9. The core mixture level reaches a minimum, and continues to increase until the core is again recovered. The three inch break does not depressurize to the accumulator setpoint. Instead, recovery is due soley to the pumped safety injection flow. The peak clad temperature occurs shortly after the core mixture level reaches its minimum level. The hot rod clad temperature transient is presented in Figure 4-10.

4.3.b Four Inch Cold Leg Break

The four inch break results are presented in Figures 4-11 through 4-21. As can be seen in Figure 4-11, this break depressurizes more rapidly than the three inch break case due to the increased rate of loss of system inventory. The inner vessel mixture level transient is shown in Figure 4-12. Again, as in the three inch break, no significant mixture level depression occurs in the core prior to the loop seal clearing. The break flows are presented in Figures 4-13 and 4-14, and the total system inventory is presented in Figure 4-15. The loop seal steam flows are shown in Figures 4-16 through 4-18. The broken loop again provided the long term steam venting path to the break. The intact loop seal adjacent to the broken loop vents only briefly and replugs. The lumped intact loop seal clears and passes steam for several hundred seconds and then also replugs for the remainder of the transient. Similar to the the three inch break, the all of the intact loop seals replug prior to the beginning of core uncovery. Core uncovery in the four inch break begins at approximately 960 seconds. The core mixture level continues to decrease until about 1650 seconds where its minimum level occurs. Also at about this time as can be viewed in Figure 4-19, the vessel mixture mass begins to increase slowly, indicating that pumped safety injection reaching the downcomer has begun to exceed the core steam production. Shortly afterward, the accumulators inject and the rate of core recovery increases until system repressurization terminates the accumulator flow. The accumulator response is shown in Figure 4-20. The accumulator injection for this break is relatively slow, and the clad continues to heat up for an additional 130 seconds after the injection begins. The peak clad temperature occurs shortly after termination of accumulator flow. Thus, both accumulator and pumped safety injection flows are important for termination of the clad heatup. The hot rod clad temperature response is shown in Figure 4-21. This particular break size was determined to be the limiting small break size for this plant.

4.3.c Six Inch Cold Leg Break

The six inch break rapidly depressurizes and the inner vessel mixture level quickly decreases to the hot leg elevation which causes the loop seals to clear very early in the transient. The pressure transient is shown in Figure 4-22, and Figure 4-23 shows the inner vessel mixture level response.

The break flows are shown in Figures 4-24 and 4-25, the total system inventory in Figure 4-26, and the loop seal steam flows in Figures 4-27 through 4-29. Again, as in the 3- and 4-inch breaks, only the broken loop clears and remains cleared for the duration of the transient. The intact loop seals vent for longer periods than smaller break sizes due to higher steam production in the six inch break, but eventually replug leaving only the broken loop seal as the path for steam to the break. Core uncovery begins at approximately 490 seconds in the six inch break, but because of the rapid rate of system depressurization in this break, accumulator injection is quickly initiated and limits the extent of the core uncovery. This break is large enough to continue depressurization even after the accumulator flow reaches the core and as a result, the accumulators continue to inject for the remainder of the core recovery process. The vessel mixture mass response and accumulator depressurization are shown in Figures 4-30 and 4-31 respectively. The peak clad temperature for the six inch break occurs shortly after the initiation of accumulator injection. This demonstrates that this break is large enough that the accumulators are effective at quickly turning around the clad temperature. The hot rod clad temperature, is shown in Figure 4-32.

4.3.d Summary of Loop Seal Behavior

The three sample small break transients for the CE NSSS all show very consistent loop seal behavior. For all three cases, the broken loop seal is the only loop seal to clear and continue to vent steam for the remainder of the transients. The intact loop seals vent briefly and then replug after varying short periods of time. Thus, there is only a limited opportunity for venting steam to condense due to interaction with pumped safety injection flow. Therefore, the behavior of the CE loop seals is not only consistent, but it is also conservative with respect to condensation potential. Because of the consistently conservative loop seal behavior during the CE small break transient, an artificial inducement to cause venting through the broken loop seal is not required.

4.3.e Summary of Cold Leg Break Results

The sample break spectrum presented in this section brackets and thus identifies the four inch break as the worst small break size for this

particular CE plant in terms of peak clad temperature. The sequence of major events for the sample break spectrum is shown in Table 4-2 and the fuel cladding information is shown in Table 4-3. Both the three and the six inch breaks caused peak clad temperatures significantly lower than the four inch break. The three inch break peak clad temperature was low in comparison to the four inch break peak clad temperature primarily because the core did not uncover deep enough. Breaks smaller than the three inch break would have even less severe core uncovery and therefore would not produce peak clad temperatures in excess of the three inch break case. The six inch break peak clad temperature was much lower than the four inch break peak clad temperature because the length of the core uncovery was sufficiently short to prevent significant clad heatup. Small break sizes larger than the six inch break would produce shorter periods of core uncovery and continuous effectiveness of the accumulators. The peak clad temperatures of those breaks would be less than the limiting small break size peak clad temperature and are bounded by large break LOCA analysis. Therefore, the four inch break is the worst break size for this plant in terms of small break peak clad temperature.

TABLE 4-2

COMPARISON OF EVENT SEQUENCE

Event	3-Inch	4-Inch	6-Inch
Start	0.0	0.0	0.0
Reactor trip signal	11.0	6.46	3.53
Top of core uncovered	1576	966	487
Accumulator injection begins	---	1670	630
Peak clad temperature occurs	2275	1810	684
Top of core covered	3530	2815	710

Unit [seconds]

TABLE 4-3

FUEL CLADDING DATA COMPARISON

Event	3-Inch	4-Inch	6-Inch
Peak clad temperature (^{o}F)	1301	1975	1165
Peak clad temperature location (ft)	11.39	11.39	10.64
Local Zr/H_2O reaction maximum (%)	0.91	9.19	0.88
Local Zr/H_2O reaction location (ft)	11.39	11.14	10.64
Total Zr/H_2O reaction (%)	<0.3	<0.3	<0.3
Hot rod burst time (sec)	—	1595	—
Hot rod burst location (ft)	—	11.14	—

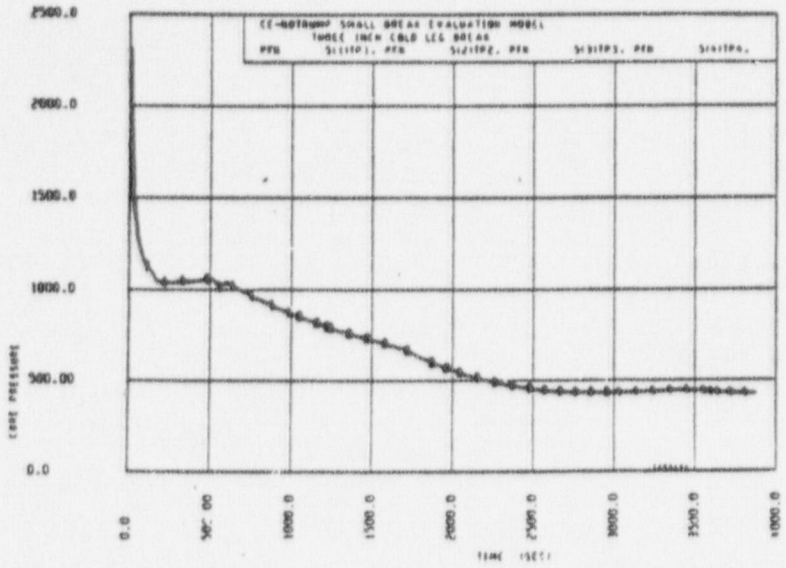


Figure 4-1. Core Pressure for Sample 3-Inch Cold Leg Break

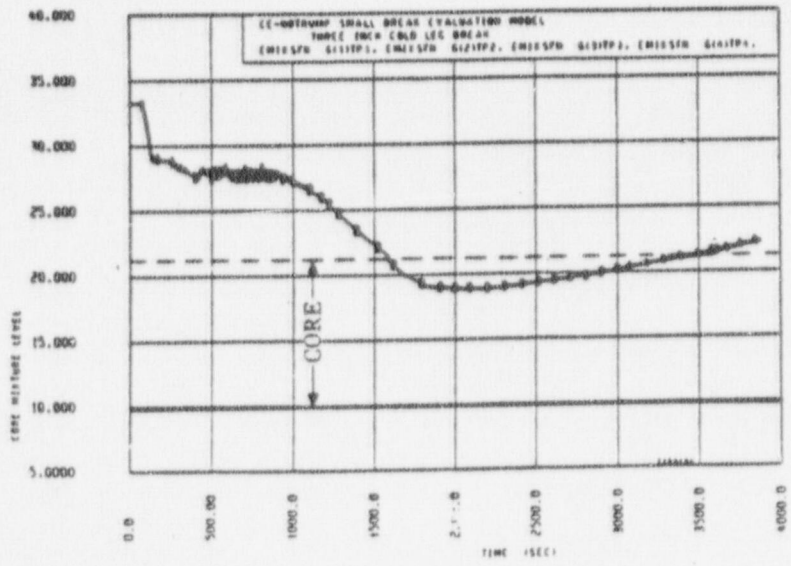


Figure 4-2. Inner Vessel Mixture Level for Sample 3-Inch Cold Leg Break

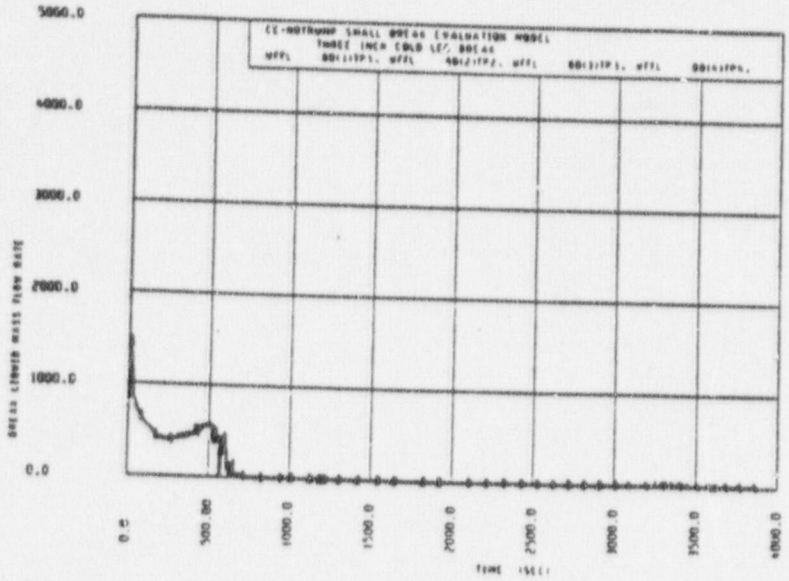


Figure 4-3. Break Liquid Flow for Sample 3-Inch Cold Leg Break

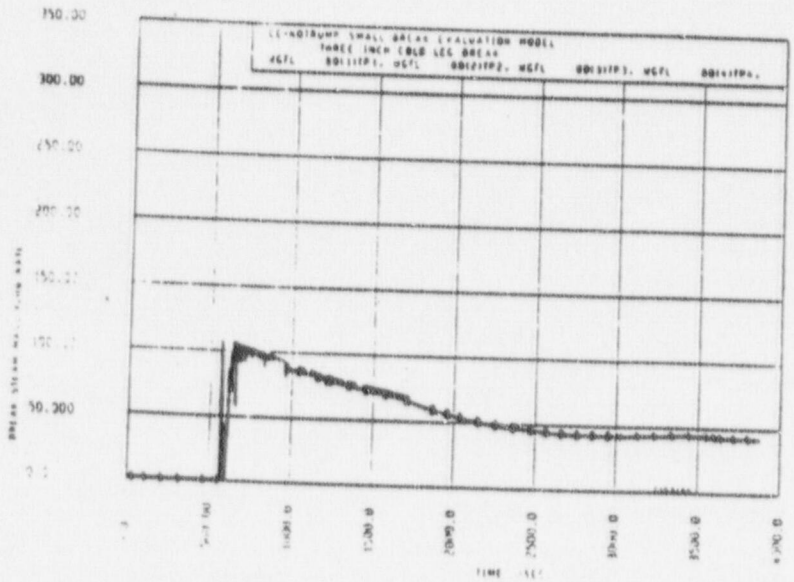


Figure 4-4. Break Steam Flow for Sample 3-Inch Cold Leg Break

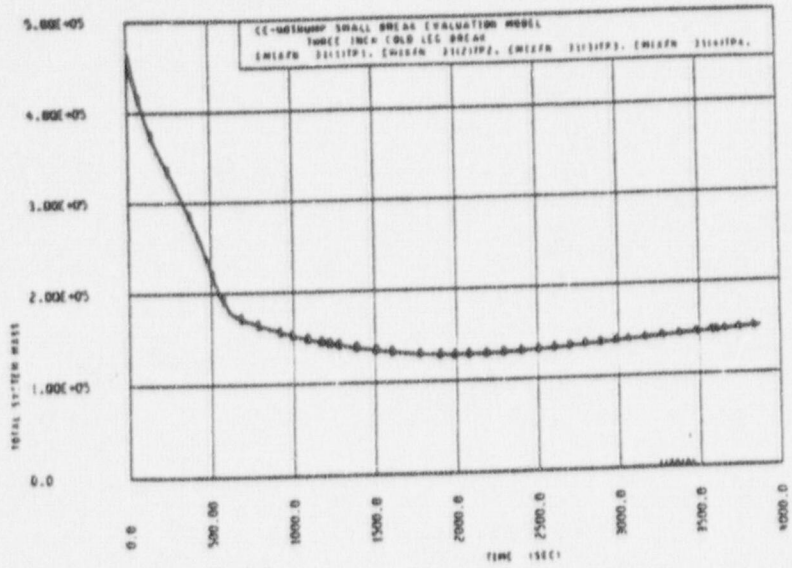


Figure 4-5. Total System Inventory for Sample 3-Inch Cold Leg Break

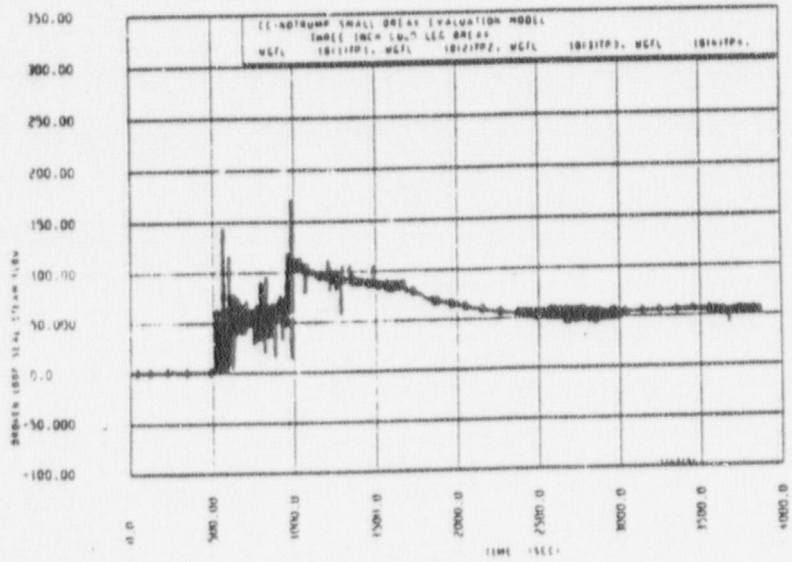


Figure 4-6. Broken Loop Seal Steam Flow for Sample 3-Inch Cold Leg Break

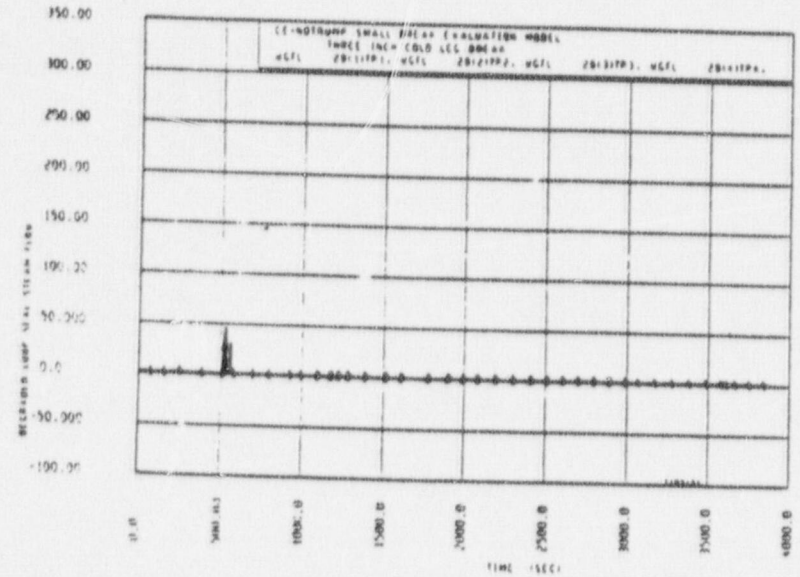


Figure 4-7. Intact Loop Seal Adjacent to Broken Leg Steam Flow for Sample 3-Inch Cold Leg Break

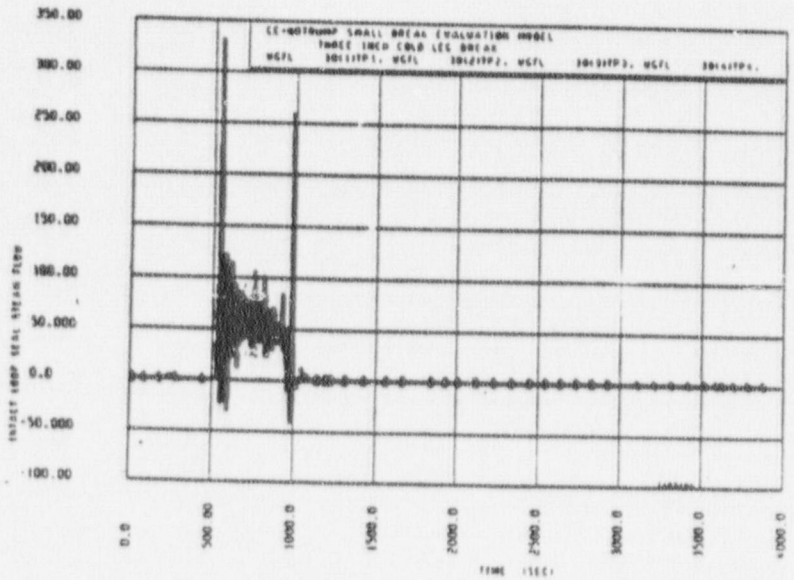


Figure 4-8. Lumped Intact Loop Seal Steam Flow for Sample 3-Inch Cold Leg Break

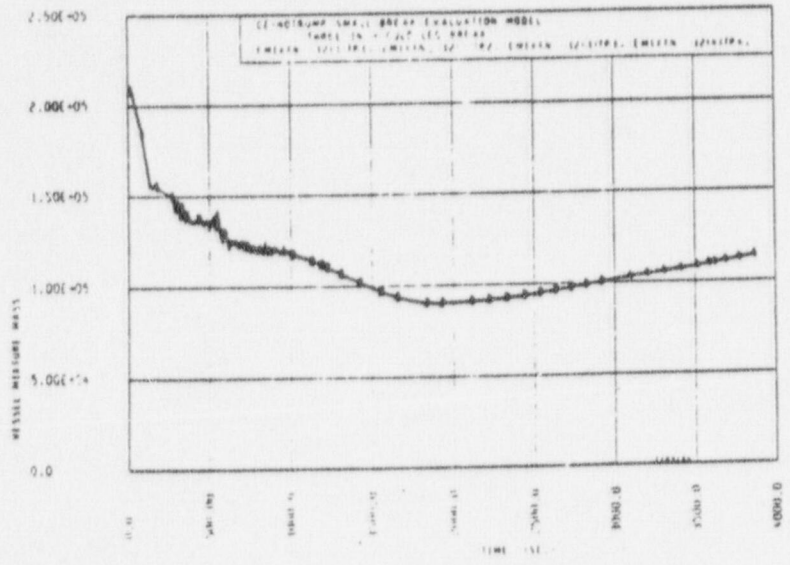


Figure 4-9. Vessel Mixture Mass for Sample 3-Inch Cold Leg Break

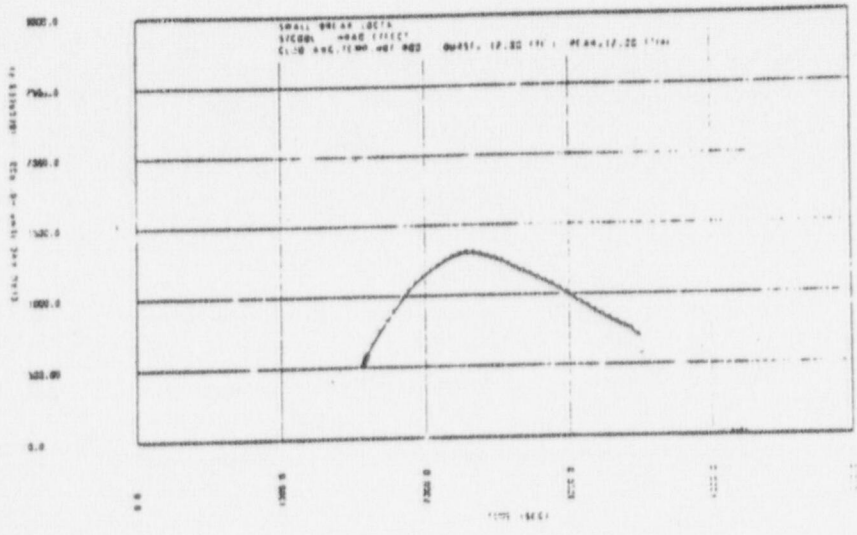


Figure 4-10. Hot Rod Clad Temperature for Sample 3-Inch Cold Leg Break

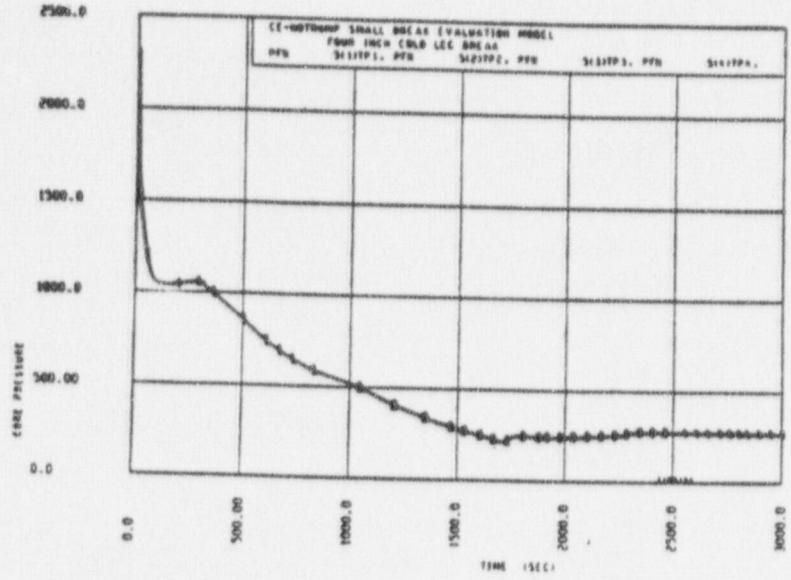


Figure 4-11. Core Pressure for Sample 4-Inch Cold Leg Break

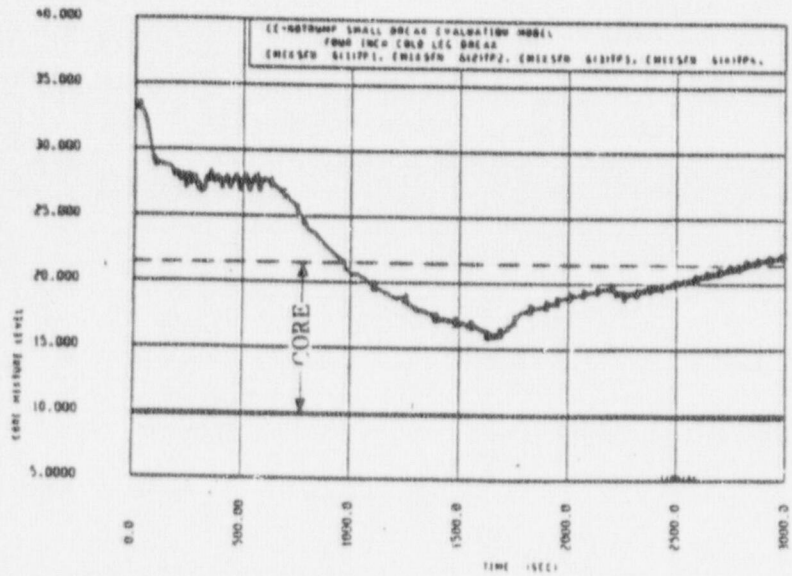


Figure 4-12. Inner Vessel Mixture Level for Sample 4-Inch Cold Leg Break

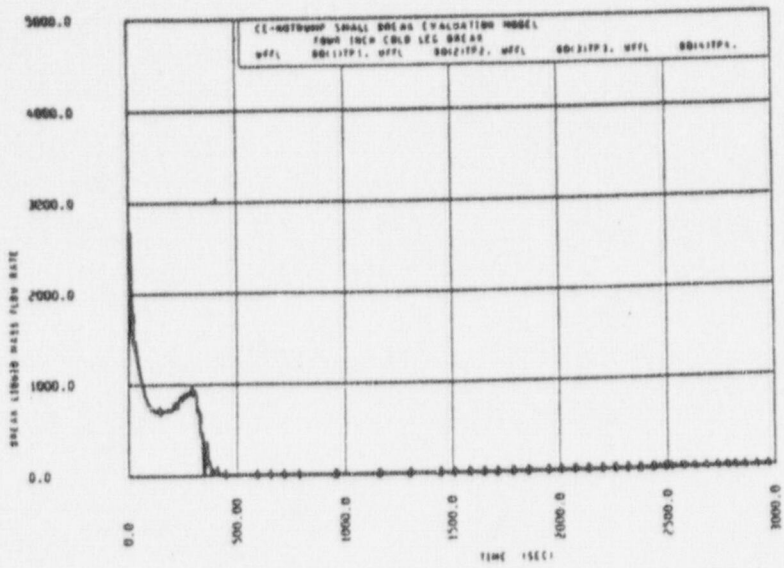


Figure 4-13. Break Liquid Flow for Sample 4-Inch Cold Leg Break

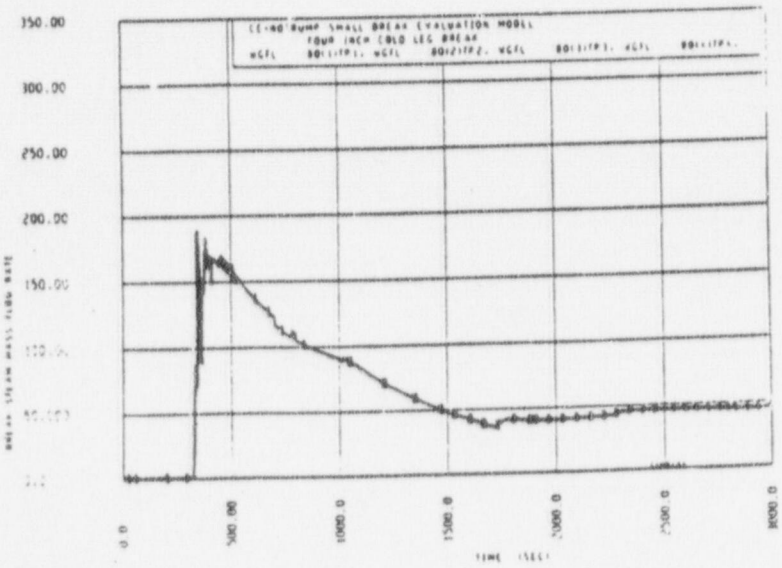


Figure 4-14. Break Steam Flow for Sample 4-Inch Cold Leg Break

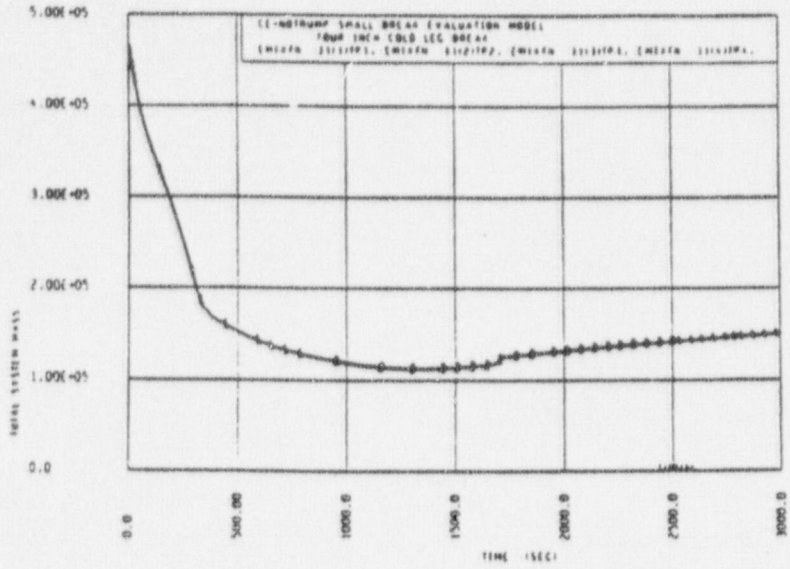


Figure 4-15. Total System Inventory for Sample 4-Inch Cold Leg Break

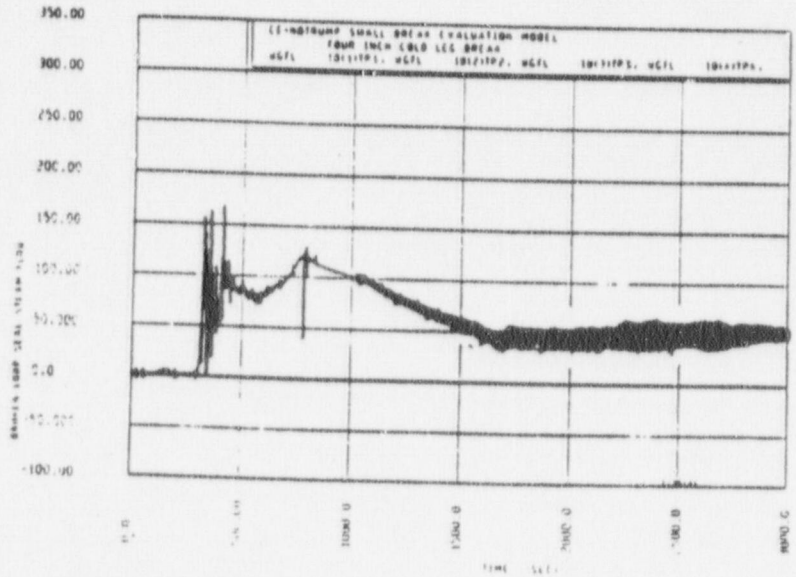


Figure 4-16. Broken Loop Seal Steam Flow for Sample 4-Inch Cold Leg Break

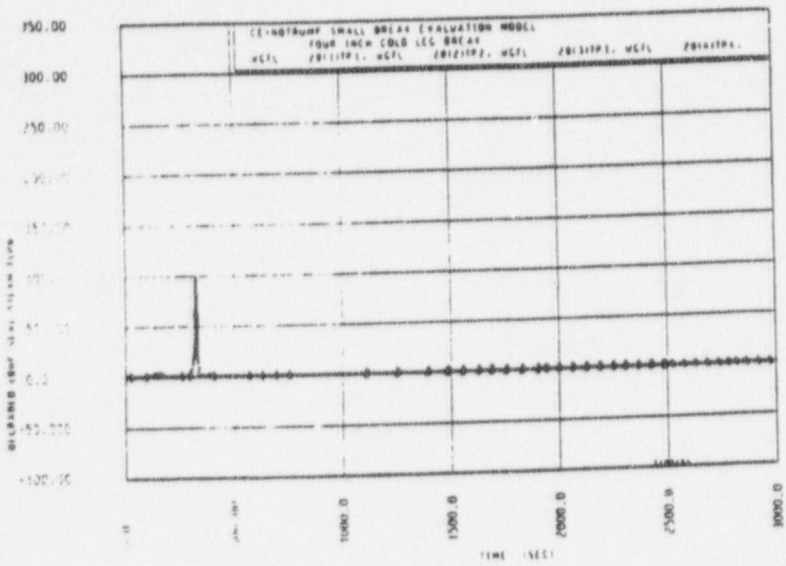


Figure 4-17. Intact Loop Seal Adjacent to Broken Loop Steam Flow for Sample 4-Inch Cold Leg Break

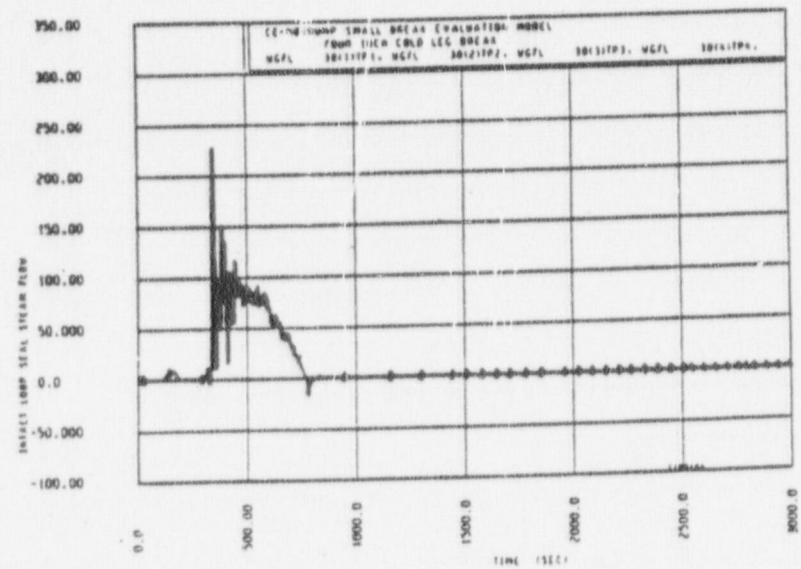


Figure 4-18. Lumped Intact Loop Seal Steam Flow for Sample 4-Inch Cold Leg Break

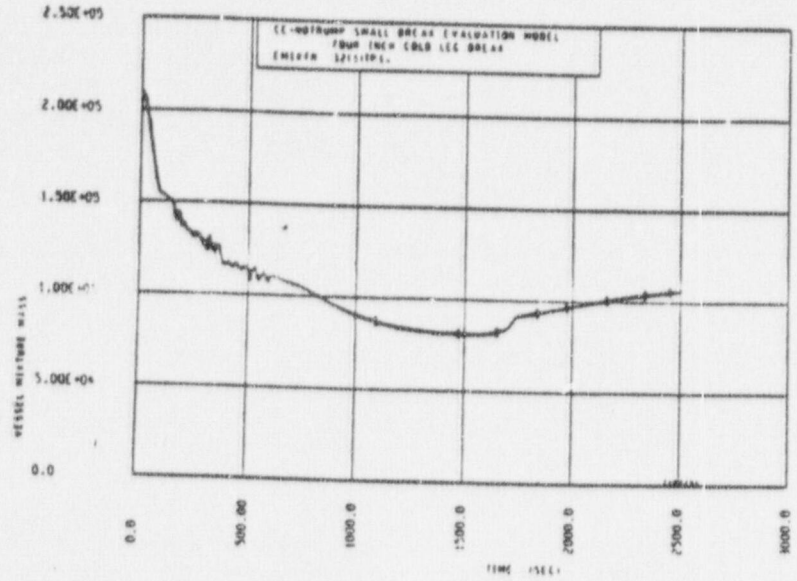


Figure 4-19. Vessel Mixture Mass for Sample 4-Inch Cold Leg Break

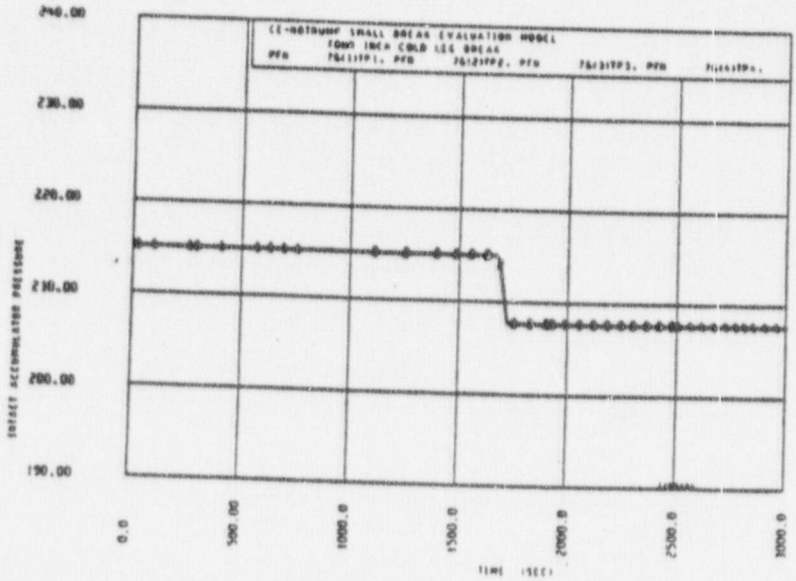


Figure 4-20. Accumulator Pressure for Sample 4-Inch Cold Leg Break

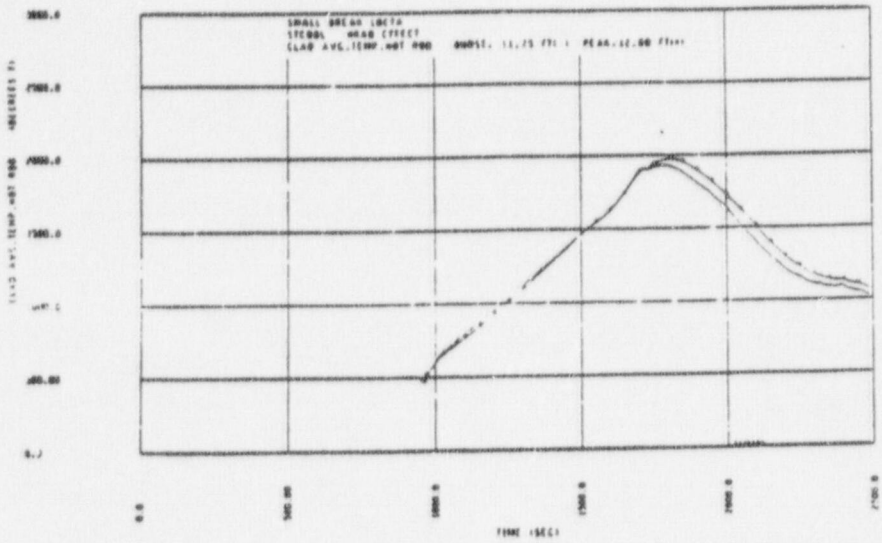


Figure 4-21. Hot Rod Clad Temperature for Sample 4-Inch Cold Leg Break.

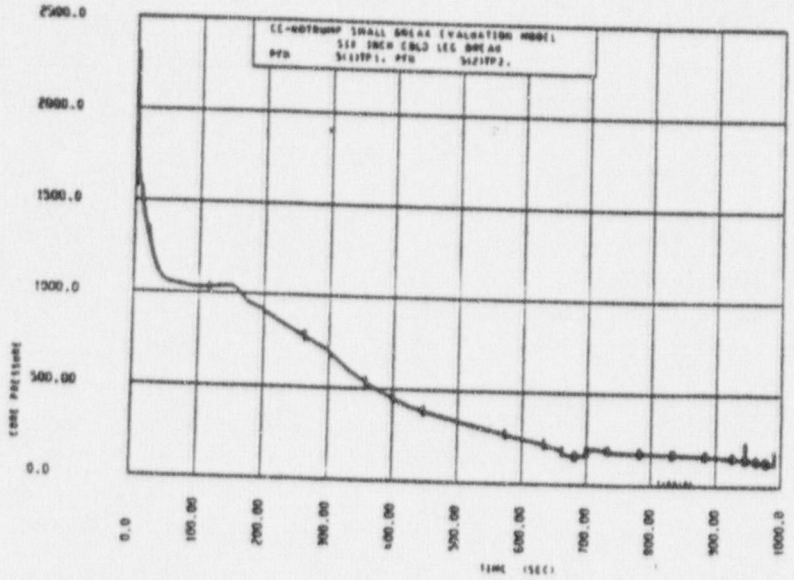


Figure 4-22. Core Pressure for Sample 6-Inch Cold Leg Break

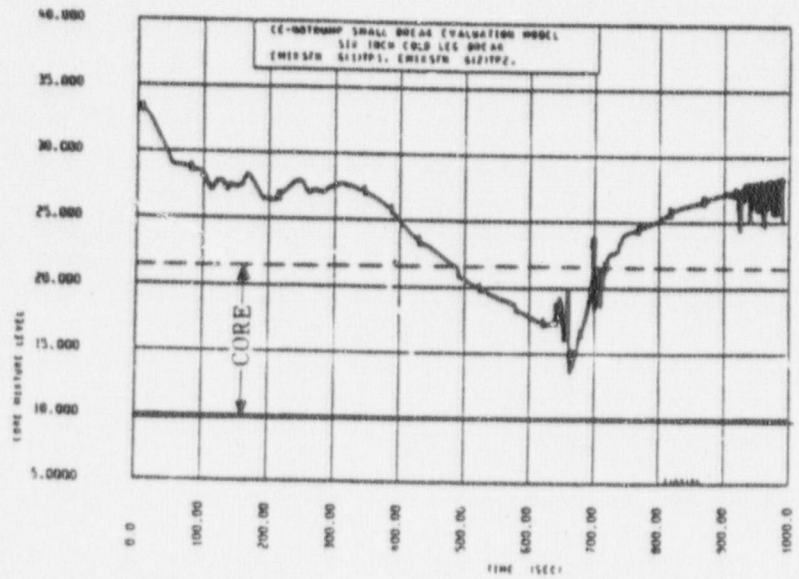


Figure 4-23. Inner Vessel Mixture Level for Sample 6-Inch Cold Leg Break

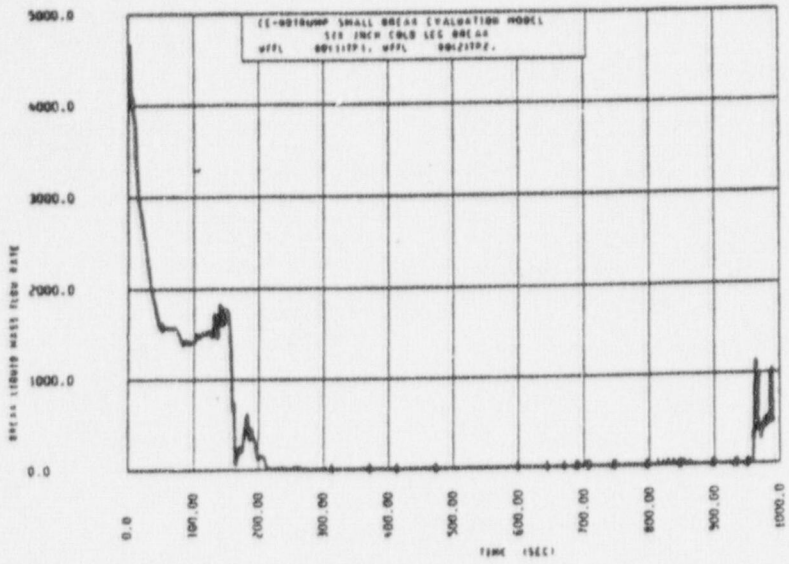


Figure 4-24. Break Liquid Flow for Sample 6-Inch Cold Leg Break

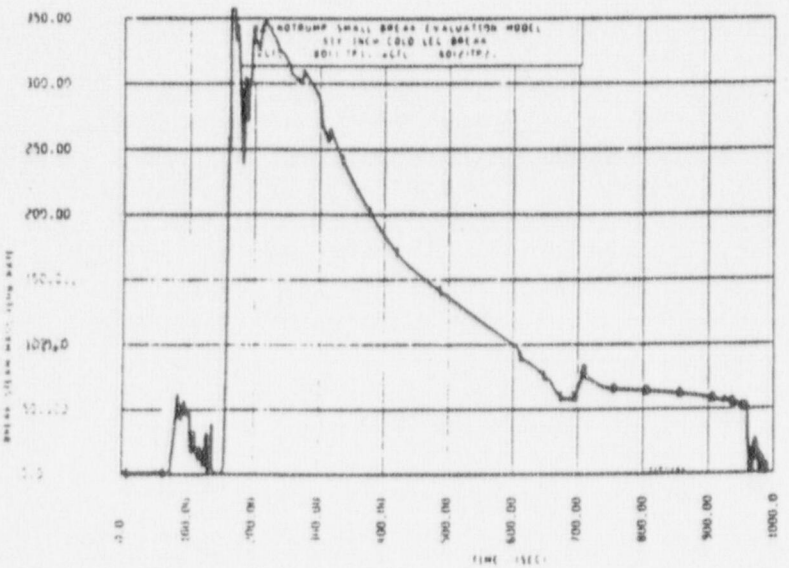


Figure 4-25. Break Steam Flow for Sample 6-Inch Cold Leg Break

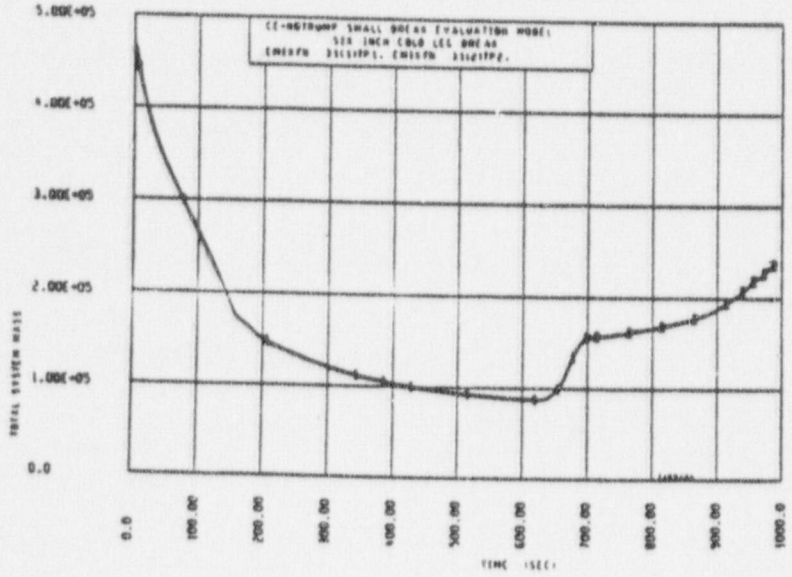


Figure 4-26. Total System Inventory for Sample 6-Inch Cold Leg Break

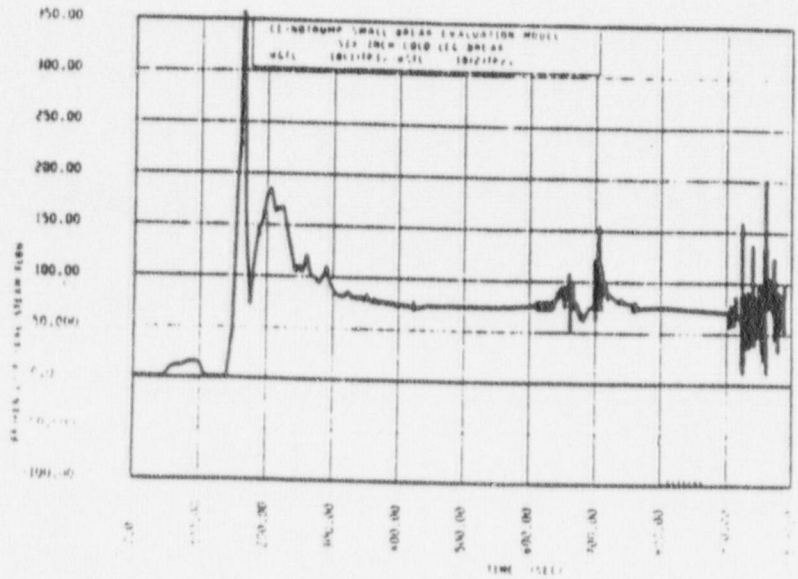


Figure 4-27. Broken Loop Seal Steam Flow for Sample 6-Inch Cold Leg Break

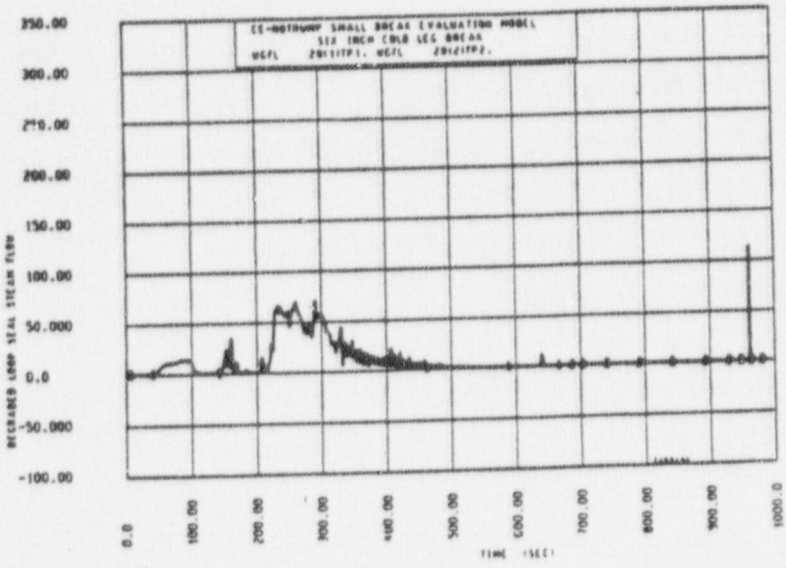


Figure 4-28. Intact Loop Seal Adjacent to Broken Loop Steam Flow for Sample 6-Inch Cold Leg Break

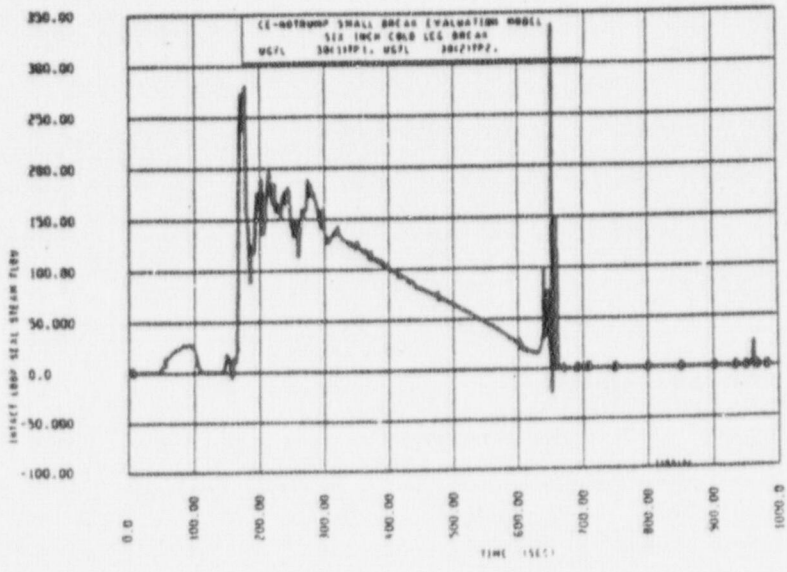


Figure 4-29. Lumped Intact Loop Seal Steam Flow for Sample 6-Inch Cold Leg Break

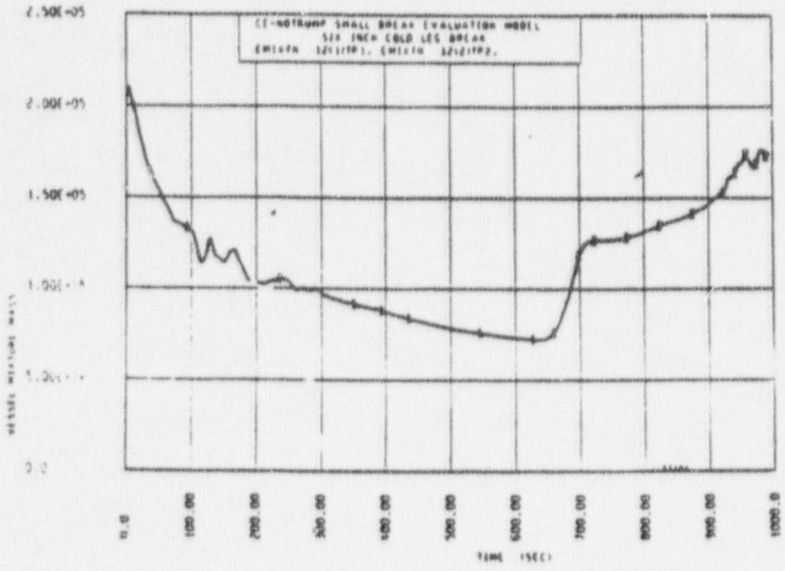


Figure 4-30. Vessel Mixture Mass for Sample 6-Inch Cold Leg Break

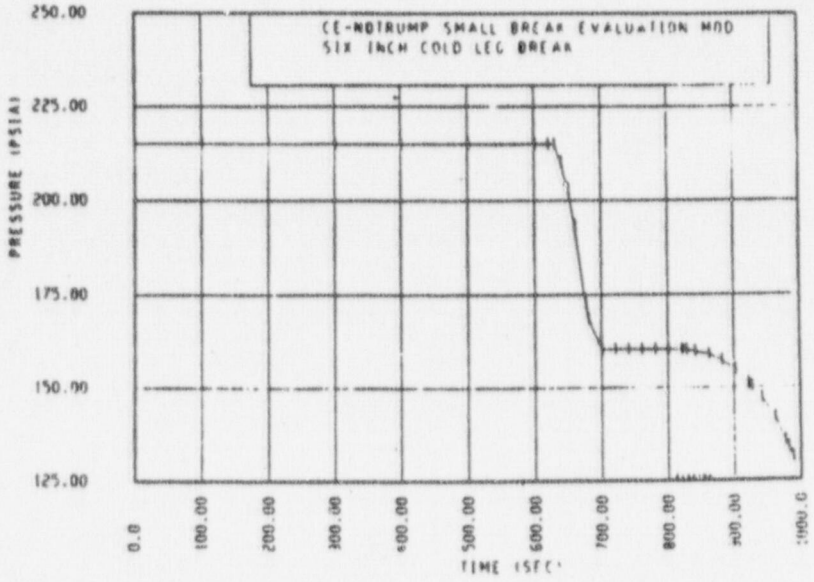


Figure 4-31. Accumulator Pressure for Sample 6-Inch Cold Leg Break

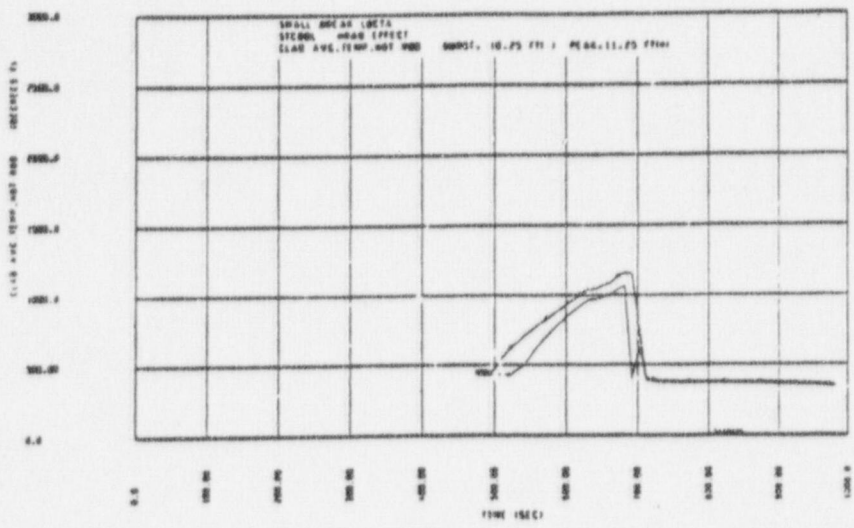


Figure 4-32. Hot Rod Clad Temperature for Sample 6-Inch Cold Leg Break

SECTION 5

SENSITIVITY STUDIES

5.1 Introduction

The purpose of this section is twofold. First, it is the intent of this section to verify that the break spectrum selected in the previous section was for the most limiting set of system breaks. Secondly, this section is also to further demonstrate the use of the Evaluation Model for small break LOCA analysis of the CE NSSS.

Two breaks were selected for this sensitivity study on break location in the CE NSSS. These were the hot leg break and the pump suction leg break. The break sizes for both of these breaks was selected as 4-inch diameter break, since that break size proved to be the most limiting in the cold leg break spectum of the previous section. Since the break location for these cases was not the cold leg, safety injection and accumulator injection to all cold legs was assumed.

5.2 4-Inch Hot Leg Break

The 4-inch hot leg break was postulated to be in the hot leg to which the pressurizer is attached in order to maximize the amount of liquid lost to the break. The results of this break are presented in Figures 5-1 through 5-10. The system rapidly depressurizes and the inner vessel mixture level quickly decreases to the hot leg elevation, as shown in Figures 5-1 and 5-2. Since the break is in the hot leg, it is not necessary to clear a loop seal in order to vent steam to the break. Also, because of the location for this break, more liquid inventory is lost out of the break in comparison to the cold leg break. The break flows are shown in Figures 5-3 and 5-4, and the total system inventory for the hot leg break is presented in Figure 5-5. Recall that in the four inch cold leg break, the loop seals cleared while the hot legs were still partially full, permitting a significant amount of liquid to become trapped there and eventually drain back to the vessel. In the four inch hot leg break however, all liquid above the bottom of the hot leg can flow out the break. As a direct consequence, the 4-inch hot leg

break inner vessel mixture level decreases into the top of the core earlier. While the inner vessel mixture level is decreasing towards the top of the core, some steam vents through the loop seals on the broken side of the plant. The loop seal steam flows are shown in Figures 5-6 through 5-8. Because no safety injection flow is spilled to containment for this break location, the core uncovery is neither as deep nor as prolonged as in the four inch cold leg break case. This can also be observed in the vessel mixture mass behavior in Figure 5-9. The accumulators did not inject for this break. The peak clad temperature occurs while the mixture level is increasing in the core. The peak clad temperature of the hot leg break was found to be significantly lower than that of the cold leg break. The hot rod clad temperature is presented in Figure 5-10.

5.3 4-Inch Pump Suction Leg Break

The 4-inch pump suction leg break was postulated to be at the base of the short vertical section of pipe leading to the inlet of the pump. This location is the lowest possible location in the primary system piping. The results of this break are shown in Figures 5-11 through 5-20. The rapid system depressurization is shown in Figure 5-11, and the inner vessel mixture level in Figure 5-12. Figures 5-13 and 5-14 present the break flows for this break. Figure 5-15 shows the total system inventory. Because the break location is lower in this case, a more noticable mixture level depression prior to sustained loop seal venting occurs. The mixture level depression does not depress the level into the top of the core. When the mixture level depression occurs, the break, which is located in the loop seal uncovers and begins to vent steam to containment. The lumped intact loop seal vents briefly and replugs. The loop seal steam flows are shown in Figures 5-16 through 5-18. The core becomes uncovered in this case at nearly the same time as core uncovery began in the four inch cold leg break. Again, since the break location is not the cold leg, the cold leg on the broken loop receives safety injection. As a result, the depth and duration of the core uncovery in the pump suction leg break is less than that of the 4-inch cold leg break. The vessel mixture mass is presented in Figure 5-19. The system depressurizes to a pressure just slightly higher than the accumulator setpoint, and thus the accumulators do not inject during the recovery period. The peak clad temperature of the pump suction leg break

was found to be much lower than that of the same sized cold leg break. The hot rod clad temperature for this case is shown in Figure 5-20.

5.4 Conclusion

The 4-inch hot leg break and the 4-inch pump suction leg break were analyzed and compared to the same sized break in the cold leg. A comparison of the results is given in Table 5-1. The results identify the cold leg as being the limiting break location for this break size in terms of peak clad temperature.

TABLE 5-1
BREAK LOCATION COMPARISON
Four Inch Diameter Break Size

Event	Break Location: Cold Leg	Hot Leg	Pump Suction
Start	0.0	0.0	0.0
Top of core uncovered (sec)	966	755	978
Accumulator injection begins (sec)	1670	---	---
Peak clad temperature (^{o}F)	1975	1664	1412
Peak clad temperature occurs (sec)	1810	1414	1673
Peak clad temperature location (ft)	11.39	11.39	11.39
Top of core covered (sec)	2815	1910	2330

5.5 Additional Sensitivity Studies

Because of the similarity in the W and CE NSSS designs, [

]^{a,c}

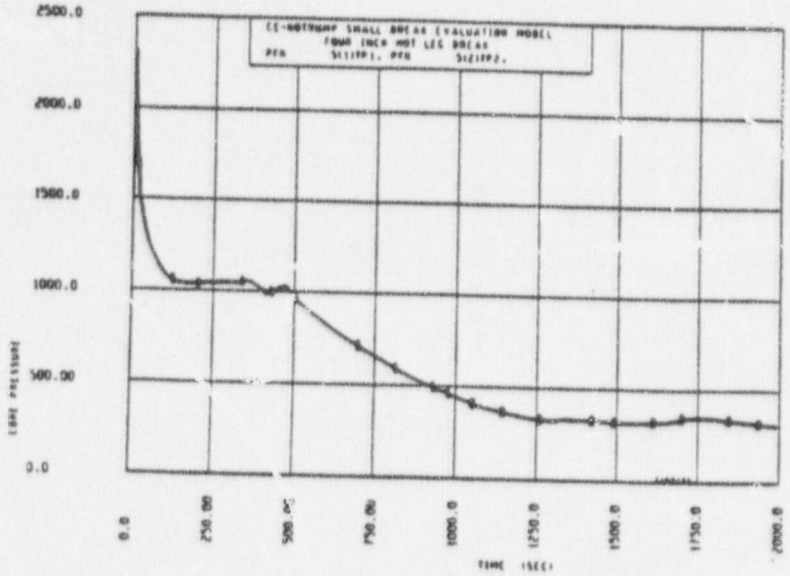


Figure 5-1. Core Pressure for 4-Inch Hot Leg Break

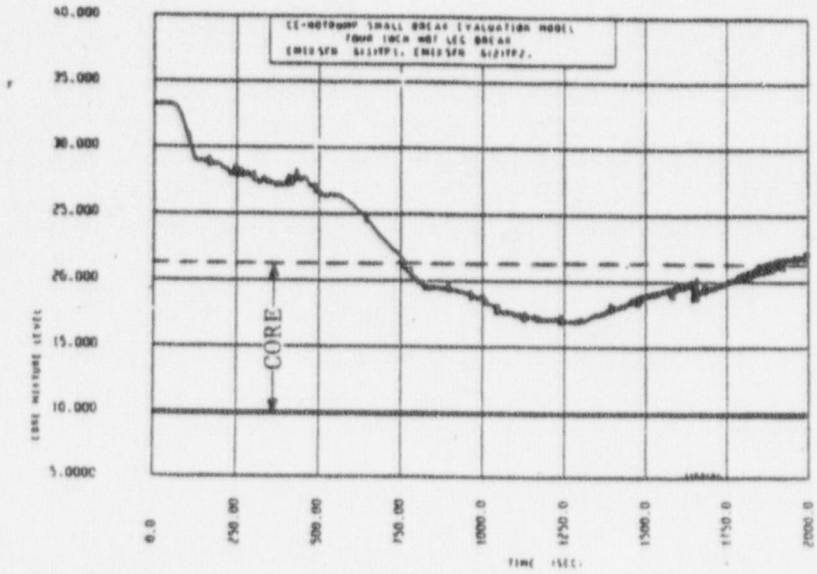


Figure 5-2. Inner Vessel Mixture Level for 4-Inch Hot Leg Break

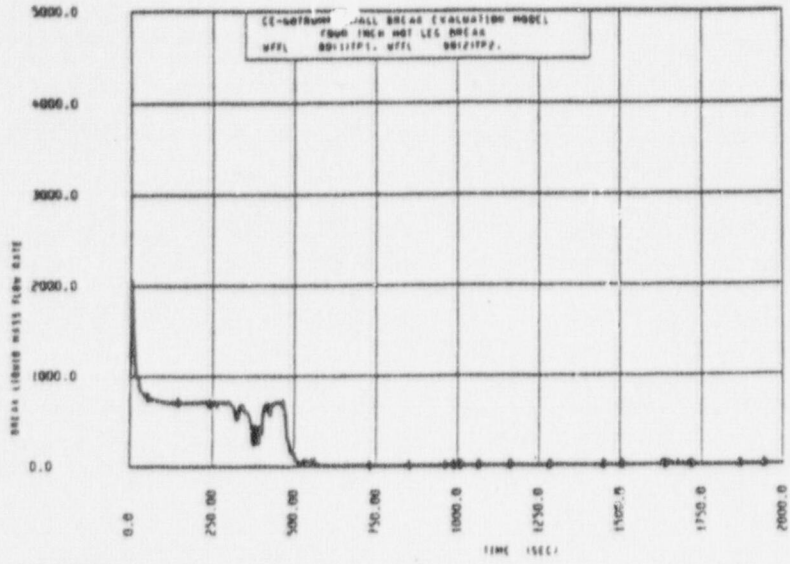


Figure 5-3. Break Liquid Flow for 4-Inch Hot Leg Break

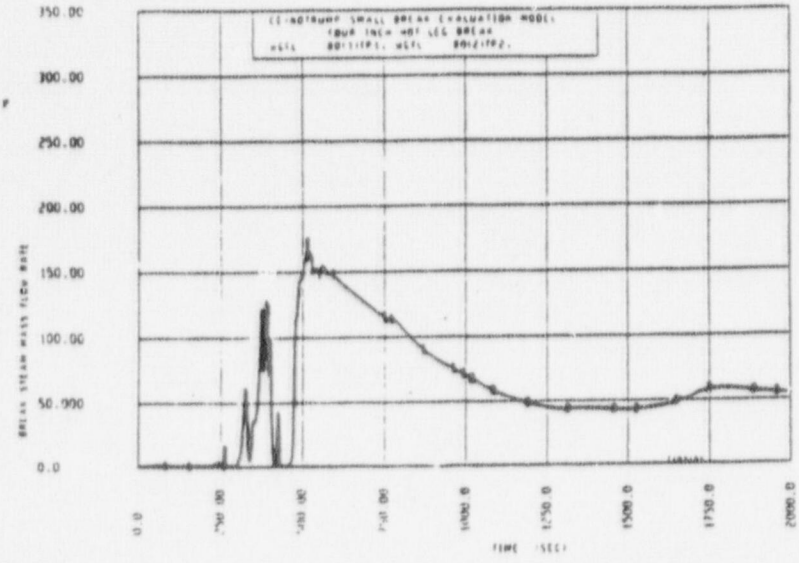


Figure 5-4. Break Steam Flow for 4-Inch Hot Leg Break

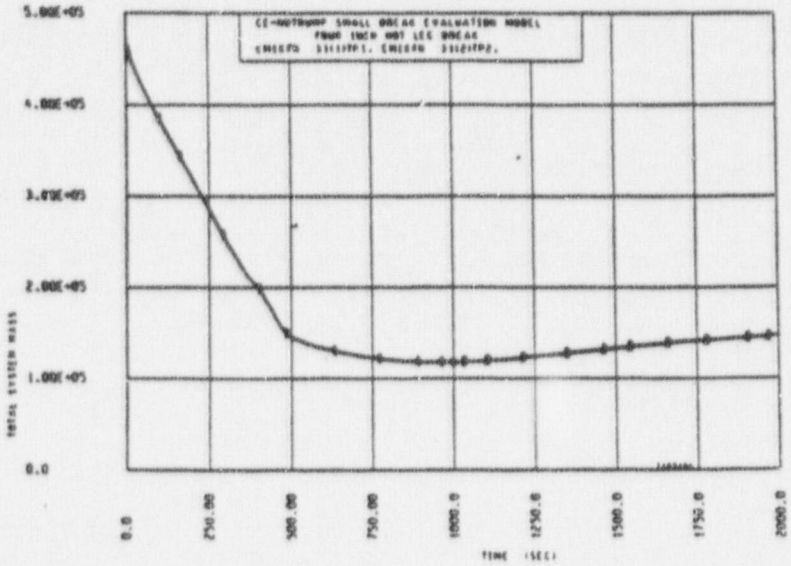


Figure 5-5. Total System Inventory for 4-Inch Hot Leg Break

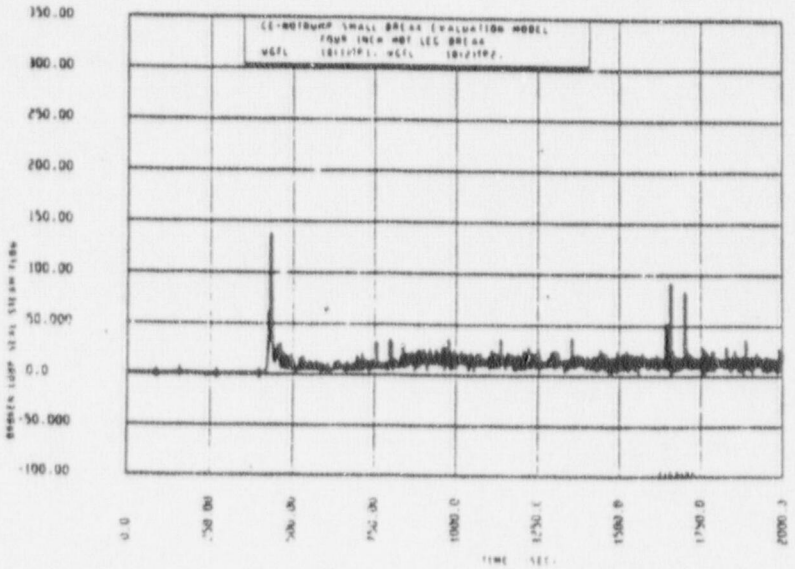


Figure 5-6. Single Intact Loop Seal Steam Flow for 4-Inch Hot Leg Break (Flow Link 18)

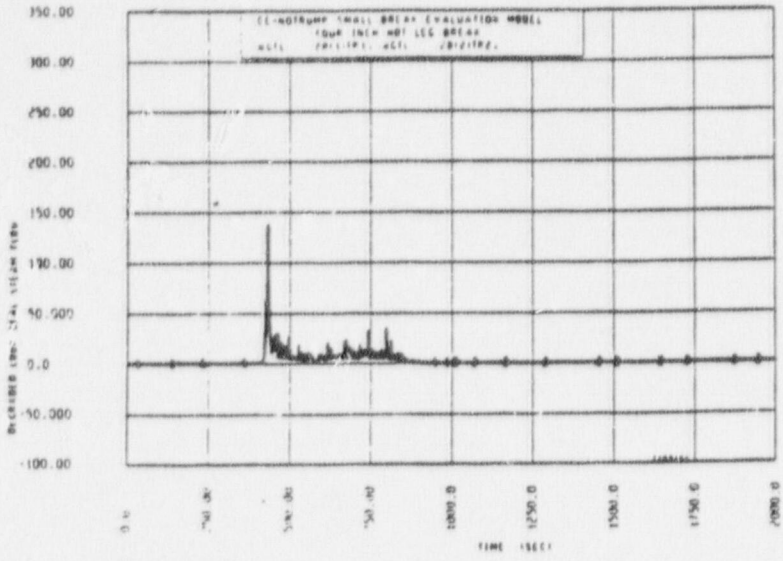


Figure 5-7. Single Intact Loop Seal Steam Flow for 4-Inch Hot Leg Break (Flow Link 28)

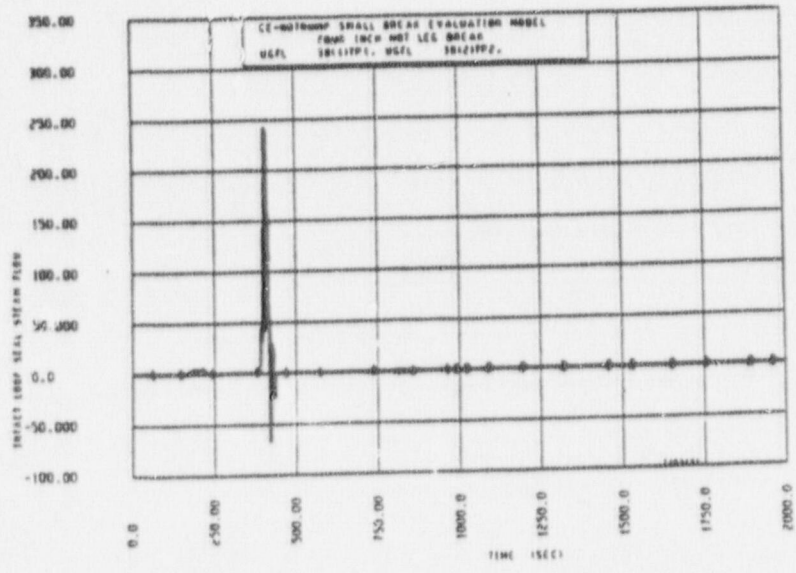


Figure 5-8. Lumped Intact Loop Seal Steam Flow for 4-Inch Hot Leg Break

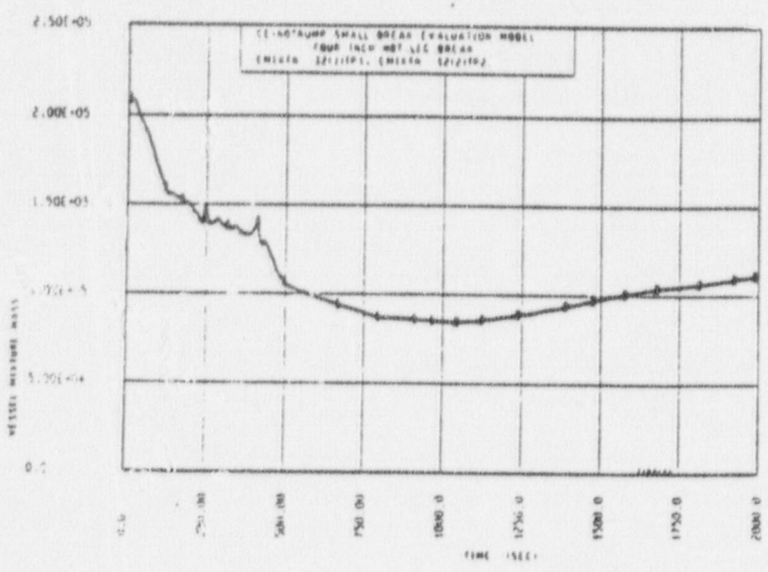


Figure 5-9. Vessel Mixture Mass for 4-Inch Hot Leg Break

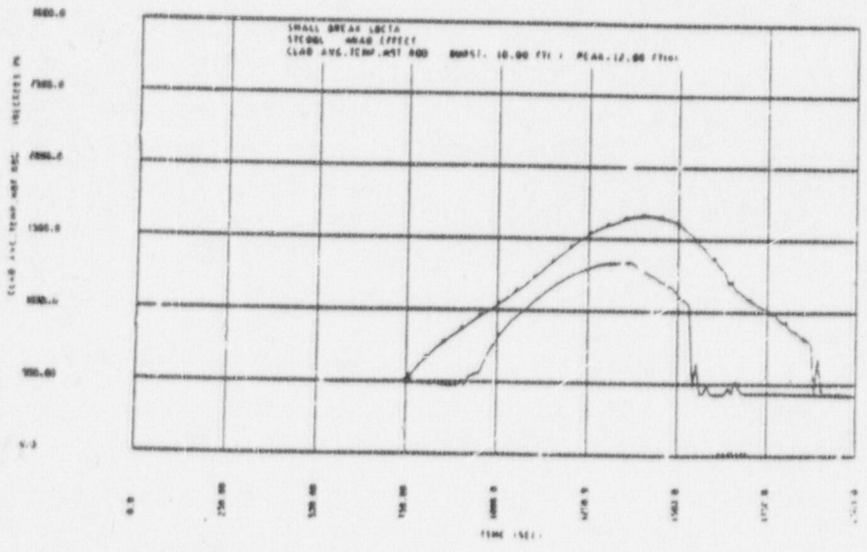


Figure 5-10. Hot Rod Clad Temperature for 4-Inch Hot Leg Break

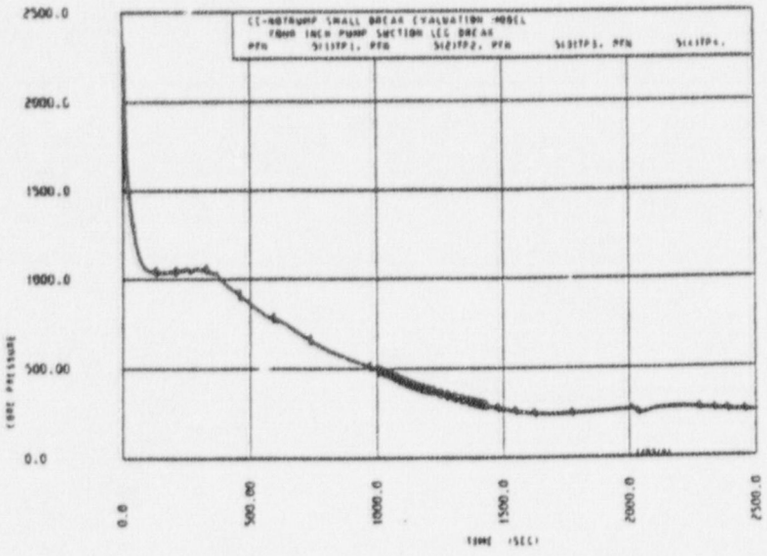


Figure 5-11. Core Pressure for 4-Inch Pump Suction Leg Break

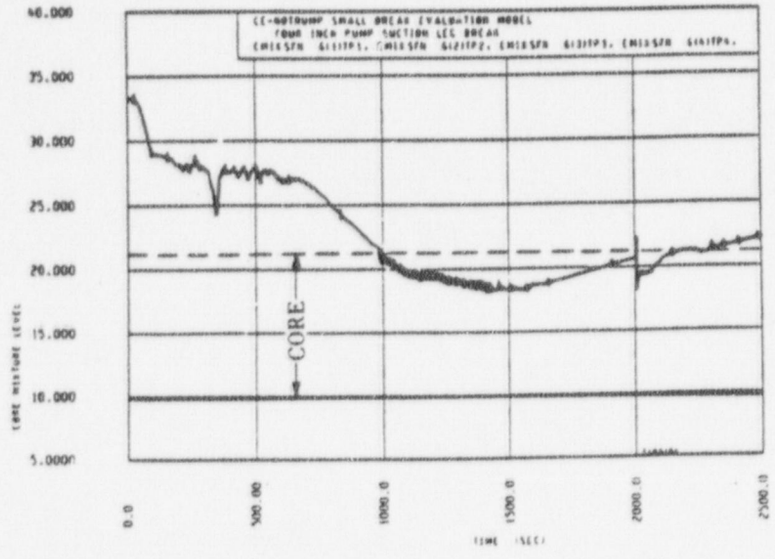


Figure 5-12. Inner Vessel Mixture Level for 4-Inch Pump Suction Leg Break

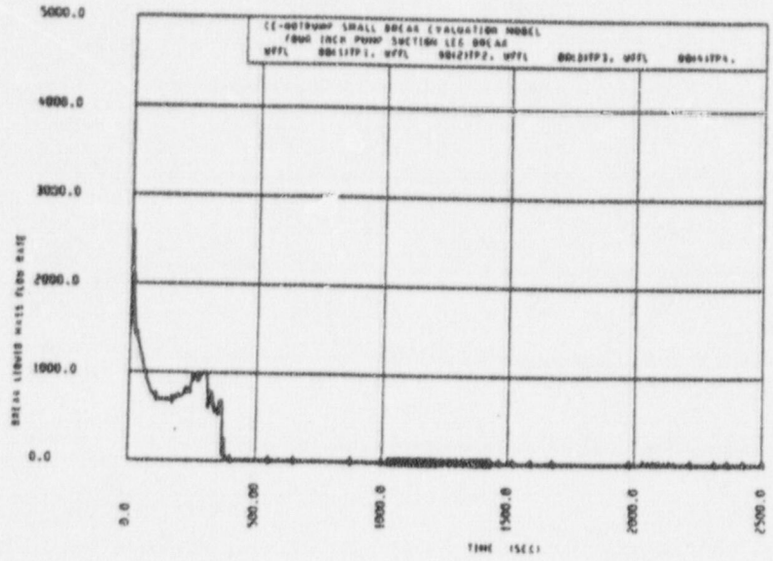


Figure 5-13. Break Liquid Flow for 4-Inch Pump Suction Leg Break

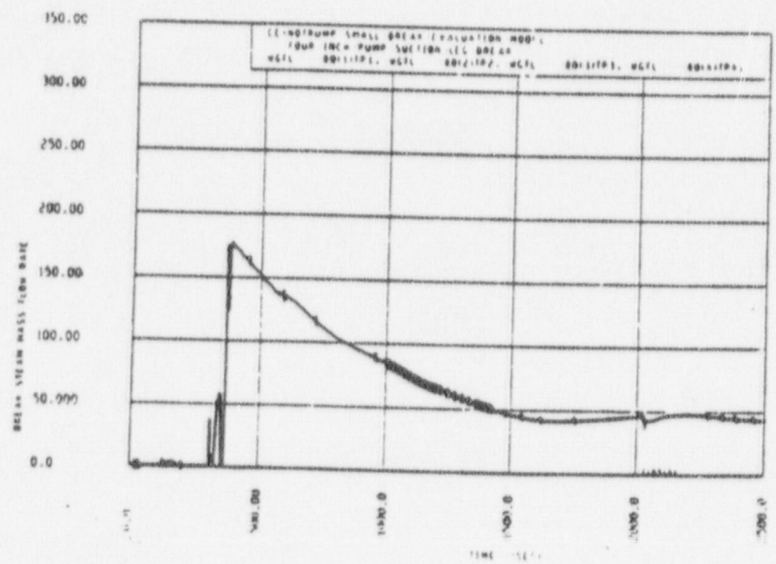


Figure 5-14. Break Steam Flow for 4-Inch Pump Suction Leg Break

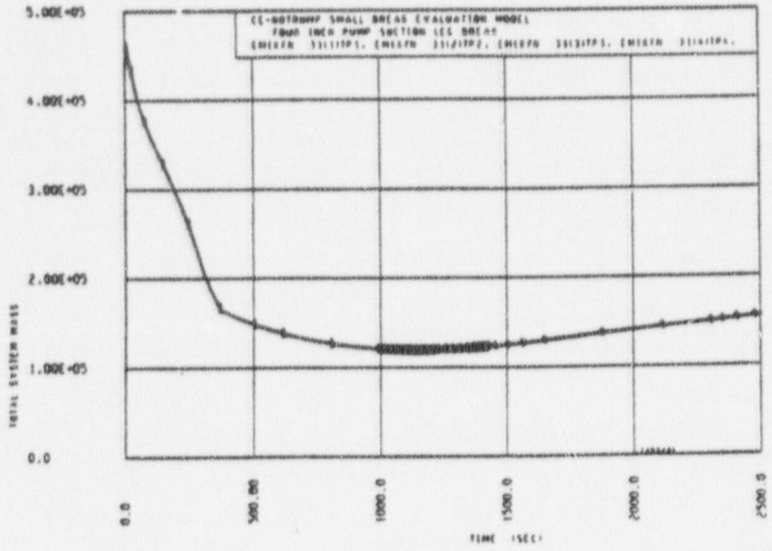


Figure 5-15. Total System Inventory for 4-Inch Pump Suction Leg Break

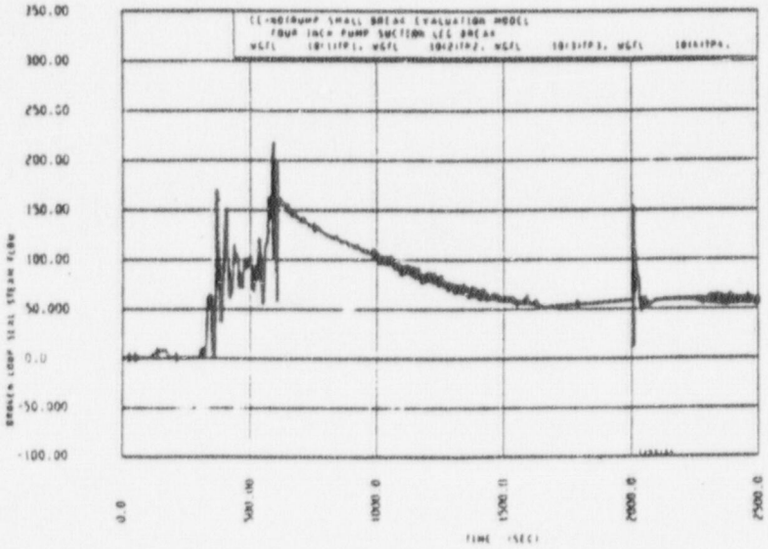


Figure 5-16. Broken Loop Seal Steam Flow for 4-Inch Pump Suction Leg Break

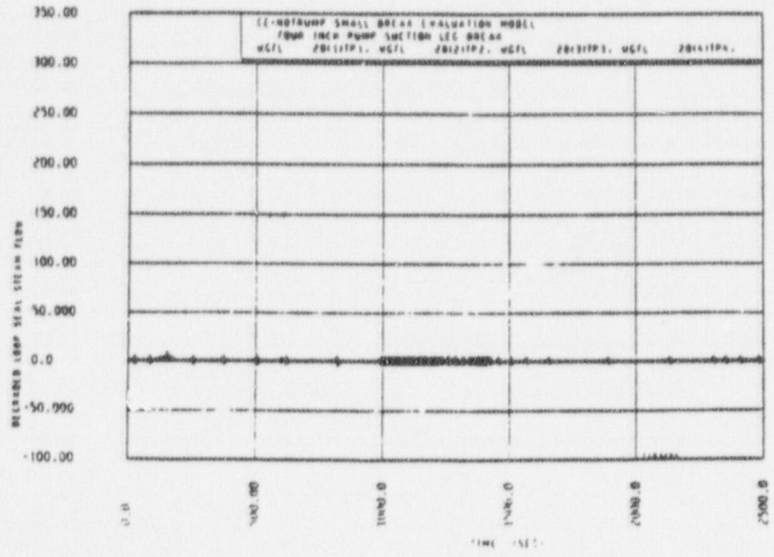


Figure 5-17. Intact Loop Seal Adjacent to Broken Loop Steam Flow for 4-Inch Pump Suction Leg Break

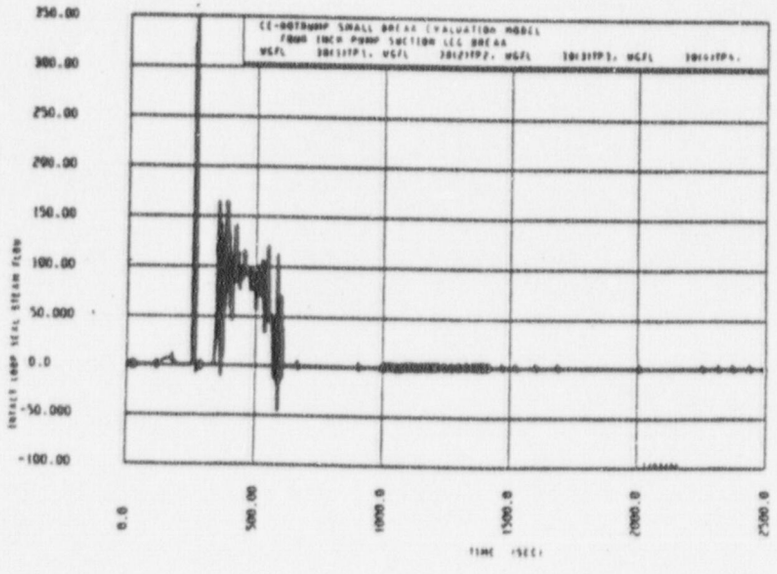


Figure 5-18. Lumped Intact Loop Seal Steam Flow for 4-Inch Pump Suction Leg Break

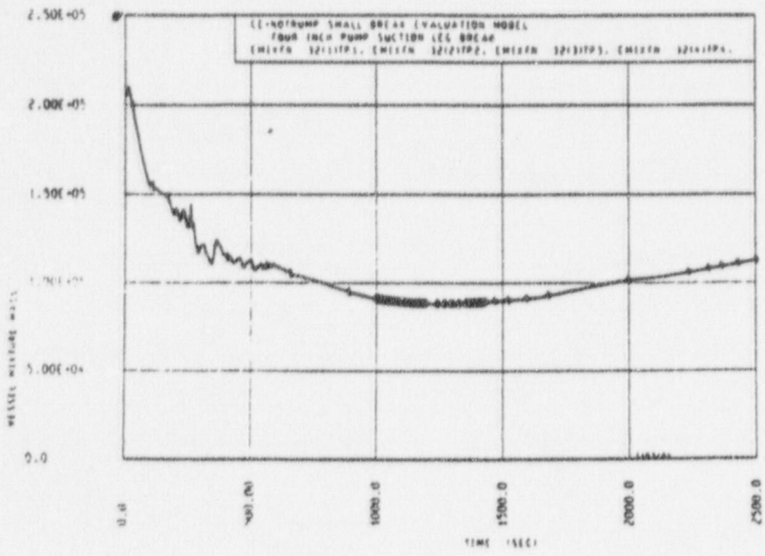


Figure 5-19. Vessel Mixture Mass for 4-Inch Pump Suction Leg Break

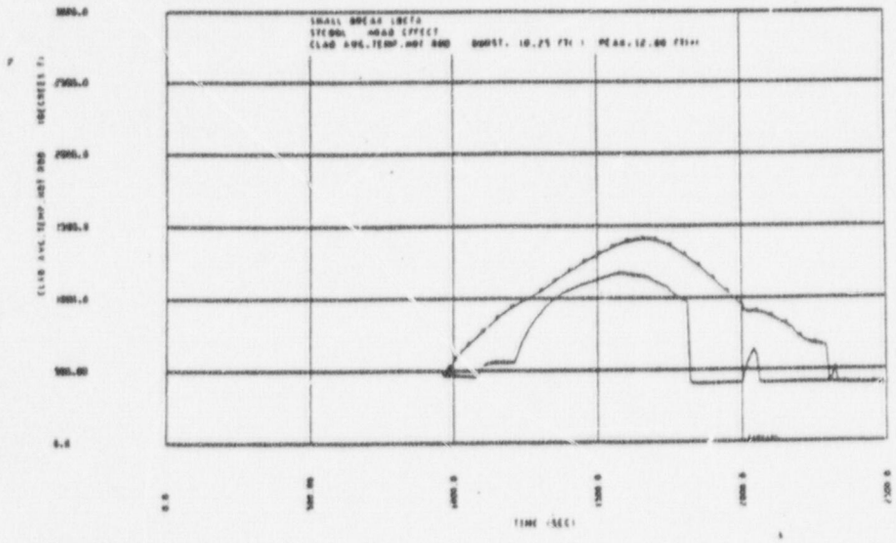


Figure 5-20. Hot Rod Clad Temperature for 4-Inch Pump Suction Leg Break

SECTION 6

CONCLUSION

This report, in conjunction with References 1 -3, has presented the application of the Westinghouse Small Break Evaluation Model using NOTRUMP and LOCTA-IV for Combustion Engineering nuclear steam supply systems. Details of the CE design have been incorporated in this new application and modifications to the application are in compliance with Appendix K of 10CFR50, as well as the requirements of the NRC Action Plan NUREG-0737 II.K.3.30. The model is acceptable for use in Final Safety Analysis Report (FSAR) small break LOCA analysis to demonstrate acceptability of the emergency core cooling system for CE nuclear steam supply systems.

SECTION 7

REFERENCES

[1] Lee, N., Rupprecht, S. D., Shwarz, W. R., Tauche, W. D., "Westinghouse Small Break ECCS Evaluation Model Using the NOTRUMP Code," WCAP-10054-P-A (Propietary) and WCAP-10081-A (Non-Proprietary), August 1985.

[2] Meyer, P. E., "NOTRUMP - A Nodal Transient Small Break and General Network Code," WCAP-10079-P-A (Proprietary) and WCAP-10080-A (Non-Proprietary), August 1985.

[3] Borderlon, F. M., et. al., "LOCTA-IV Program: Loss of Coolant Transient Analysis, WCAP-8305 (Proprietary), June 1974.

[4] Yeh, H. C., et. al., "Heat Transfer Above the Two-Phase Mixture Level Under Core Uncovery Conditions in a 336-Rod Bundle," EPRI-NP-2161, December 1981.

[5] Ferguson, K. L., Kemper, R. M., "ECCS Evaluation Model for Westinghouse Reloads of Combustion Engineering NSSS," WCAP-9528 (Proprietary), June 1979.

APPENDIX A

RESPONSE TO THE NRC REQUEST FOR ADDITIONAL INFORMATION
ON TOPICAL REPORT WCAP-10054, ADDENDUM 1

1. "In Appendix J of WCAP-10079-P-A, the mechanical separator models available in NOTRUMP are described. Discuss how the mechanical separators for the CE plants are modeled in the small break LOCA analysis. Where models based upon the Westinghouse design are used, justify their applicability to the CE design."

Response:

The swirl vane and Peerless vane mechanical separator models, described in Appendix J of WCAP-10079, are based upon the consideration of the physical phenomena, such as the velocity and momentum, of the fluid entering the separator. The models are, by design, general in nature and should be applicable to the CE design with the appropriate values of input to this model.

Currently, the evaluation model used for small break analyses for Westinghouse plants does not use the mechanical separator models. On this basis, the CE small break evaluation does not currently use the mechanical separator models. Should Westinghouse decide to incorporate the mechanical separator models into CE small break LOCA analyses at a later date, justification of their applicability to the CE design will be provided.

2. "Specific noding studies for modeling of the steam generator tubes for the CE plants was not performed; rather, the noding studies for the Westinghouse plant design was used. Because the loop layouts are different between the plants and their impact on the accident may be different, provide specific noding studies for the modeling of the steam generator tubes for the CE plants."

Response:

The advanced heat transfer correlations in the NOTRUMP computer code are regime dependant and span all reasonable heat transfer situations during a small break LOCA. The correlations consider the effects of geometry through the input. The two-phase flow characteristics calculated in the NOTRUMP computer code through the use of state-of-the-art flow regime [ ]^{a,c,e} correlations span all

reasonable single and two-phase flow situations during a small break LOCA. The correlations consider the effects of geometry through the code input. Consequently, the basic heat transfer and fluid flow models available in NOTRUMP are appropriate to the CE design, particularly in the steam generator since the basic CE steam generator design is similar to the Westinghouse design.

Steam generator noding sensitivity studies were performed and documented in WCAP-10054. The sensitivity studies examined the effect of a variation in the noding on the basic heat transfer, fluid flow and flooding effects. More detailed noding showed only small variations in the primary to secondary heat transfer, natural circulation flow rates, and amount of liquid hold up in the steam generator U-tubes. Overall, the simplified noding was shown to be conservative in the peak clad temperature. Westinghouse has examined the design and geometry differences in the CE plants.

The major difference in design which would affect the transient response of a small break LOCA is the hot leg to steam generator inlet plenum geometry. Westinghouse uses a [

]^{a,c,e} WCAP-10054, Addendum 1 documents a detailed evaluation of the applicability of the Westinghouse [ ]^{a,c,e} correlation to the CE design. Sensitivity studies to a [ ]^{a,c,e} were also performed and documented in WCAP-10054, Addendum 1.

Westinghouse has concluded that there are no other differences in the basic design which affect the fundamental phenomena associated with a small break LOCA which would invalidate the previous noding sensitivity study conclusions.

3. "The accumulator polytropic expansion coefficient utilized in NOTRUMP is based on the accumulator blowdown test performed at the Callaway site in 1982. For CE plants with accumulators with a 600 psig initial backfill, this coefficient appears to be appropriate. The staff notes that the Callaway test is not appropriate for the 200 psig accumulators as the tests show a temperature differential between the accumulator wall and the nitrogen gas as well as an inappropriate water to gas volume ratio. Provide additional justification for the expansion coefficient used for the 200 psig accumulators."

Response:

In addition to the Callaway test results, a sensitivity study was performed by [ ]^{a,c,e} the polytropic expansion

coefficient for the Westinghouse small break evaluation model using NOTRUMP at an initial accumulator backfill of 600 psig. From this sensitivity it was shown that there was [ ]^{a,c,e} on results by [ ]^{a,c,e} the polytropic expansion coefficient. Even though some CE plants have accumulators at an initial backfill of 200 psig, the sensitivity study for the expansion coefficient can be used to demonstrate that the accumulator polytropic expansion coefficient used in the CE small break evaluation model is conservative for Appendix K analyses.

4. "The sample small break spectrum analysis provided in Section 4 is sufficient to demonstrate the performance of the generic model. However, since these analyses have only been performed for a single CE plant, it is the staff's position that these analyses are not sufficient to provide compliance with Section C.1 of Appendix K for all CE plants. The staff has tentatively concluded that if these analyses are referenced by a licensee with a CE plant as its spectrum analysis, the licensee should demonstrate that the input assumptions utilized are appropriate for that plant. If you believe there are reasons why this should not be the case, please provide the information necessary to support an alternate position."

Response:

It is recognized, that the work performed in WCAP-10054, Addendum 1 is based on the CE plant at Millstone 2. Currently, Millstone 2 is the only plant referencing WCAP-10054, Addendum 1 to identify the limiting small break. Analyses performed in the future for a licensee with a CE plant will analysis a representative spectrum of small breaks to identify the limiting small break.

5. "For the specific plant analyzed in Section 4, it was concluded that the four-inch line break was the worst case break. The staff notes that the brief accumulator injection which occurred for that break increased the core mixture level approximately 1-1/2 feet and terminated the cladding temperature rise. It appears that a slightly smaller break, which would not result in accumulator actuation, could result in a initial inventory loss and a higher cladding temperature due to the lack of the accumulator injection. Provide additional justification, or an analysis of the slightly smaller break, to support the conclusion in the maximum cladding temperature."

Response:

The choice of the break spectrum for Combustion Engineering designed plants has evolved from the vast Westinghouse experience with small break LOCA thermal- hydraulic transient

phenomena and the detailed analysis calculations of the plant response. The transient response determines the limiting break size. The physical phenomena governing the transient response of a Combustion Engineering plant is fundamentally the same as in a Westinghouse designed plant. The competing effects of the rate of RCS depressurization, as governed by the mass inventory depletion through the break with the decay heat removal processes, and the emergency core cooling system response, will determine the limiting break. The limiting small break size choice is determined from the evaluation of the Millstone Unit 2 transient analysis results.

10 CFR 50.46 requires that 'ECCS cooling performance shall be calculated in accordance with an acceptable evaluation model, and shall be calculated for a number of postulated loss of coolant accidents of different sizes, locations, and other properties sufficient to provide assurance that the entire spectrum of postulated loss of coolant accidents is covered.' Currently, for small break loss of coolant accidents, the spectrum of breaks to be analyzed per Westinghouse methodology consists of standard break sizes of 2, 3, 4, 6 and 8 inch diameter breaks.

Specifically in WCAP-10054, Addendum 1, a 3, 4, and 6 inch diameter pump discharge break was analyzed using Millstone 2 as the CE-plant. From these results it was shown that the peak clad temperature was bounded between a diameter of 3 and 6 inches, and a discrete break diameter of 4 inches produced the limiting peak clad temperature. It does appear that the limiting break size would be the largest break in which the clad temperature excursion would be terminated by safety injection flow alone. However, recent Westinghouse small break LOCA analyses have shown that, even with accumulator injection, a larger break resulting in [

]^{a,c,e}. This is particularly true for the Millstone Unit 2 analysis with the non-equilibrium NOTRUMP computer code. While an equilibrium model of accumulator injection during a small break LOCA may result in massive amounts of accumulator injection due to local depressurization, the NOTRUMP non-equilibrium model will realistically calculate the amount of accumulator injection appropriate to the local conditions. On the basis of the current methodology used by Westinghouse, a spectrum of break sizes was analyzed for the generic CE plant to assure the worst break size has been identified.

The dominating factors in determining whether or not accumulator actuation will occur in a small break loss of coolant accident are the accumulator backpressure and the pressure transient of the associated small break. For a Combustion Engineering plant with an accumulator backpressure of 215 psia, the determination of accumulator injection could be important in terminating the clad heatup. For instance, in WCAP-10054, Addendum 1, the 4 inch diameter pump discharge break does have accumulator actuation at 1670 seconds with the peak clad temperature occurring at 1810 seconds. On the other hand, in WCAP-10054, Addendum 1, the 3 inch diameter pump discharge break does not have accumulator actuation with the peak clad temperature occurring at 2275 seconds. From these two small break cases performed in WCAP-10054, Addendum 1, it is conceivable that there could be a break size between the 3 and 4 inch break sizes that will depressurize to a point just above the accumulator injection cover gas pressure.

System pressure, core power, core mixture level, and core steam flow are the important parameters that go into the calculation of the clad heatup. So to better understand what could happen for a break between 3 and 4 inches in diameter without accumulator actuation, these parameters will be investigated in detail.

First, to determine the break diameter at which the pressure of the reactor coolant system will stay above the accumulator backpressure, the pressure transient for the proposed break size must level off at a pressure just above 215 psia. The pressure transient for the 3 inch break in WCAP-10054, Addendum 1 levels off at a pressure of about [ ]^{a,c,e}, while the pressure transient for the 4 inch break, right before accumulator injection, is decreasing at a rate of [ ]^{a,c,e} as can be seen in Figure A-1 (for Figures A-1 to A-8, the 4 inch curves are plotted up to accumulator injection). For the 3 inch break between 1200 to 2300 the rate of decrease is about [ ]^{a,c,e}. The rate of decrease for the 3 inch break does not slow down until about [ ]^{a,c,e}.

For the proposed break size the pressure transient would follow a [ ]^{a,c,e} pressure transient and level off at 215 psia [ ]^{a,c,e}. At [ ]^{a,c,e} for the 3 inch the pressure is [ ]^{a,c,e}. A pressure transient curve for the proposed break will be generated by [ ]^{a,c,e}. The dashed line in Figure A-1 is this curve. At [ ]^{a,c,e} there is enough information at the 3 and 4 inch pressure transients to interpolate a proposed break size for the new pressure curve.

At [ ]^{a,c,e} the pressure for the 3 inch break is [ ]^{a,c,e} and the pressure for the 4 inch break is [ ]^{a,c,e}. Subtracting [ ]^{a,c,e} for the new proposed break curve at [ ]^{a,c,e}. By interpolation between the 3 and 4 inch breaks a new proposed break diameter of [ ]^{a,c,e} is estimated to be the break size where accumulator actuation will not occur.

Using Figure A-2 a new core uncovery time can be estimated for a [ ]^{a,c,e} break, using a core uncovery time of 1576 seconds for the 3 inch break and 966 seconds for the 4 inch break. For the [ ]^{a,c,e} break an estimated core uncovery time of [ ]^{a,c,e}. Core steam flow is used in the clad heatup calculation after core uncovery and from Figure A-3 the core steam flows, after core uncovery, are similar for the 3 and 4 inch breaks with the 3 inch break case having [ ]^{a,c,e} steam flows. For instance, [ ]^{a,c,e} after core uncovery the steam flow for the 3 inch break is [ ]^{a,c,e} while the steam flow for the 4 inch break, [ ]^{a,c,e} after core uncovery is [ ]^{a,c,e}. Table A-2 gives the Fraction of core power for each break. The core power in the 3 inch break at core uncovery is [ ]^{a,c,e} than the core power of the 4 inch break at core uncovery.

Other key parameters effecting the transient that will be looked at are break flow, vessel liquid mass, and total system mass. Figures A-4 and A-5 are a comparison of the break flows for the 3 and 4 inch breaks. Late in the transient the pressure in the 3 inch break case is [ ]^{a,c,e} than the 4 inch case, which results in [ ]^{a,c,e} steam flow for the 3 inch break as seen in Figure A-4. So the [ ]^{a,c,e} break will result in a [ ]^{a,c,e} than the 3 inch break case at the time of peak clad temperature.

A very important observation in the 4 inch break is the vessel liquid mass and the total system mass have [ ]^{a,c,e} with the core mixture elevation [ ]^{a,c,e}. So by using the minimum mass values from the 3 and 4 inch breaks, an estimated minimum vessel mass and a minimum total system mass for the proposed break size of [ ]^{a,c,e} can be determined. For the vessel liquid mass the minimum mass for the 3 inch break is [ ]^{a,c,e}, and [ ]^{a,c,e} for the 4 inch break. An estimated minimum vessel mass of [ ]^{a,c,e} is

calculated for the proposed [ ]a,c,e break as seen in Figure A-6. For the total system mass, the minimum mass is [ ]a,c,e for the 3 inch break, and [ ]a,c,e for the 4 inch break. An estimated minimum total system mass of [ ]a,c,e is calculated for the [ ]a,c,e break.

For the core mixture level, the minimum core mixture elevation for the 3 inch break is [ ]a,c,e, and [ ]a,c,e for the 4 inch break. An estimated minimum core mixture level of [ ]a,c,e is calculated for the proposed break size of [ ]a,c,e as can be seen in Figure A-2.

Now an estimate of the clad heatup can be performed for the proposed break size of [ ]a,c,e. For the first [ ]a,c,e of core uncovery, the heatup rate of the fuel clad is [ ]a,c,e for the 4 inch break, and for the first [ ]a,c,e of core uncovery, the clad heatup is [ ]a,c,e for the 3 inch break. Between 1000 to 1600 seconds the clad heatup rate for the 4 inch break is [ ]a,c,e, and between 1610 to 1900 seconds for the 3 inch break the clad heatup rate is [ ]a,c,e. The cladding heatup rate for a postulated [ ]a,c,e break will be lower than the 4-inch case, but higher than the 3-inch case. For conservatism, the cladding heatup rate for the [ ]a,c,e case may be used to estimate the cladding heatup, even though the core power will be [ ]a,c,e break because of the [ ]a,c,e than the [ ]a,c,e break heatup rates, the heatup rates for the [ ]a,c,e case will be used to generate a clad temperature curve from core uncovery to 1900 seconds for the proposed [ ]a,c,e break. From [ ]a,c,e a heatup rate of [ ]a,c,e will be used and from 1300 seconds to 1900 seconds a clad heatup rate of [ ]a,c,e will be used, resulting in a clad temperature of [ ]a,c,e. For the seconds for the proposed [ ]a,c,e break clad temperature curve from 1900 seconds to time of peak clad temperature, the [ ]a,c,e clad heatup rate information will be used to estimate the clad temperature, since the minimum mixture level has been [ ]a,c,e and the system mass and mixture level will be [ ]a,c,e. The time of peak clad temperature will be assumed as the [ ]a,c,e. This is a conservative assumption since it is shown that the minimum vessel mass, the minimum total mass and the core mixture level [ ]a,c,e, and the time of minimum mass and minimum mixture level have a definite effect on the time of peak clad temperature.

At 1900 seconds the clad temperature for the 3 inch break is [ ]^{a,c,e} between the proposed [ ]^{a,c,e} break and the 3 inch break. Adding the difference of [ ]^{a,c,e} to the 3 inch peak clad temperature of 1301.5°F gives an estimated peak clad temperature of [ ]^{a,c,e} for the proposed break size of [ ]^{a,c,e} diameter pump discharge break without accumulator actuation as seen in Figure A-8.

From this evaluation it is shown that the proposed break without accumulator injection is bounded by the 3 and 4 inch breaks and the worst break case has been identified for the generic CE plant in compliance with 10 CFR 50.46.

6. "WCAP-10054, Addendum 1 was provided to demonstrate compliance of the NOTRUMP code, as modified, to TMI Action Item II.K.3.30 of NUREG-0737 for the CE plants. NUREG-0635 documents the staff's concerns with respect to small break LOCA analyses for CE plants. Based upon the review of these documents, information on the following concerns in NUREG-0635 is requested:"

   a. "Address the effects of noncondensible gases on condensation heat transfer for CE plants."

   b. "Confirm that adequate accounting of stored energy (heat) within the primary system metal structures are included in the CE plant model."

   c. "Validate the acceptability of applying a 1.0 discharge coefficient on both the subcooled and saturated break flow models."

Response to 6.a:

In WCAP-10054-P-A, Section 3-4-10 discusses the effect of non-condensible gases on a small break LOCA. The effects on CE plant response via heat transfer would be the same.

Response to 6.b:

WCAP-10079-P-A, Section 6 discusses the interaction of the metal with the fluid in NOTRUMP. Through the appropriate inputs, the following components are modeled with respect to metal heat. Metal [ ]^{a,c,e} is currently being modeled for CE plants in the small break evaluation model using NOTRUMP. In WCAP-10054-P-A, Section 7 is a comparison of calculated results from NOTRUMP to LOFT and Semiscale simulation test data. The studies show appropriate steam flashing, metal heat and fluid enthalpy distribution. On this basis the metal heat is adequately accounted for in the current evaluation model used for CE plants.

Response to 6.c:

The NOTRUMP small break LOCA ECCS evaluation model uses a [ ]^{a,c,e} correlation for the subcooled stagnation state and the Moody correlation for the saturated stagnation state to calculate the mass discharge through the break. The critical mass discharge rate is determined by the fluid conditions in the approach region to the break and by the break geometry. The parameters used to characterize the fluid conditions in the approach region to the break are

1. The fluid pressure,
2. The fluid temperature,and
3. The fluid state (subcooled, two-phase, all steam).

The NOTRUMP model explicitly includes the effect of the fluid conditions in the critical mass discharge flow calculations but does not explicitly account for variations in the break geometry. The effect of the break geometry may be represented by the use of a discharge coefficient.

The break geometry influences the critical flow rate in part by the degree of fluid metastability or nonequilibrium that exists at the exit plane of the critical flow section. Geometric configurations that enhance the degree of nonequilibrium cause higher critical flow rates. Three factors exert a major influence on fluid conditions at the break, namely;

1. The approach region configuration; sharp edged versus rounded entrance,
2. The flow passage diameter, and
3. The flow passage length.

A break geometry with a rounded entrance and a small flow path length would result in the most metastable fluid condition at the exit plane. Other break geometries would exhibit lower critical flow rates.

Review of the NOTRUMP small LOCA break flow model as applied to evaluation model analysis calculations reveals that the break effluent is predominantly either subcooled liquid or all steam. There is only a breif period of two-phase flow for the limiting cold leg small break LOCAs. Maximazation of the amount of subcooled break flow during a small break transient leads to the most conservative prediction of peak cladding temperature for a given break size since it results in the greatest system mass inventory depletion. The uncertainty in the subcooled break discharge model and the sensitivity to a discharge coefficient on subcooled break flow is addressed in references A-1 and A-2. The conclusions of those studies are valid for the NOTRUMP small break LOCA ECCS evaluation model.

Furthermore, there is very little uncertainty associated with the prediction of all steam critical discharge mass flow. The Moody model with a discharge coefficient of 1.0 provides a best estimate of the critical discharge flow rate when the flow is all steam. Calculations of the discharge rate do not vary appreciably between the homogeneous equilibrium model (HEM), the Henry-Fauske model (HF), or the Moody model when the break flow is all steam. This is summarized in table A-1 which presents the ratio of the HEM break mass flux to the Moody break mass flux and the ratio of the Henry-Fauske break mass flux to the Moody break mass flux for various pressures.

TABLE A-1

All Steam Break Flow Model Comparisons

Pressure (psia)	G_{HEM}/G_{Moody}	G_{HF}/G_{Moody}
600	[	] a,c,e
800		
1000		
1400		

In conclusion, the NOTRUMP small break LOCA evaluation model break flow calculation is appropriate. A discharge coefficient of 1.0 used with the [ ]^{a,c,e} correlation results in a slight over prediction of subcooled break flow through rounded entrance, short L/D configurations. This is conservative in terms of the system inventory and peak clad temperature response. A discharge coefficient of 1.0 in the Moody steam break flow model provides an accurate calculation of the break flow. Uncertainties in the two-phase period of critical mass discharge are not expected to have a significant impact on the system response or peak clad temperature. The uncertainties are bounded by the fact that a range of break sizes is analyzed. Therefore, a discharge coefficient of 1.0 is appropriate in the NOTRUMP small break evaluation model.

Ref. A-1 Letter dated Nov. 16,1978, T. M. Anderson to R. J. Mattson, NS-TMA-1989.

Ref. A-2 WCAP-9600, "Report on Small Break Accidents for Westinghouse NSSS System", Section 2.8.

TABLE A-2

Fraction of Core Power

Time (sec)	Break Size	
	3 inch	4 inch
900	[	] a,c,e
1000		
1100		
1200		
1300		
1400		
1500		
1600		
1700		
1800		
1900		
2000		
2100		
2200		
2300		

FIGURE A-1 PRESSURE COMPARISON

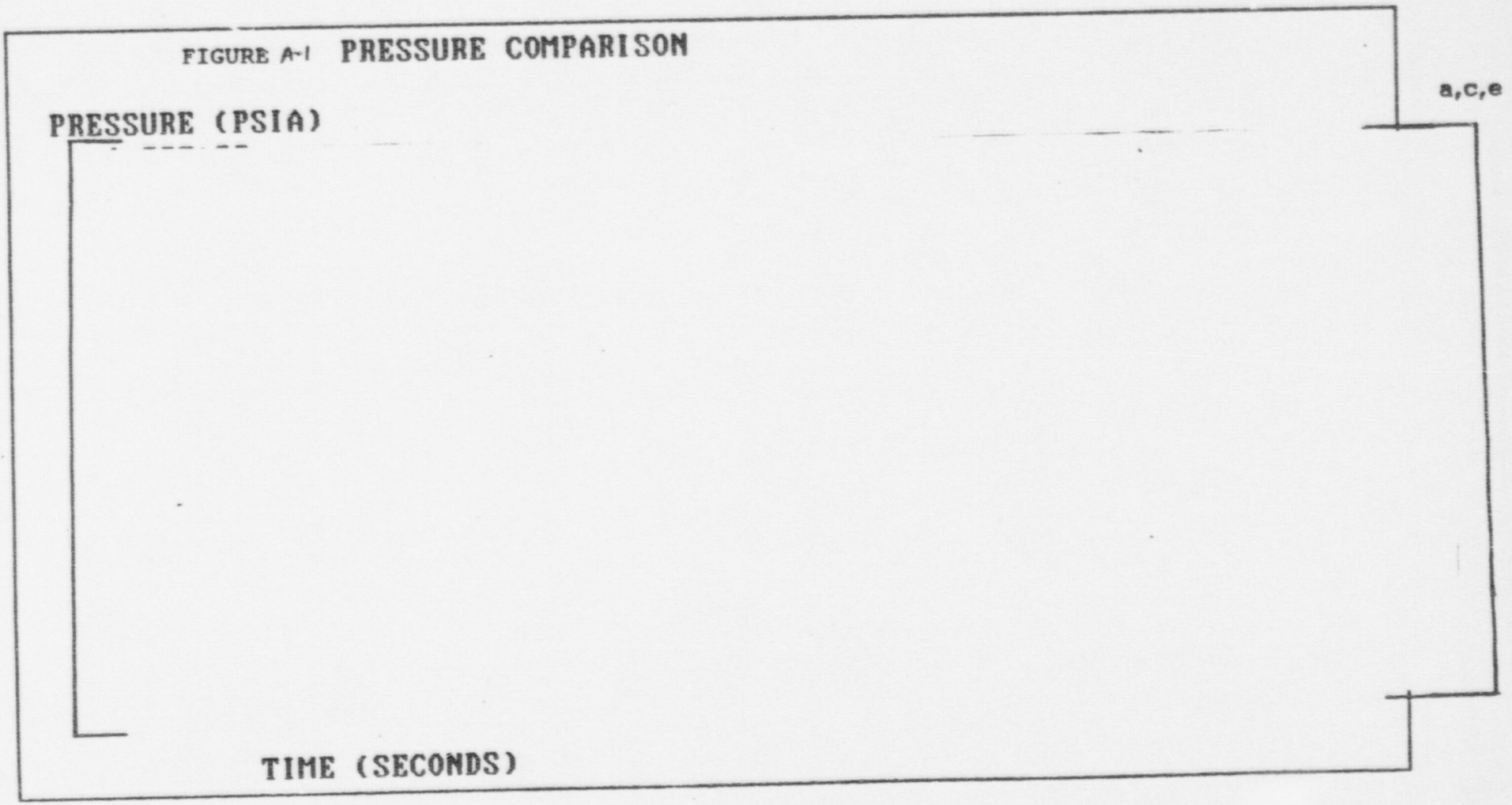


FIGURE A-2 MIXTURE LEVEL COMPARISON TOP OF CORE = 11.392 FEET

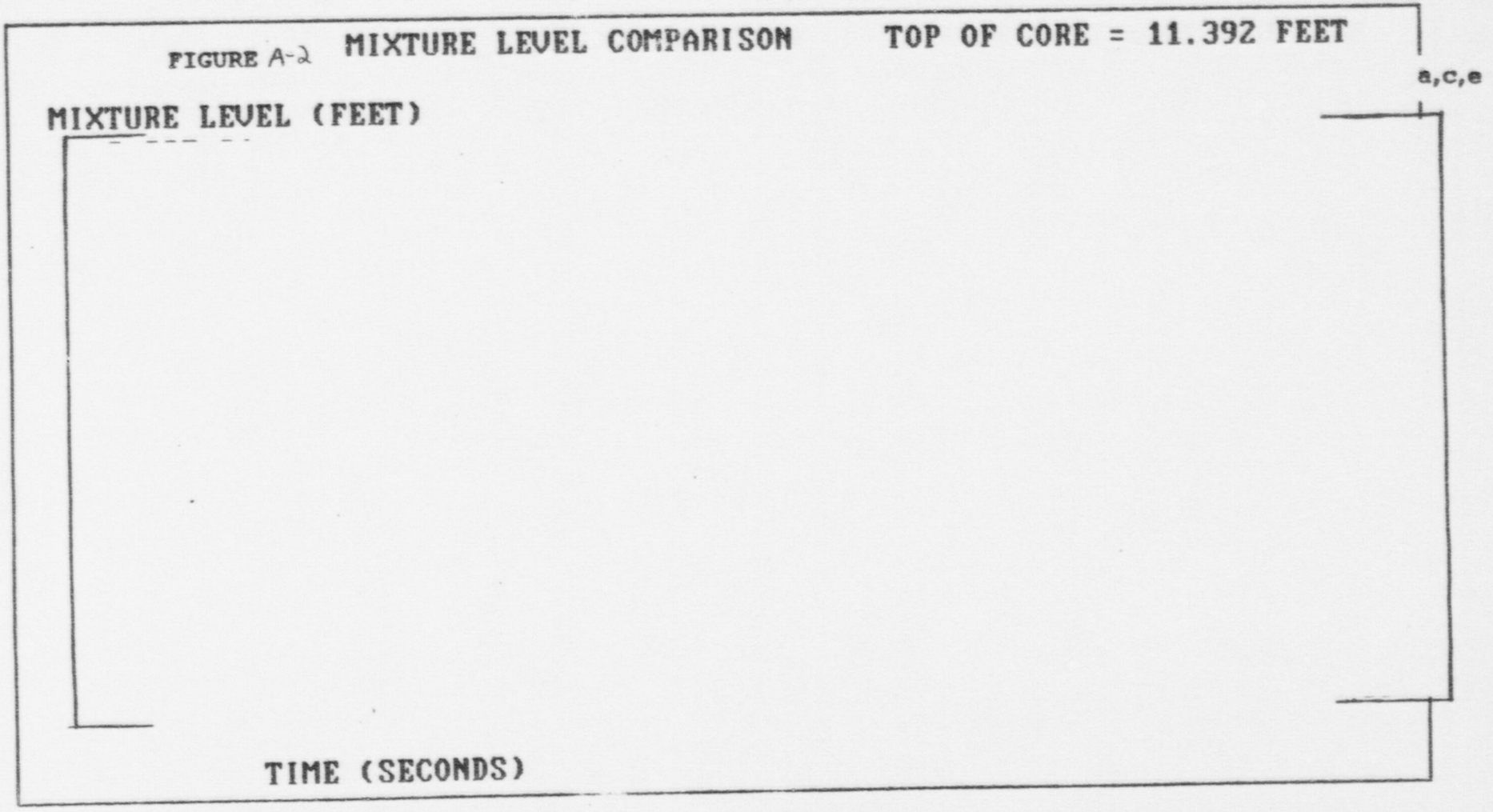
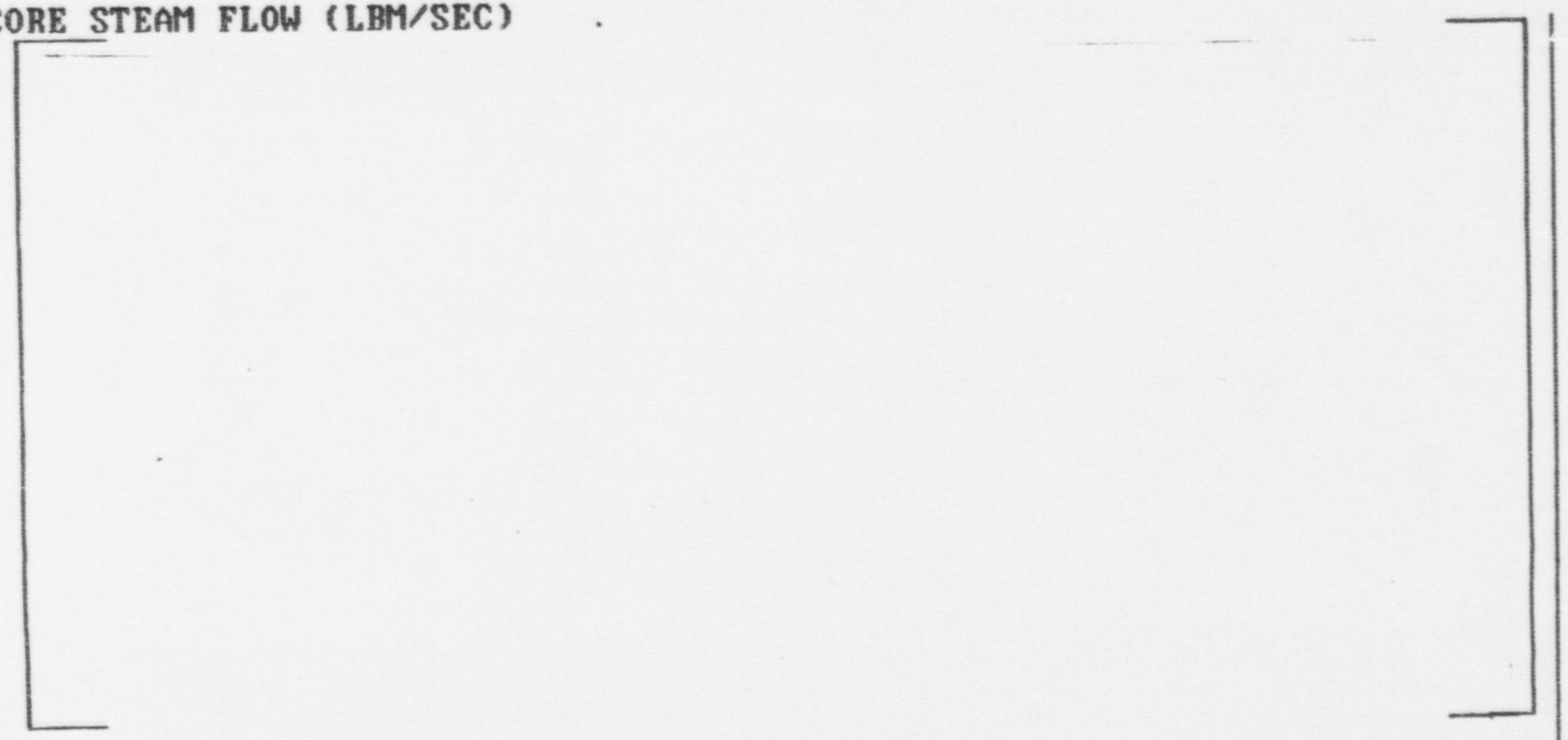


FIGURE A-3 CORE STEAM FLOW COMPARISON

a,c,e

CORE STEAM FLOW (LBM/SEC)



TIME (SECONDS)

FIGURE A-4 BREAK STEAM FLOW COMPARISON

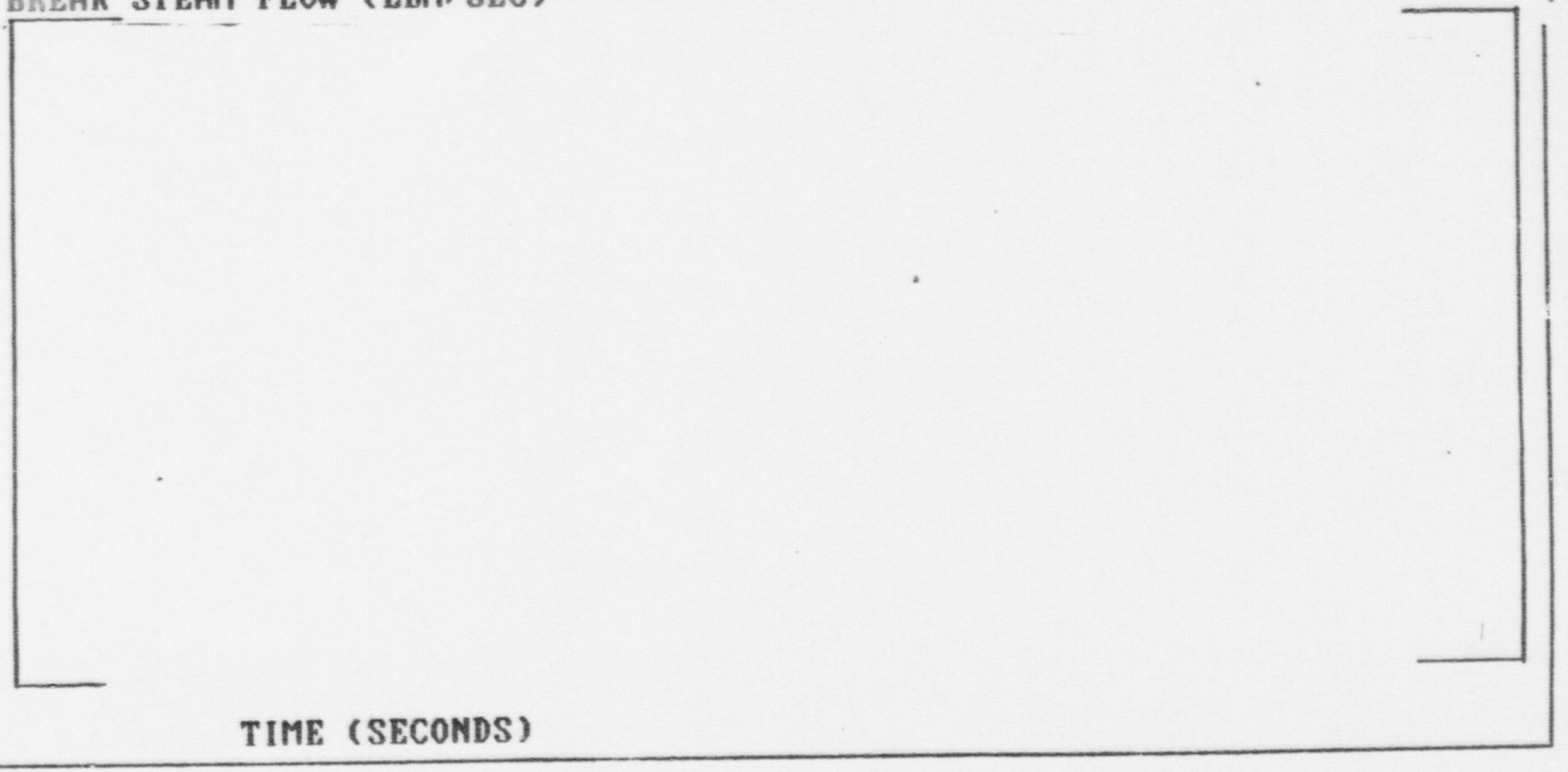


FIGURE A-5 BREAK LIQUID FLOW COMPARISON

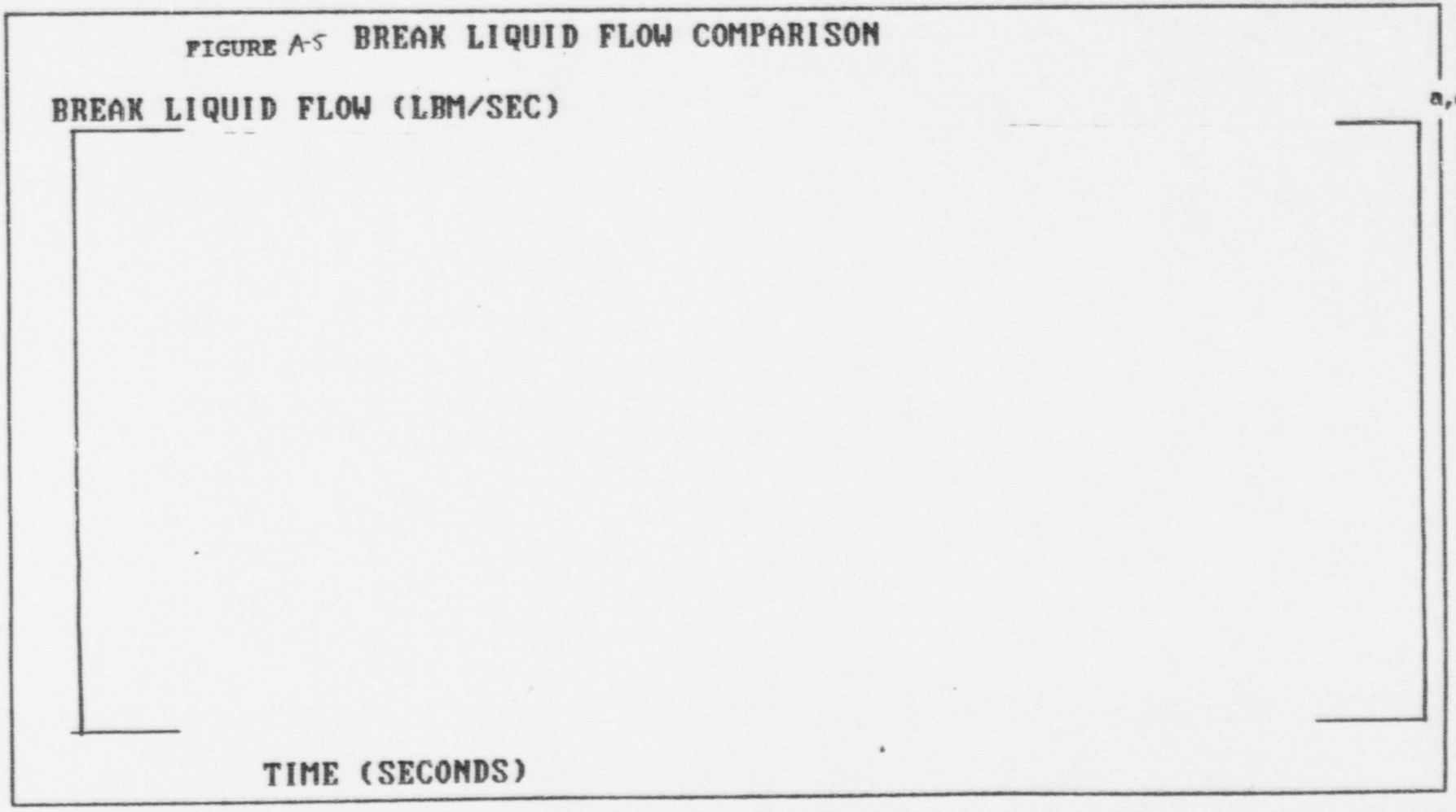


FIGURE A-6 VESSEL LIQUID MASS COMPARISON

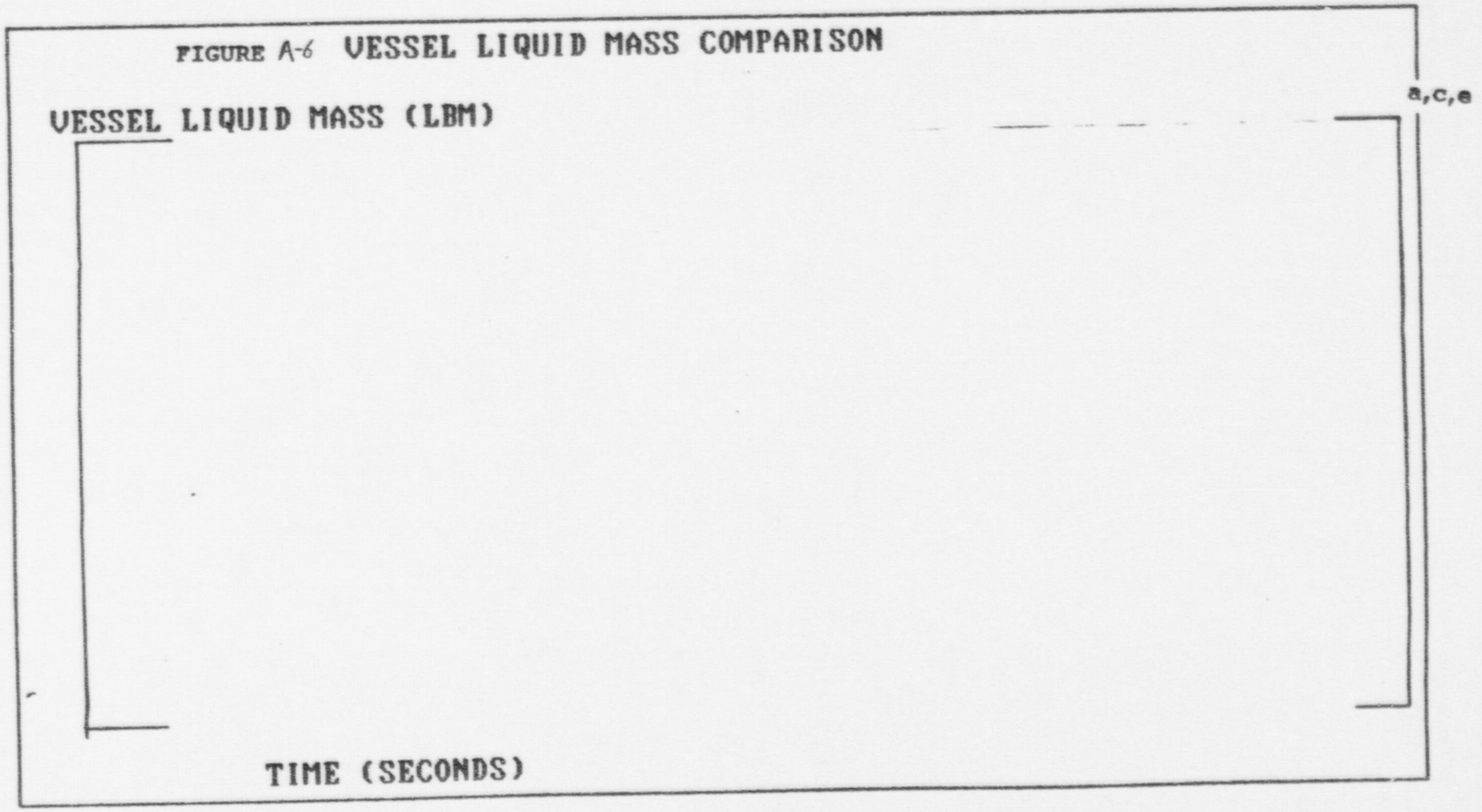


FIGURE A-7 TOTAL SYSTEM MASS COMPARISON

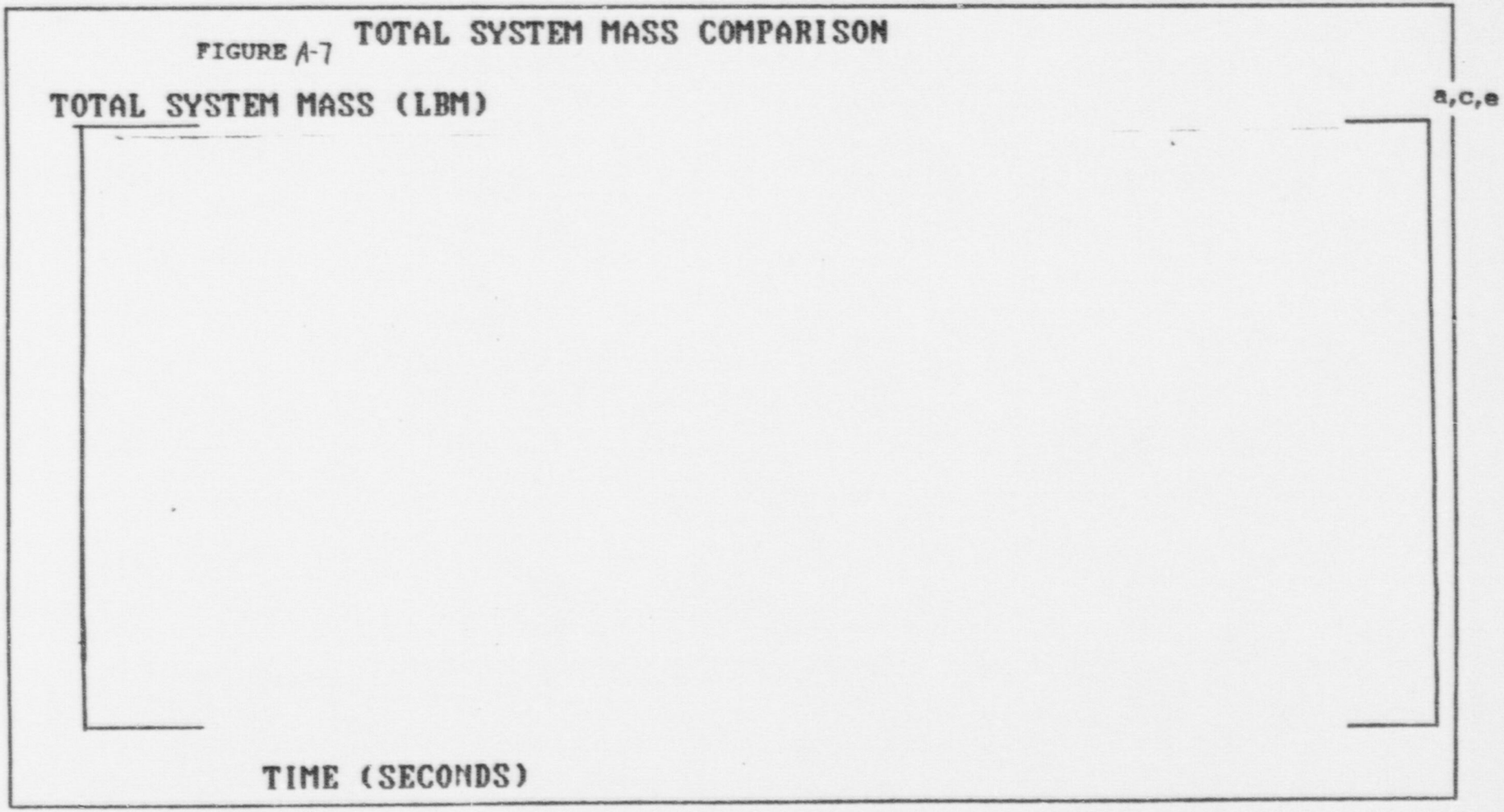


FIGURE A-8 CLAD AVERAGE TEMPERATURE (HOT ROD)

a,c,e

